# MANY-PARTICLE APPROACH TO THE IMAGE-CHARGE EFFECT

Riku Tuovinen

Jyväskylän yliopisto
Fysiikan laitos

Pro gradu -tutkielma
Ohjaaja: Robert van Leeuwen
23. helmikuuta 2011

## Abstract

In this master's thesis microscopical systems of molecules and atomic chains are studied to obtain information about quantum-transport phenomena. Both exact diagonalization method through second quantization and perturbation theory approach with Feynman diagrams are described, and then the energy spectra for the studied systems are calculated using the two methods.

The essential part of the method of exact diagonalization is simply to consider different quantum configurations of the studied system. After this the Hamiltonian matrix is constructed from all the possible states, and finally solving the actual problem is finding the eigenvalues and eigenvectors of this matrix. Only problem is, when the studied systems are large, that the dimension of the Hamiltonian matrix grows rapidly leading the diagonalization being quite a demanding task (even with powerful computers).

For the perturbation-theory approach, on the other hand, lots of preparations are needed before any results arise. These preparations include a wide background information about Green's functions, equations of motions, not forgetting the perturbative expansion with Feynman diagrams. Once ready and prepared, the non-interacting Green's functions for the studied systems can be constructed, after which the self-energy calculations with Feynman rules can be done. From the self-energy the total Green's function for the interacting system can be derived, and ultimately from the total Green's function all the essential physical properties of the studied systems are obtained.

The studied system includes a two-site molecule and an $N$-site tight-binding chain with interactions between the molecule and the chain. The main focus involves adding and removing particles to the molecule, and then studying the response of the chain next to the molecule. In this kind of study the so-called image-charge effect arises when the added or removed particle on the molecule affects the electron density on the terminal site of the chain.

The actual findings of the thesis are limited to comparing the results obtained from perturbation theory to the exact ones. It is seen clearly that the perturbation theory in first order (Hartree–Fock) does not take into account the interactions of the studied system, but already the second-order calculations converge almost to the exact result.

# Contents

## List of symbols

| | |
|---|---|
| $\hat{A}_{(H)}$ | Operator in Schrödinger (Heisenberg) picture |
| $\hat{A}^{(\dagger)}$ | General annihilation (creation) operator |
| $G_{(N)}(1,\dots,N;N',\dots,1')$ | $N$-particle propagator, i.e., Green's function from $(\mathbf{x}'_i, t'_i)$ to $(\mathbf{x}_i, t_i)$ |
| $\varphi_n(\mathbf{x})$ | One-particle orbitals |
| $\psi(x)$ | Single-particle wavefunction (in one dimension) |
| $\Psi(\mathbf{x}_1,\dots,\mathbf{x}_N)$ | Many-particle wavefunction |
| $\hat{\psi}^{(\dagger)}(\mathbf{x})$ | Field operator for annihilating (creating) particle from (to) $\mathbf{x}$ |
| $\Sigma$ | Self-energy |
| $\mathcal{T}_{(C)}$ | Time (contour) ordering operator |
| $\hat{U}(t,t')$ | Time-evolution operator from $t'$ to $t$ |
| $\mathbf{x}$ | Collective vector for position vector $\mathbf{r}$ and spin index $\sigma$: $\mathbf{x} = (\mathbf{r}, \sigma)$ |
| $\mathcal{Z}$ | Partition function |

## Conventions

- Vectors are expressed with bold-face letters, matrices have indices as subscripts.
- Operators are marked with a hat ˆ .
- In numerical calculations we use units: $\hbar = m_e = e = (4\pi\epsilon_0)^{-1} = 1$ .

# Chapter 1

# Introduction

Quantum theory is (so far) the most accurate representation of the Nature at the microscopic level. The theory has been applied succesfully to different phenomena of matter and energy, which can differ considerably in the order of magnitude. This so-called standard model of particle physics covers the research fields from elementary particles, to many-particle materials science, and even further to neutron stars and to other astrophysical objects in cosmological scale. Apart from these the most everyday interaction – gravity – remains an open problem in fundamental quantum theory.

At first quantum physics concerned the movement of particles as mechanical objects leaving, e.g., the electromagnetic interaction completely to Maxwell's era. Because of this the name quantum *mechanics* has remained to describe many phenomena at the microscopic level. The elementary quantum mechanics was developed mainly by Heisenberg, Schrödinger and Dirac during the years 1925–1926 [15, 27, 6]. It did not, however, take very long time until also the electromagnetic field was quantized and soon after this also the material fields for fermions and bosons. These theories combined to quantum electrodynamics (QED) and quantum field theory (QFT). The original single-particle quantum mechanics is often called first quantization, whereas the quantum-field theoretical description is called second quantization.

In this project we aim to study electron dynamics in many-particle systems. The motion of electrons naturally corresponds to charge transport and eventually to the quantity known as current. Microscopical devices can already be constructed and they can be utilized in, e.g., nanotechnology and molecular electronics. Namely solid–molecule interfaces are typical components, but the actual quantum-level physics in the background of these applications is known quite restrictedly. The theoretical models rely mostly on density functional theory which emanates from single-particle quantum mechanics. Obtaining results from these theoretical models can be quite a tedious task when considering the numerical methods. Many-particle perturbation theory provides another method to study the interesting model systems corresponding to, e.g., nanoscale electronics chips.

Computationally speaking the many-particle perturbation theory might not be any more profitable method than the ones with density functional theory, but the idea of capturing the essential physics from studied system through a collection of Feynman diagrams is (at least intuitively) advantageous. More explicitly, in many-particle perturbation theory the system is first assumed to be non-interacting. Then the interactions (due to Coulomb force or tunneling for instance) are assumed to be small enough that they can be interpreted perturbatively. The terms of the perturbation series are then described as symbolic diagrams for which certain calculation rules arise.

The outline of this thesis is as follows. After this short introduction we present a theoretical background by stating the many-particle problem in terms of quantum field theory. After this a little more background information about many-particle perturbation theory is described, after which it follows a short introduction to complex analysis because of the needed mathematical methods. Then the present study is described and analyzed in detail with the help of the stated background theory. After the actual calculations we present the results and discuss them thoroughly. The last chapter contains a conclusion and an outlook for future considerations.

# Chapter 2

# Many-particle problem in terms of quantum field theory

In this chapter we will set the basis for the field of study. The framework we will be working is the quantum field theory, and for for the many-particle phenomena we introduce essential parts of this particular theory. We will be following the representation of Refs. [20,24,28,33] and the lecture notes of a course in many-particle quantum mechanics by Robert van Leeuwen.

## 2.1 Second quantization

The formalism of second quantization is a quantum field theoretical representation of many-particle systems. This formalism is especially necessary when we are dealing with systems in which the number of particles is itself variable. Originally, second quantization was developed for the study of photons in radiation theory by P. Dirac in 1927 [7]. The method was later extended to bosons (by P. Jordan and O. Klein) in 1927 and to fermions (by P. Jordan and E. Wigner) in 1928 [17,32].

Usually, the elementary quantum mechanics is formulated via first quantization, i.e., the normal observables for position $\mathbf{x}$ and momentum $\mathbf{p}$ are replaced by operators $\hat{\mathbf{x}}$ and $\hat{\mathbf{p}}$, which in turn obey the so-called canonical commutation relation $[\hat{\mathbf{x}}, \hat{\mathbf{p}}] = \mathrm{i}\hbar$. However, in second quantization we quantize the wave function itself by replacing the complex-valued function $\psi(\mathbf{x})$ by an operator $\hat{\psi}(\mathbf{x})$. The terminology here can be rather misleading since first quantization refers to the quantization of a single-particle system while second quantization refers to the quantization of a many-particle system, but both systems are being quantized only once and separately.

Quantum mechanics of an $N$-particle system is strongly based on the wave function $\Psi\left(\mathbf{x}_1, \ldots, \mathbf{x}_N\right)$, where both the position $\mathbf{r}_i$ and the spin projection $\sigma_i$ of the $i$:th particle are included in the coordinate $\mathbf{x}_i$. When studying indentical particles, their exchange must not change any physical quantities, i.e.,

$$\Psi\left(\mathbf{x}_1, \ldots, \mathbf{x}_i, \ldots, \mathbf{x}_j, \ldots, \mathbf{x}_N\right) = \mathrm{e}^{\mathrm{i}\theta}\Psi\left(\mathbf{x}_1, \ldots, \mathbf{x}_j, \ldots, \mathbf{x}_i, \ldots, \mathbf{x}_N\right) , \tag{2.1}$$

where $\mathrm{e}^{\mathrm{i}\theta}$ is a phase factor. Interchanging any pair $(i, j)$ of particles twice should amount to no interchange, hence, $(\mathrm{e}^{\mathrm{i}\theta})^2 = 1$ gives $\mathrm{e}^{\mathrm{i}\theta} = \pm 1$. This (anti)symmetry of the wave function for (fermions) bosons is called *Spin-statistics theorem* [25]. This theorem follows from the assumptions of 1) Lorentz invariance, 2) causality and 3) unitarity. It should, however, be noted that the theorem holds only in three spatial dimensions (and above) because in one and two dimensions the exchange of particles is more restricted, as there must be some plane where the particles are rotating (2D) or a line where the particles are colliding with each other (1D). Next thing to consider is, what kind of basis we need to construct for the general wave function in Eq. (2.1). When studying $N$ identical fermions[1] we need to have a fully antisymmetrized wave function. Although it is possible to expand the total wave function in an orthonormal basis $\{\varphi_n(\mathbf{x})\}$ [with $\varphi_n(\mathbf{x}) = \langle \mathbf{x}|\varphi_n\rangle$ being a projection on the position-spin eigenbra $\langle \mathbf{x}| = \langle \mathbf{r}\sigma|$ of the basis ket $|\varphi_n\rangle$], the antisymmetry property makes calculations somewhat difficult. The $N$-particle basis function, with respect to the expansion is to be done, is a sum of all different permutations of one-particle basis functions

$$\sum_P \operatorname{sgn}(P)\varphi_{n_1}(\mathbf{x}_{P(1)})\varphi_{n_2}(\mathbf{x}_{P(2)})\cdots\varphi_{n_N}(\mathbf{x}_{P(N)}) \,, \tag{2.2}$$

where $P$ refers to permutations of $1, 2, \ldots, N$. The sign of the permutation $\operatorname{sgn}(P)$ is either plus for even permutations or minus for odd permutations. The sum in Eq. (2.2) contains $N!$ terms, and it easy to imagine how convoluted, e.g., actions of certain operators become when we express the basis functions as projections on the normalized position-spin eigenbra of the corresponding normalized basis ket

$$\left[\frac{1}{\sqrt{N!}}\sum_P \operatorname{sgn}(P)\langle \mathbf{x}_{P(N)}|\cdots\langle \mathbf{x}_{P(2)}|\langle \mathbf{x}_{P(1)}|\right]\left[\frac{1}{\sqrt{N!}}\sum_P \operatorname{sgn}(P)|\varphi_{n_{P(1)}}\rangle|\varphi_{n_{P(2)}}\rangle\cdots|\varphi_{n_{P(N)}}\rangle\right] . \tag{2.3}$$

Fortunately, the formalism of second quantization gives us a shortcut for the stated headache above, as the expressions become more compact. It turns out that there are certain operators which have all the symmetry properties of the system built into them.

One remarkable thing to mention before tackling the formal development of the occupation number representation in detail, is the idea by V. Fock from 1932 [12]. He showed a one-to-one correspondence between wave-function description and occupation number representation, and introduced the so-called *Fock space*. If we consider the number of particles as an observable capable of assuming various values ($N = 0, 1, 2, \ldots$), we have one Hilbert space corresponding to the one-particle system, a different Hilbert space for the two-particle system and so on. The Fock space is a collection of all these Hilbert spaces with different number of particles. In fact, the Fock space is a direct sum of $i$-particle Hilbert spaces

$$\mathcal{F} = \bigoplus_{i=0}^{N} \mathcal{H}_i \,, \tag{2.4}$$

where also the zero-particle Hilbert space is included, which is simply an empty, one-dimensional space.

### 2.1.1 Occupation number representation

We notice that the form of the basis functions in Eq. (2.2) is the definition of a determinant. The fully antisymmetrized wave function can therefore be represented as a so-called *Slater*

---

[1] In this thesis we will be considering fermions only.

*determinant*

$$\Psi(\mathbf{x}_1,\ldots,\mathbf{x}_N) = \frac{1}{\sqrt{N!}} \begin{vmatrix} \varphi_{n_1}(\mathbf{x}_1) & \ldots & \varphi_{n_1}(\mathbf{x}_N) \\ \vdots & \ddots & \vdots \\ \varphi_{n_N}(\mathbf{x}_1) & \ldots & \varphi_{n_N}(\mathbf{x}_N) \end{vmatrix} . \tag{2.5}$$

As said earlier, the determinant expression is a bit clumsy to carry around, and because of this, we adopt a compact way of writing the wave function in Eq. (2.5) by noticing that the particles are indistinguishable: The essential information then is, how many particles there are in a single-particle state. We can then equally well specify the non-interacting state as (without normalization)

$$\Psi(\mathbf{x}_1,\ldots,\mathbf{x}_N) = \langle \mathbf{x}_N,\ldots,\mathbf{x}_1 | n_1,\ldots,n_N \rangle , \tag{2.6}$$

meaning, that there is $n_1$ particles in state $\varphi_{n_1}$ and $n_N$ particles in state $\varphi_{n_N}$, with $n_i$ being either 1 or 0 because of the Pauli's exclusion principle. The form of the wave function in Eq. (2.6) is called the *occupation number representation*. It is also important to note that the states in occupation number representation form a complete orthonormal set of basis functions (just as the original Slater determinants do), i.e., we have

$$\langle n'_N,\ldots,n'_1 | n_1,\ldots,n_N \rangle = \delta_{n'_1,n_1} \ldots \delta_{n'_N,n_N} , \tag{2.7}$$

and

$$\sum_{n_1,\ldots,n_N} |n_1,\ldots,n_N\rangle\langle n_N,\ldots,n_1| = \mathbb{1} . \tag{2.8}$$

The particle number operator is easily accessible in occupation number representation. When we act with a number operator to a state, we get exactly the number of particles in that particular state

$$\hat{n}_i |n_1,\ldots,n_i,\ldots,n_N\rangle = n_i |n_1,\ldots,n_i,\ldots,n_N\rangle , \tag{2.9}$$

and the total number of particles $N$ in a system is then given simply by

$$\hat{N}|n_1,\ldots,n_N\rangle = \sum_i n_i |n_1,\ldots,n_N\rangle . \tag{2.10}$$

### 2.1.2 Creation and annihilation operators

We can look into the occupation number representation more precisely by introducing so-called *creation* and *annihilation* operators. These operators map the space of $N$-particle states to spaces with $N \pm 1$-particle states, i.e., add or remove particles. For the consideration here, we follow the representation given in [28].

Due to the Pauli's exclusion principle, two identical fermions must not occupy the same state. When we consider adding particles, i.e., acting to a state with creation operators, we must pay attention to the fermion statistics: applying them twice should amount to zero. Consider now an $N$-particle state

$$|n_1,n_2,\ldots,n_N\rangle = \hat{a}_1^\dagger,\hat{a}_2^\dagger,\ldots,\hat{a}_N^\dagger|0\rangle , \tag{2.11}$$

where the operators $\hat{a}^\dagger$ are creation operators acting to a vacuum state $|0\rangle$. If we interchange first two occupancies we get the same state except for the sign (antisymmetricity)

$$|n_2,n_1,\ldots,n_N\rangle = -\hat{a}_2^\dagger,\hat{a}_1^\dagger,\ldots,\hat{a}_N^\dagger|0\rangle . \tag{2.12}$$

We then realize that $\hat{a}_1^\dagger \hat{a}_2^\dagger = -\hat{a}_2^\dagger \hat{a}_1^\dagger$, i.e., the operators anticommute: $\left\{\hat{a}_1^\dagger, \hat{a}_2^\dagger\right\} = 0$. Naturally, this generalizes to any two creation operators in Eq. (2.11) and we have

$$\left\{\hat{a}_i^\dagger, \hat{a}_j^\dagger\right\} = 0\,. \tag{2.13}$$

The impossibility of double occupation[2] is naturally included in Eq. (2.13). By fermionic nature of particles we can now rewrite our $N$-particle state in Eq. (2.11) as

$$|n_1, n_2, \ldots, n_N\rangle = \left(\hat{a}_1^\dagger\right)^{n_1} \left(\hat{a}_2^\dagger\right)^{n_2} \ldots \left(\hat{a}_N^\dagger\right)^{n_N} |0\rangle\,, \tag{2.14}$$

with $n_i \in \{0, 1\}$. If we then consider the addition of a particle into state $i$ we have

$$\hat{a}_i^\dagger |\ldots, n_i, \ldots\rangle = (1 - n_1)(-1)^{\sum_{j<i} n_j} |\ldots, n_i + 1, \ldots\rangle\,, \tag{2.15}$$

where the term $(1 - n_i)$ forbids the double occupation, as $1 - n_i = 0$ if there already is a particle in the state $i$ ($n_i = 1$). The sign term $(-1)^{\sum_{j<i} n_j}$ arises from the fact that we need to anticommute the creation operator $\hat{a}_i^\dagger$ to the correct place, and by one anticommutation we get a minus sign. To obtain an expression for the annihilation operator $\hat{a}_i$ we take the adjoint of Eq. (2.15) and then multiply it from right with an $N$-particle ket state (labeled with primes)

$$\langle \ldots, n_i, \ldots |\hat{a}_i| \ldots, n_i', \ldots\rangle = (1 - n_i)(-1)^{\sum_{j<i} n_j} \underbrace{\langle \ldots, n_i + 1, \ldots | \ldots, n_i', \ldots\rangle}_{=\delta_{n_1,n_1'} \ldots \delta_{n_i+1,n_i'} \ldots \delta_{n_N,n_N'}}\,. \tag{2.16}$$

Then we calculate the action of an annihilation operator $\hat{a}_i$ to an $N$-particle state by using the completeness relation in Eq. (2.8) of the $N$-particle states

$$\begin{aligned}
\hat{a}_i |\ldots, n_i', \ldots\rangle &= \sum_{n_1,\ldots,n_N} |\ldots, n_i, \ldots\rangle \underbrace{\langle \ldots, n_i, \ldots |\hat{a}_i| \ldots, n_i', \ldots\rangle}_{\text{insert Eq. (2.16)}} \\
&= \sum_{n_1,\ldots,n_N} |\ldots, n_i, \ldots\rangle (1 - n_i)(-1)^{\sum_{j<i} n_j} \delta_{n_1,n_1'} \ldots \underbrace{\delta_{n_i+1,n_i'}}_{=\delta_{n_i,n_i'-1}} \ldots \delta_{n_N,n_N'} \\
&= |\ldots, n_i' - 1, \ldots\rangle [1 - (n_i' - 1)](-1)^{\sum_{j<i} n_j} n_i' \\
&= n_i'(2 - n_i')(-1)^{\sum_{j<i} n_j} |\ldots, n_i' - 1, \ldots\rangle \\
&= n_i'(-1)^{\sum_{j<i} n_j} |\ldots, n_i' - 1, \ldots\rangle\,.
\end{aligned} \tag{2.17}$$

On the third line we added a term $n_i'$ to the expression to ensure that we are not removing a particle from state $i$ if there is not one ($n_i = 0$). We are allowed to add this term since the Kronecker delta $\delta_{n_i+1,n_i'}$ always gives zero for $n_i' = 0$. This way we may also forget about the term $(2 - n_i)$ because this gives simply 1 with $n_i' = 1$ and for $n_i' = 0$ the whole expression is zero, so that the extra 2 will not bother us. It now follows that

$$\begin{aligned}
\hat{a}_i \hat{a}_i^\dagger |\ldots, n_i, \ldots\rangle &= \hat{a}_i (1 - n_i)(-1)^{\sum_{j<i} n_j} |\ldots, n_i + 1, \ldots\rangle \\
&= (1 - n_i)(-1)^{\sum_{j<i} n_j} (n_i + 1)(-1)^{\sum_{j<i} n_j} |\ldots, n_i, \ldots\rangle \\
&= (1 - n_i)(n_i + 1) \underbrace{[(-1)^2]^{\sum_{j<i} n_j}}_{=1} |\ldots, n_i, \ldots\rangle \\
&= (n_i + 1 - \underbrace{n_i^2}_{=n_i} - n_i) |\ldots, n_i, \ldots\rangle \\
&= (1 - n_i) |\ldots, n_i, \ldots\rangle
\end{aligned} \tag{2.18}$$

---

[2] $\left\{\hat{a}_i^\dagger, \hat{a}_i^\dagger\right\} = \hat{a}_i^\dagger \hat{a}_i^\dagger + \hat{a}_i^\dagger \hat{a}_i^\dagger = 0 \quad \Rightarrow \quad 2\hat{a}_i^\dagger \hat{a}_i^\dagger = 0 \quad \Rightarrow \quad \left(\hat{a}_i^\dagger\right)^2 = 0.$

and

$$\begin{aligned}
\hat{a}_i^\dagger \hat{a}_i|\ldots,n_i,\ldots\rangle &= \hat{a}_i^\dagger n_i(-1)^{\sum_{j<i} n_j}|\ldots,n_i-1,\ldots\rangle \\
&= n_i(-1)^{\sum_{j<i} n_j}[1-(n_i-1)](-1)^{\sum_{j<i} n_j}|\ldots,n_i,\ldots\rangle \\
&= n_i(2-n_i)\underbrace{\left((-1)^2\right)^{\sum_{j<i} n_j}}_{=1}|\ldots,n_i,\ldots\rangle \\
&= (2n_i - \underbrace{n_i^2}_{=n_i})|\ldots,n_i,\ldots\rangle \\
&= n_i|\ldots,n_i,\ldots\rangle \,. 
\end{aligned} \tag{2.19}$$

If we add Eqs. (2.18) and (2.19) together we get

$$\hat{a}_i^\dagger \hat{a}_i + \hat{a}_i \hat{a}_i^\dagger \equiv \left\{\hat{a}_i^\dagger, \hat{a}_i\right\} = 1 - n_i + n_i = 1 \,. \tag{2.20}$$

Consider then an action of operators as in Eqs. (2.18) and (2.19) but with different indices, i.e., we add a particle to state $j$ and remove a particle from state $i$, and then the same in different order: (here we have $j > i$ as particle labeling indices)

$$\begin{aligned}
\hat{a}_i\hat{a}_j^\dagger|\ldots,n_i,\ldots,n_j,\ldots\rangle &= (1-n_j)\underbrace{(-1)^{\sum_{k<j} n_k}}_{=(-1)^{\sum_{k<i}}(-1)^{\sum_{i\le k<j}}} n_i(-1)^{\sum_{k<i} n_k}|\ldots,n_i-1,\ldots,n_j+1,\ldots\rangle \\
&= (1-n_j)n_i\underbrace{\left[(-1)^2\right]^{\sum_{k<i} n_k}}_{=1}(-1)^{\sum_{i\le k<j} n_k}|\ldots,n_i-1,\ldots,n_j+1,\ldots\rangle \\
&= (1-n_j)n_i(-1)^{\sum_{i\le k<j} n_k}|\ldots,n_i-1,\ldots,n_j+1,\ldots\rangle
\end{aligned} \tag{2.21}$$

$$\begin{aligned}
\hat{a}_j^\dagger\hat{a}_i|\ldots,n_i,\ldots,n_j,\ldots\rangle &= n_i(-1)^{\sum_{k<i}}(1-n_j)\underbrace{(-1)^{\sum_{k<j-1} n_k}}_{=(-1)^{\sum_{k<i} n_k}(-1)^{\sum_{i\le k<j-1} n_k}}|\ldots,n_i-1,\ldots,n_j+1,\ldots\rangle \\
&= -(1-n_j)n_i\underbrace{\left[(-1)^2\right]^{\sum_{k<i} n_k}}_{=1}(-1)^{\sum_{i\le k<j} n_k}|\ldots,n_i-1,\ldots,n_j+1,\ldots\rangle \\
&= -(1-n_j)n_i(-1)^{\sum_{i\le k<j} n_k}|\ldots,n_i-1,\ldots,n_j+1,\ldots\rangle
\end{aligned} \tag{2.22}$$

In the first line of Eq. (2.22) we have the summing over index $k$ up to $j-1$ since the operator $\hat{a}_i$ already annihilated the particle from state $i$, and hence, there is one anticommutation less for operator $\hat{a}_j^\dagger$ than in Eq. (2.21). This sum over index $k$ can be extended from $j-1$ to $j$ if we add a minus sign in front of the whole expression. Then, combining Eqs. (2.21) and (2.22) gives

$$\hat{a}_i\hat{a}_j^\dagger + \hat{a}_j^\dagger\hat{a}_i \equiv \left\{\hat{a}_i, \hat{a}_j^\dagger\right\} = 0 \,. \tag{2.23}$$

Also, for the annihilation operators we have

$$\begin{aligned}
\hat{a}_i\hat{a}_j|\ldots,n_i,\ldots,n_j,\ldots\rangle &= n_j(-1)^{\sum_{k<j} n_k} n_i(-1)^{\sum_{k<i} n_k}|\ldots,n_i-1,\ldots,n_j-1,\ldots\rangle \\
&= n_j n_i\underbrace{\left[(-1)^2\right]^{\sum_{k<i} n_k}}_{=1}(-1)^{\sum_{i\le k<j} n_k}|\ldots,n_i-1,\ldots,n_j-1,\ldots\rangle \\
&= n_j n_i(-1)^{\sum_{i\le k<j} n_k}|\ldots,n_i-1,\ldots,n_j-1,\ldots\rangle
\end{aligned} \tag{2.24}$$

$$\begin{aligned}\hat{a}_j\hat{a}_i|\ldots,n_i,\ldots,n_j,\ldots\rangle &= n_i(-1)^{\sum_{k<i}n_k}n_j(-1)^{\sum_{k<j-1}n_k}|\ldots,n_i-1,\ldots,n_j-1,\ldots\rangle\\ &= -n_in_j\underbrace{\left[(-1)^2\right]^{\sum_{k<i}n_k}}_{=1}(-1)^{\sum_{i\le k<j-1}n_k}|\ldots,n_i-1,\ldots,n_j-1,\ldots\rangle\\ &= -n_jn_i(-1)^{\sum_{i\le k<j}n_k}|\ldots,n_i-1,\ldots,n_j-1,\ldots\rangle \qquad (2.25)\end{aligned}$$

where we used similar arguments for the summings as in Eq. (2.22). Eqs. (2.24) and (2.25) together now yield $\left\{\hat{a}_i,\hat{a}_j\right\}=0$. We have then obtained the fermionic operator algebra:

$$\left\{\hat{a}_i,\hat{a}_j\right\}=0=\left\{\hat{a}_i^\dagger,\hat{a}_j^\dagger\right\} \qquad \text{and} \qquad \left\{\hat{a}_i,\hat{a}_j^\dagger\right\}=\delta_{i,j}\,. \tag{2.26}$$

As a remark of Eq. (2.19), we may regard the operation $\hat{a}_i^\dagger\hat{a}_i$ as the occupation number operator for the state $i$, i.e., $\hat{n}_i=\hat{a}_i^\dagger\hat{a}_i$.

So far, we have been discussing adding and removing particles in a general basis $\{|i\rangle\}$. We then consider another basis $\{|\alpha\rangle\}$ and examine the relationship between the creation and annihilation operators in these particular bases. As we are studying orthonormal bases, we may expand one in terms of the other, i.e.,

$$|\alpha\rangle=\sum_i|i\rangle\langle i|\alpha\rangle\,. \tag{2.27}$$

Here we may regard $\langle i|\alpha\rangle$ as a change-of-basis matrix from $|i\rangle$ to $|\alpha\rangle$. As the operator $\hat{a}_i^\dagger$ creates a fermion in the state $i$, we must have the creation of a fermion in the state $\alpha$ as

$$\hat{a}_\alpha^\dagger=\sum_i\langle i|\alpha\rangle\hat{a}_i^\dagger\,. \tag{2.28}$$

The adjoint of Eq. (2.28) then gives us the annihilation operator in the other basis

$$\hat{a}_\alpha=\sum_i\langle\alpha|i\rangle^*\hat{a}_i\,. \tag{2.29}$$

Although the discussion still remains in a general basis, we may now take a concrete, yet very important, example. We were trying to find a suitable basis for the general many-particle wave function in Eq. (2.1) and came up with single-particle eigenstates in position representation $\varphi_n(\mathbf{x})=\langle\mathbf{x}|\varphi_n\rangle$. We may now represent our creation and annihilation operators corresponding to the eigenstates of position as

$$\hat{\psi}^\dagger(\mathbf{x})=\sum_n\varphi_n^*(\mathbf{x})\hat{a}_n^\dagger\,, \tag{2.30}$$

$$\hat{\psi}(\mathbf{x})=\sum_n\varphi_n(\mathbf{x})\hat{a}_n\,. \tag{2.31}$$

The operators in Eqs. (2.30) and (2.31) are called *field operators*, and because of their important nature they are denoted with different letter $\hat{\psi}$ instead of $\hat{a}$. This is now a concrete example of adding (removing) a particle to (from) the position $\mathbf{x}$. It is essential to remember that we use notation $\mathbf{x}=(\mathbf{r},\sigma)$, i.e., the spin is included to the coordinate $\mathbf{x}$. The field operators obey similar anticommutation relations as operators $\hat{a}^\dagger$ and $\hat{a}$ do. In fact, we may calculate

$$\begin{aligned}\left\{\hat{\psi}^{(\dagger)}(\mathbf{x}),\hat{\psi}^{(\dagger)}(\mathbf{x}')\right\} &= \sum_{n,m}\left[\varphi_n^{(*)}(\mathbf{x})\hat{a}_n^{(\dagger)}\varphi_m^{(*)}(\mathbf{x}')\hat{a}_m^{(\dagger)}+\varphi_m^{(*)}(\mathbf{x}')\hat{a}_m^{(\dagger)}\varphi_n^{(*)}(\mathbf{x})\hat{a}_n^{(\dagger)}\right]\\ &= \sum_{n,m}\varphi_n^{(*)}(\mathbf{x})\varphi_m^{(*)}(\mathbf{x}')\underbrace{\left\{\hat{a}_n^{(\dagger)},\hat{a}_m^{(\dagger)}\right\}}_{=0}\\ &= 0\,, \qquad (2.32)\end{aligned}$$

where we calculated both creation and annihilation operators simultaneously as $(\dagger)$ and $(*)$ are to be understood as the exponent either is there, or it is not. Similarly, we have

$$\begin{aligned}
\left\{\hat{\psi}(\mathbf{x}),\hat{\psi}^{\dagger}(\mathbf{x}')\right\} &= \sum_{n,m}\left[\varphi_n(\mathbf{x})\hat{a}_n\varphi^*_m(\mathbf{x}')\hat{a}^{\dagger}_m + \varphi^*_m(\mathbf{x}')\hat{a}^{\dagger}_m\varphi_n(\mathbf{x})\hat{a}_n\right] \\
&= \sum_{n,m}\varphi_n(\mathbf{x})\varphi^*_m(\mathbf{x}')\underbrace{\left\{\hat{a}_n,\hat{a}^{\dagger}_m\right\}}_{=\delta_{n,m}} \\
&= \sum_{n}\varphi_n(\mathbf{x})\varphi^*_n(\mathbf{x}') \\
&= \delta^{(3)}(\mathbf{x}-\mathbf{x}')\,, \qquad (2.33)
\end{aligned}$$

where, on the last step, we used the fact that the single-particle eigenstates are orthonormal.[3] Summarizing our results, we have obtained creation and annihilation operators ($\hat{a}^{\dagger}$, $\hat{a}$) that work in occupation number representation by either increasing or decreasing the particle number in a particular state. On the other hand we have obtained creation and annihilation operators (field operators) that work in single-particle eigenbasis by adding (removing) particles to (from) a particular coordinate $\mathbf{x}$.

We will now discuss shortly the utilization of the field operators. We may express an $N$-particle state in coordinate representation by

$$|\mathbf{x}_1,\ldots,\mathbf{x}_N\rangle = \hat{\psi}^{\dagger}(\mathbf{x}_1)\ldots\hat{\psi}^{\dagger}(\mathbf{x}_N)|0\rangle\,, \qquad (2.34)$$

and then calculate the action of an operator $\hat{\psi}^{\dagger}(\mathbf{x})\hat{\psi}(\mathbf{y})$ on this particular state:

$$\hat{\psi}^{\dagger}(\mathbf{x})\hat{\psi}(\mathbf{y})|\mathbf{x}_1,\ldots,\mathbf{x}_N\rangle = \hat{\psi}^{\dagger}(\mathbf{x})\hat{\psi}(\mathbf{y})\hat{\psi}^{\dagger}(\mathbf{x}_1)\ldots\hat{\psi}^{\dagger}(\mathbf{x}_N)|0\rangle\,. \qquad (2.35)$$

To evaluate this, we need to anticommute the annihilation operator $\hat{\psi}(\mathbf{y})$ next to the vacuum state $|0\rangle$ which then will be vanished. For the anticommutations, we use a standard result $\hat{A}\hat{B} = \left\{\hat{A},\hat{B}\right\} - \hat{B}\hat{A}$, which is readily proven by the definition of an anticommutator. During the anticommutation process, we obtain terms as follows

$$\begin{aligned}
& \hat{\psi}^{\dagger}(\mathbf{x})\underbrace{\hat{\psi}(\mathbf{y})\hat{\psi}^{\dagger}(\mathbf{x}_1)}_{\{\hat{\psi}(\mathbf{y}),\hat{\psi}^{\dagger}(\mathbf{x}_1)\}-\hat{\psi}^{\dagger}(\mathbf{x}_1)\hat{\psi}(\mathbf{y})}\ldots\hat{\psi}^{\dagger}(\mathbf{x}_N)|0\rangle \\
= \;& \hat{\psi}^{\dagger}(\mathbf{x})\left[\delta^{(3)}(\mathbf{y}-\mathbf{x}_1)|\mathbf{x}_2,\ldots,\mathbf{x}_N\rangle - \hat{\psi}^{\dagger}(\mathbf{x}_1)\underbrace{\hat{\psi}(\mathbf{y})\hat{\psi}^{\dagger}(\mathbf{x}_2)}_{\{\hat{\psi}(\mathbf{y}),\hat{\psi}^{\dagger}(\mathbf{x}_2)\}-\hat{\psi}^{\dagger}(\mathbf{x}_2)\hat{\psi}(\mathbf{y})}\ldots\hat{\psi}^{\dagger}(\mathbf{x}_N)|0\rangle\right] \\
= \;& \hat{\psi}^{\dagger}(\mathbf{x})\Big[\delta^{(3)}(\mathbf{y}-\mathbf{x}_1)|\mathbf{x}_2,\ldots,\mathbf{x}_N\rangle - \delta^{(3)}(\mathbf{y}-\mathbf{x}_2)|\mathbf{x}_1,\mathbf{x}_3,\ldots,\mathbf{x}_N\rangle \\
& \quad + (-1)^{k-1}|\mathbf{x}_1,\ldots,\mathbf{x}_{k-1},\mathbf{x}_{k+1},\ldots,\mathbf{x}_N\rangle + \ldots\Big] \\
= \;& \delta^{(3)}(\mathbf{y}-\mathbf{x}_1)|\mathbf{x},\mathbf{x}_2,\ldots,\mathbf{x}_N\rangle + \delta^{(3)}(\mathbf{y}-\mathbf{x}_2)|\mathbf{x}_1,\mathbf{x},\mathbf{x}_3\ldots,\mathbf{x}_N\rangle + \ldots \\
& \quad + \delta^{(3)}(\mathbf{y}-\mathbf{x}_k)|\mathbf{x},\ldots,\mathbf{x}_{k-1},\mathbf{x},\mathbf{x}_{k+1},\ldots,\mathbf{x}_N\rangle + \ldots \\
= \;& \sum_{k=1}^{N}\delta^{(3)}(\mathbf{y}-\mathbf{x}_k)|\mathbf{x},\ldots,\mathbf{x}_{k-1},\mathbf{x},\mathbf{x}_{k+1},\ldots,\mathbf{x}_N\rangle\,. \qquad (2.36)
\end{aligned}$$

---

[3] From Eqs. (2.7) and (2.8) we have $\langle n_i|n_j\rangle = \delta_{n_i,n_j}$ and $\sum_{n_i}|n_i\rangle\langle n_i| = \mathbb{1}$, and therefore

$$\sum_{n_i}\varphi_{n_i}(\mathbf{x})\varphi^*_{n_i}(\mathbf{x}') = \sum_{n_i}\langle\mathbf{x}|n_i\rangle\langle n_i|\mathbf{x}'\rangle = \langle\mathbf{x}|\mathbf{x}'\rangle = \delta^{(3)}(\mathbf{x}-\mathbf{x}').$$

Notice, how the minus signs vanish on the fourth line as we anticommute the creation operator $\hat{\psi}^\dagger(\mathbf{x})$ to the place corresponding to the minus signs on the third line. The density operator on coordinate $\mathbf{x}$ is defined as $n(\mathbf{x}) = \hat{\psi}^\dagger(\mathbf{x})\hat{\psi}(\mathbf{x})$, i.e., we get from Eq. (2.36) by replacing $\mathbf{y}$ with $\mathbf{x}$, and noticing that the deltafunction is an even distribution for which $\delta(x) = \delta(-x)$, a representation for the density operator in $N$-particle Hilbert space

$$n(\mathbf{x}) = \sum_{k=1}^{N} \delta^{(3)}(\mathbf{x}_k - \mathbf{x})\ . \tag{2.37}$$

We would then like to see how an operator describing, e.g., an external potential looks like when it is expressed in terms of the field operators. First we need to get back to Eqs. (2.30) and (2.31) shortly. For the operators that act in occupation number representation, we need to convert the definitions for the field operators as follows

$$\begin{aligned} \hat{a}_n^\dagger &= \sum_m \delta_{n,m}\hat{a}_m^\dagger = \sum_m \int \mathrm{d}\mathbf{x}\, \varphi_n(\mathbf{x})\varphi_m^*(\mathbf{x})\hat{a}_m^\dagger \\ &= \int \mathrm{d}\mathbf{x}\, \varphi_n(\mathbf{x}) \sum_m \varphi_m^*(\mathbf{x})\hat{a}_m^\dagger \\ &= \int \mathrm{d}\mathbf{x}\, \varphi_n(\mathbf{x})\hat{\psi}^\dagger(\mathbf{x})\ , \end{aligned} \tag{2.38}$$

and

$$\begin{aligned} \hat{a}_n &= \sum_m \delta_{n,m}\hat{a}_m = \sum_m \int \mathrm{d}\mathbf{x}\, \varphi_m(\mathbf{x})\varphi_n^*(\mathbf{x})\hat{a}_m \\ &= \int \mathrm{d}\mathbf{x}\, \varphi_n^*(\mathbf{x}) \sum_m \varphi_m(\mathbf{x})\hat{a}_m \\ &= \int \mathrm{d}\mathbf{x}\, \varphi_n^*(\mathbf{x})\hat{\psi}(\mathbf{x})\ . \end{aligned} \tag{2.39}$$

Then we consider an external (spin-independent) potential $u(\mathbf{r})$. As this is expressed in coordinate representation, we may give an expression in occupation number representation via the field operators

$$\hat{U} = \int \mathrm{d}\mathbf{x}\, u(\mathbf{r})\hat{\psi}^\dagger(\mathbf{x})\hat{\psi}(\mathbf{x}) = \int \mathrm{d}\mathbf{x}\, u(\mathbf{r})\hat{n}(\mathbf{x})\ . \tag{2.40}$$

The operator $\hat{U}$ is *hermitean*, i.e.,

$$\hat{U}^\dagger = \left[\int \mathrm{d}\mathbf{x}\, u(\mathbf{r})\hat{\psi}^\dagger(\mathbf{x})\hat{\psi}(\mathbf{x})\right]^\dagger = \int \mathrm{d}\mathbf{x}\, u(\mathbf{r})\hat{\psi}^\dagger(\mathbf{x})\hat{\psi}(\mathbf{x}) = \hat{U}\ , \tag{2.41}$$

because for arbitrary operators $\hat{A}$ and $\hat{B}$ we have $(\hat{A}\hat{B})^\dagger = \hat{B}^\dagger\hat{A}^\dagger$, and $(\hat{A}^\dagger)^\dagger = \hat{A}$. Then consider an action to an $N$-particle state such that

$$\begin{aligned}
\hat{U}\Psi(\mathbf{x}_1,\ldots,\mathbf{x}_N) &= \langle \mathbf{x}_N,\ldots,\mathbf{x}_1|\hat{U}|\Psi\rangle = \langle\Psi|\hat{U}^\dagger|\mathbf{x}_1,\ldots,\mathbf{x}_N\rangle^* \\
&= \int \mathrm{d}\mathbf{x}\, u(\mathbf{r})\langle\Psi|\hat{n}(\mathbf{x})|\mathbf{x}_1,\ldots,\mathbf{x}_N\rangle^* \\
&= \int \mathrm{d}\mathbf{x}\, u(\mathbf{r})\langle\Psi|\sum_{k=1}^{N}\delta^{(3)}(\mathbf{x}_k-\mathbf{x})|\mathbf{x}_1,\ldots,\mathbf{x}_N\rangle^* \\
&= \int \mathrm{d}\mathbf{x}\, u(\mathbf{r})\sum_{k=1}^{N}\delta^{(3)}(\mathbf{x}_k-\mathbf{x})\langle\Psi|\mathbf{x}_1,\ldots,\mathbf{x}_N\rangle^* \\
&= \sum_{k=1}^{N} u(\mathbf{r}_k)\Psi(\mathbf{x}_1,\ldots,\mathbf{x}_N)\,, \qquad (2.42)
\end{aligned}$$

where, on third line, we used Eq. (2.37). The expression in Eq. (2.42) is exactly the action of an external potential $u(\mathbf{r})$ in coordinate representation. This means that the definition in Eq. (2.40) for the operator $\hat{U}$ is indeed the correct one.

We can similarly show that an operator for kinetic energy

$$\hat{T} = -\frac{\hbar^2}{2m}\int \mathrm{d}\mathbf{x}\,\hat{\psi}^\dagger(\mathbf{x})\nabla^2\hat{\psi}(\mathbf{x}) \qquad (2.43)$$

is hermitean because for any arbitrary states $|\chi\rangle$ and $|\phi\rangle$ we have

$$\begin{aligned}
\langle\chi|\hat{T}|\phi\rangle &= -\frac{\hbar^2}{2m}\int \mathrm{d}\mathbf{x}\,\langle\chi|\hat{\psi}^\dagger(\mathbf{x})\nabla^2\hat{\psi}(\mathbf{x})|\phi\rangle \\
&= -\frac{\hbar^2}{2m}\int \mathrm{d}\mathbf{x}\,\langle\phi|[\hat{\psi}^\dagger(\mathbf{x})\nabla^2\hat{\psi}(\mathbf{x})]^\dagger|\chi\rangle^* \\
&= -\frac{\hbar^2}{2m}\int \mathrm{d}\mathbf{x}\,\langle\phi|\nabla^2\hat{\psi}^\dagger(\mathbf{x})\hat{\psi}(\mathbf{x})|\chi\rangle^* \\
&= -\frac{\hbar^2}{2m}\int \mathrm{d}\mathbf{x}\,\langle\phi|\hat{\psi}^\dagger(\mathbf{x})\nabla^2\hat{\psi}(\mathbf{x})|\chi\rangle^* \\
&= \langle\phi|\hat{T}|\chi\rangle^*\,, \qquad (2.44)
\end{aligned}$$

where, on fourth line, we used integration by parts. We assume that the boundary terms vanish because of the properties of the field operators. Eq. (2.44) tells us that $\hat{T} = \hat{T}^\dagger$. Furthermore, by considering an action to an $N$-particle state, we get

$$\begin{aligned}
\hat{T}\Psi(\mathbf{x}_1,\ldots,\mathbf{x}_N) &= \langle \mathbf{x}_N,\ldots,x_1|\hat{T}|\Psi\rangle = \langle\Psi|\hat{T}^\dagger|\mathbf{x}_1,\ldots,\mathbf{x}_N\rangle^* \\
&= -\frac{\hbar^2}{2m}\int d\mathbf{x}\,\langle\Psi|\hat{\psi}^\dagger(\mathbf{x})\nabla^2\hat{\psi}(\mathbf{x})|\mathbf{x}_1,\ldots,\mathbf{x}_N\rangle^* \\
&= -\frac{\hbar^2}{2m}\int d\mathbf{x}\,\langle\Psi|\hat{\psi}^\dagger(\mathbf{x})\nabla^2_{\mathbf{y}}\hat{\psi}(\mathbf{y})|\mathbf{x}_1,\ldots,\mathbf{x}_N\rangle^*_{\mathbf{y}=\mathbf{x}} \\
&= -\frac{\hbar^2}{2m}\int d\mathbf{x}\,\langle\Psi|\nabla^2_{\mathbf{y}}\hat{\psi}^\dagger(\mathbf{x})\hat{\psi}(\mathbf{y})|\mathbf{x}_1,\ldots,\mathbf{x}_N\rangle^*_{\mathbf{y}=\mathbf{x}} \\
&= -\frac{\hbar^2}{2m}\int d\mathbf{x}\,\langle\Psi|\nabla^2_{\mathbf{y}}\sum_{k=1}^{N}\delta^{(3)}(\mathbf{x}_k-\mathbf{y})|\mathbf{x}_1,\ldots,\mathbf{x}_{k-1},\mathbf{x},\mathbf{x}_{k+1},\ldots,\mathbf{x}_N\rangle^*_{\mathbf{y}=\mathbf{x}} \\
&= -\frac{\hbar^2}{2m}\sum_{k=1}^{N}\int d\mathbf{x}\,\delta^{(3)}(\mathbf{x}_k-\mathbf{x})\nabla^2_{\mathbf{x}}\Psi(\mathbf{x}_1,\ldots,\mathbf{x}_{k-1},\mathbf{x},\mathbf{x}_{k+1},\ldots,\mathbf{x}_N) \\
&= -\frac{\hbar^2}{2m}\sum_{k=1}^{N}\nabla^2_{\mathbf{x}_k}\Psi(\mathbf{x}_1,\ldots,\mathbf{x}_N)\,, \qquad (2.45)
\end{aligned}$$

and we used Eq. (2.36) on fifth line. Eq. (2.45) gives us exactly the corresponding action in coordinate representation. Also in here we may confirm that the definition for the operator $\hat{T}$ in Eq. (2.43) gives the correct result.

Finally we would like to think of two-particle interactions such as

$$\hat{V} = \frac{1}{2}\sum_{i\neq j} v(\mathbf{r}_i,\mathbf{r}_j)\,, \qquad (2.46)$$

with a simple property

$$\hat{V}|\mathbf{x}_1,\ldots,\mathbf{x}_N\rangle = \frac{1}{2}\sum_{i\neq j} v(\mathbf{r}_i,\mathbf{r}_j)|\mathbf{x}_1,\ldots,\mathbf{x}_N\rangle\,. \qquad (2.47)$$

We will now manipulate the expression in Eq. (2.46) as follows

$$\begin{aligned}
\hat{V} &= \frac{1}{2}\sum_{i\neq j} v(\mathbf{r}_i,\mathbf{r}_j) = \frac{1}{2}\left[\sum_{i,j=1}^{N} v(\mathbf{r}_i,\mathbf{r}_j) - \sum_{i=1}^{N} v(\mathbf{r}_i,\mathbf{r}_i)\right] \\
&= \frac{1}{2}\int \mathrm{d}\mathbf{x} \int \mathrm{d}\mathbf{x}' \overbrace{\sum_{i=1}^{N}\delta^{(3)}(\mathbf{x}-\mathbf{x}_i)}^{=\hat{n}(\mathbf{x})} \underbrace{\sum_{j=1}^{N}\delta^{(3)}(\mathbf{x}'-\mathbf{x}_j)}_{=\hat{n}(\mathbf{x}')}\, v(\mathbf{r},\mathbf{r}') \\
&- \frac{1}{2}\int \mathrm{d}\mathbf{x} \underbrace{\sum_{i=1}^{N}\delta^{(3)}(\mathbf{x}-\mathbf{x}_i)}_{=\hat{n}(\mathbf{x})}\, v(\mathbf{r},\mathbf{r}) \\
&= \frac{1}{2}\Big[\int \mathrm{d}\mathbf{x} \int \mathrm{d}\mathbf{x}'\, \hat{n}(\mathbf{x})\hat{n}(\mathbf{x}')v(\mathbf{r},\mathbf{r}') - \underbrace{\int \mathrm{d}\mathbf{x}\, \hat{n}(\mathbf{x})v(\mathbf{r},\mathbf{r})}_{=\int \mathrm{d}\mathbf{x} \int \mathrm{d}\mathbf{x}'\, \delta^{(3)}(\mathbf{x}-\mathbf{x}')\hat{n}(\mathbf{x})v(\mathbf{r},\mathbf{r}')}\Big] \\
&= \frac{1}{2}\int \mathrm{d}\mathbf{x} \int \mathrm{d}\mathbf{x}'\, v(\mathbf{r},\mathbf{r}')\left[\hat{n}(\mathbf{x})\hat{n}(\mathbf{x}') - \delta^{(3)}(\mathbf{x}-\mathbf{x}')\hat{n}(\mathbf{x})\right] . \qquad (2.48)
\end{aligned}$$

Then, by considering an expression

$$\begin{aligned}
\hat{\psi}^{\dagger}(\mathbf{x})\hat{\psi}^{\dagger}(\mathbf{x}')\underbrace{\hat{\psi}(\mathbf{x}')\hat{\psi}(\mathbf{x})}_{=-\hat{\psi}(\mathbf{x})\hat{\psi}(\mathbf{x}')} &= -\hat{\psi}^{\dagger}(\mathbf{x})\underbrace{\hat{\psi}^{\dagger}(\mathbf{x}')\hat{\psi}(\mathbf{x})}_{=\delta^{(3)}(\mathbf{x}'-\mathbf{x})-\hat{\psi}(\mathbf{x})\hat{\psi}^{\dagger}(\mathbf{x}')}\hat{\psi}(\mathbf{x}') \\
&= -\hat{\psi}^{\dagger}(\mathbf{x})\left[\delta^{(3)}(\mathbf{x}'-\mathbf{x}) - \hat{\psi}(\mathbf{x})\hat{\psi}^{\dagger}(\mathbf{x}')\right]\hat{\psi}(\mathbf{x}') \\
&= \hat{\psi}^{\dagger}(\mathbf{x})\hat{\psi}(\mathbf{x})\hat{\psi}^{\dagger}(\mathbf{x}')\hat{\psi}(\mathbf{x}') - \delta^{(3)}(\mathbf{x}'-\mathbf{x})\hat{\psi}^{\dagger}(\mathbf{x})\hat{\psi}(\mathbf{x}') \\
&= \hat{n}(\mathbf{x})\hat{n}(\mathbf{x}') - \delta^{(3)}(\mathbf{x}',\mathbf{x})\hat{n}(\mathbf{x}) , \qquad (2.49)
\end{aligned}$$

we see that this is exactly the same as in Eq. (2.48). Hence, we have

$$\hat{V} = \frac{1}{2}\int \mathrm{d}\mathbf{x} \int \mathrm{d}\mathbf{x}'\, v(\mathbf{r},\mathbf{r}')\hat{\psi}^{\dagger}(\mathbf{x})\hat{\psi}^{\dagger}(\mathbf{x}')\hat{\psi}(\mathbf{x}')\hat{\psi}(\mathbf{x}) . \qquad (2.50)$$

We are now ready to give an expression for a Hamiltonian $\hat{H} = \hat{T} + \hat{U} + \hat{V}$ in terms of the field operators, i.e., the Hamiltonian in second quantization

$$\hat{H} = \int \mathrm{d}\mathbf{x}\, \hat{\psi}^{\dagger}(\mathbf{x})\left[-\frac{\hbar^2}{2m}\nabla^2 + u(\mathbf{r})\right]\hat{\psi}(\mathbf{x}) + \frac{1}{2}\int \mathrm{d}\mathbf{x} \int \mathrm{d}\mathbf{x}'\, v(\mathbf{r},\mathbf{r}')\hat{\psi}^{\dagger}(\mathbf{x})\hat{\psi}^{\dagger}(\mathbf{x}')\hat{\psi}(\mathbf{x}')\hat{\psi}(\mathbf{x}) \qquad (2.51)$$

The Hamiltonian in Eq. (2.51) can also be expressed in a general basis (e.g. occupation number representation) by using Eqs. (2.30) and (2.31) as

$$\hat{H} = \sum_{i,j} h_{ij}\hat{a}_i^{\dagger}\hat{a}_j + \frac{1}{2}\sum_{i,j,k,l} v_{ijkl}\hat{a}_i^{\dagger}\hat{a}_j^{\dagger}\hat{a}_k\hat{a}_l , \qquad (2.52)$$

where we defined

$$h_{ij} = \int \mathrm{d}\mathbf{x}\, \varphi_i^{*}(\mathbf{x})\left[-\frac{\hbar^2}{2m}\nabla^2 + u(\mathbf{r})\right]\varphi_j(\mathbf{x}) \qquad (2.53)$$

and

$$v_{ijkl} = \int \mathrm{d}\mathbf{x} \int \mathrm{d}\mathbf{x}'\, v(\mathbf{r},\mathbf{r}')\varphi_i^*(\mathbf{x})\varphi_j^*(\mathbf{x}')\varphi_k(\mathbf{x}')\varphi_l(\mathbf{x}) \,. \tag{2.54}$$

The expressions for the Hamiltonian in Eqs. (2.51) and (2.52) become very useful when we study some applications of many-particle systems next and also later, in Chap. 5.

### 2.1.3 Field operators and time-evolution

The field operators, introduced in Eqs. (2.30) and (2.31), play a very important role in many-particle physics. Especially, when doing perturbation theory, we study quantum systems and operators via various *pictures*. These pictures relate to time-dependent phenomena: while in one picture the operators are time-independent, in another picture they are time-independent. These concepts are discussed more in detail in the next chapter when doing many-particle perturbation theory.

Now we are mostly interested in a case where the field operators are time-dependent, the so-called Heisenberg picture. The operators in Heisenberg picture, with subscript '$H$', satisfy the equations of motion

$$\partial_t \hat{O}_H(t) = -\frac{\mathrm{i}}{\hbar}\left[\hat{O}_H(t), \hat{H}(t)\right] , \tag{2.55}$$

where the Hamiltonian $\hat{H}(t) = \hat{T}(t) + \hat{U}(t) + \hat{V}(t)$ is split into three pieces. The different pieces of the Hamiltonian are now used in their second quantized forms in Eqs. (2.40), (2.43) and (2.50) – only with the field operators being in Heisenberg picture. We first study the equations of motion for the creation operator $\hat{\psi}_H^\dagger$. Before evaluating the commutator in Eq. (2.55), we make shorthand notations $\hat{A} = \hat{\psi}_H(\mathbf{y},t)$ and $\hat{B} = \hat{\psi}_H^\dagger(\mathbf{y},t)\left(-\frac{\hbar^2}{2m}\nabla_\mathbf{y}^2 + u(\mathbf{r_y},t)\right)$. With these notations we have for the commutator

$$\begin{aligned}
\left[\hat{\psi}_H^\dagger(\mathbf{x},t), \hat{T}(t)+\hat{U}(t)\right] &= \hat{\psi}_H^\dagger(\mathbf{x},t)\int \mathrm{d}\mathbf{y}\, \hat{\psi}_H^\dagger(\mathbf{y},t)\left(-\frac{\hbar^2}{2m}\nabla_\mathbf{y}^2 + u(\mathbf{r_y},t)\right)\hat{\psi}_H(\mathbf{y},t) \\
&- \int \mathrm{d}\mathbf{y}\, \hat{\psi}_H^\dagger(\mathbf{y},t)\left(-\frac{\hbar^2}{2m}\nabla_\mathbf{y}^2 + u(\mathbf{r_y},t)\right)\hat{\psi}_H(\mathbf{y},t)\hat{\psi}_H^\dagger(\mathbf{x},t) \\
&= \int \mathrm{d}\mathbf{y}\, \left[\hat{\psi}_H^\dagger(\mathbf{x},t), \hat{B}\hat{A}\right] \,.
\end{aligned} \tag{2.56}$$

This is easy to evaluate by using a relation $\left[\hat{C},\hat{B}\hat{A}\right] = \left\{\hat{C},\hat{B}\right\}\hat{A} - \hat{B}\left\{\hat{C},\hat{A}\right\}$. By this manner we need to calculate two anticommutators instead. For the first one we have

$$\begin{aligned}
\left\{\hat{\psi}_H^\dagger(\mathbf{x},t), \hat{B}\right\} &= \hat{\psi}_H^\dagger(\mathbf{x},t)\hat{\psi}_H^\dagger(\mathbf{y},t)\left(-\frac{\hbar^2}{2m}\nabla_\mathbf{y}^2 + u(\mathbf{r_y},t)\right) + \hat{\psi}_H^\dagger(\mathbf{y},t)\left(-\frac{\hbar^2}{2m}\nabla_\mathbf{y}^2 + u(\mathbf{r_y},t)\right)\hat{\psi}_H^\dagger(\mathbf{x},t) \\
&= u(\mathbf{r_y},t)\left\{\hat{\psi}_H^\dagger(\mathbf{x},t), \hat{\psi}_H^\dagger(\mathbf{y},t)\right\} - \frac{\hbar^2}{2m}\left\{\hat{\psi}_H^\dagger(\mathbf{x},t), \hat{\psi}_H^\dagger(\mathbf{y},t)\right\} \\
&= 0 \,,
\end{aligned} \tag{2.57}$$

and for the second one

$$\left\{\hat{\psi}_H^\dagger(\mathbf{x},t), \hat{A}\right\} = \left\{\hat{\psi}_H^\dagger(\mathbf{x},t), \hat{\psi}_H^\dagger(\mathbf{y},t)\right\} = \delta^{(3)}(\mathbf{x}-\mathbf{y}) \,. \tag{2.58}$$

Inserting Eqs. (2.57) and (2.58) back into Eq. (2.56) we obtain

$$\begin{aligned}\left[\hat{\psi}_H^\dagger(\mathbf{x},t),\hat{T}(t)+\hat{U}(t)\right] &= -\int d\mathbf{y}\,\hat{\psi}_H^\dagger(\mathbf{y},t)\left(-\frac{\hbar^2}{2m}\nabla_{\mathbf{y}}^2+u(\mathbf{r}_{\mathbf{y}},t)\right)\delta^{(3)}(\mathbf{x}-\mathbf{y}) \\ &= -\left(-\frac{\hbar^2}{2m}\nabla_{\mathbf{x}}^2+u(\mathbf{r}_{\mathbf{x}},t)\right)\hat{\psi}_H^\dagger(\mathbf{x},t)\ . \qquad (2.59)\end{aligned}$$

Similarly, we evaluate the commutator $\left[\hat{\psi}_H^\dagger(\mathbf{x},t),\hat{V}(t)\right]$ by first introducing the following notations: $\hat{A}=\hat{\psi}_H^\dagger(\mathbf{y},t)\hat{\psi}_H^\dagger(\mathbf{y}',t)$ and $\hat{B}=\hat{\psi}_H(\mathbf{y}',t)\hat{\psi}_H(\mathbf{y},t)$. This way we have

$$\begin{aligned}\left[\hat{\psi}_H^\dagger(\mathbf{x},t),\hat{V}(t)\right] &= \hat{\psi}_H^\dagger(\mathbf{x},t)\frac{1}{2}\int d\mathbf{y}\int d\mathbf{y}'\,v(\mathbf{r}_{\mathbf{y}},\mathbf{r}_{\mathbf{y}'},t)\hat{\psi}_H^\dagger(\mathbf{y},t)\hat{\psi}_H^\dagger(\mathbf{y}',t)\hat{\psi}_H(\mathbf{y}',t)\hat{\psi}_H(\mathbf{y},t) \\ &- \frac{1}{2}\int d\mathbf{y}\int d\mathbf{y}'\,v(\mathbf{r}_{\mathbf{y}},\mathbf{r}_{\mathbf{y}'},t)\hat{\psi}_H^\dagger(\mathbf{y},t)\hat{\psi}_H^\dagger(\mathbf{y}',t)\hat{\psi}_H(\mathbf{y}',t)\hat{\psi}_H(\mathbf{y},t)\hat{\psi}_H^\dagger(\mathbf{x},t) \\ &= \frac{1}{2}\int d\mathbf{y}\int d\mathbf{y}'\,\left[\hat{\psi}_H^\dagger(\mathbf{x},t),\hat{A}\hat{B}\right]v(\mathbf{r}_{\mathbf{y}},\mathbf{r}_{\mathbf{y}'},t)\ . \qquad (2.60)\end{aligned}$$

Then we use a relation $\left[\hat{C},\hat{A}\hat{B}\right]=\left[\hat{C},\hat{A}\right]\hat{B}+\hat{A}\left[\hat{C},\hat{B}\right]$ to calculate the commutator in the integrand. For the first part we have

$$\begin{aligned}\left[\hat{\psi}_H^\dagger(\mathbf{x},t),\hat{\psi}_H^\dagger(\mathbf{y},t)\hat{\psi}_H^\dagger(\mathbf{y}',t)\right] &= \hat{\psi}_H^\dagger(\mathbf{x},t)\hat{\psi}_H^\dagger(\mathbf{y},t)\hat{\psi}_H^\dagger(\mathbf{y}',t)-\hat{\psi}_H^\dagger(\mathbf{y},t)\hat{\psi}_H^\dagger(\mathbf{y}',t)\hat{\psi}_H^\dagger(\mathbf{x},t) \\ &= 0\ , \qquad (2.61)\end{aligned}$$

which gives simply zero because an even number (two) of anticommutations is needed for the other term become identical to another. For the second part of the commutator in Eq. (2.60) we have both creation and annihilation operators, hence, the anticommutations involving deltafunctions require a little more book keeping:

$$\begin{aligned}&\left[\hat{\psi}_H^\dagger(\mathbf{x},t),\hat{\psi}_H(\mathbf{y}',t)\hat{\psi}_H(\mathbf{y},t)\right] \\ &= \underbrace{\hat{\psi}_H^\dagger(\mathbf{x},t)\hat{\psi}_H(\mathbf{y}',t)}_{=\delta^{(3)}(\mathbf{x}-\mathbf{y}')-\hat{\psi}_H(\mathbf{y}',t)\hat{\psi}_H^\dagger(\mathbf{x},t)}\hat{\psi}_H(\mathbf{y},t)-\hat{\psi}_H(\mathbf{y}',t)\hat{\psi}_H(\mathbf{y},t)\hat{\psi}_H^\dagger(\mathbf{x},t) \\ &= \delta^{(3)}(\mathbf{x}-\mathbf{y}')\hat{\psi}_H(\mathbf{y},t)-\hat{\psi}_H(\mathbf{y}',t)\underbrace{\hat{\psi}_H^\dagger(\mathbf{x},t)\hat{\psi}_H(\mathbf{y},t)}_{=\delta^{(3)}(\mathbf{x}-\mathbf{y})-\hat{\psi}_H(\mathbf{y},t)\hat{\psi}_H^\dagger(\mathbf{x},t)}-\hat{\psi}_H(\mathbf{y}',t)\hat{\psi}_H(\mathbf{y},t)\hat{\psi}_H^\dagger(\mathbf{x},t) \\ &= \delta^{(3)}(\mathbf{x}-\mathbf{y}')\hat{\psi}_H(\mathbf{y},t)-\hat{\psi}_H(\mathbf{y}',t)\delta^{(3)}(\mathbf{x}-\mathbf{y})\ . \qquad (2.62)\end{aligned}$$

By substituting Eqs. (2.61) and (2.62) into Eq. (2.60) we get

$$\begin{aligned}&\left[\hat{\psi}_H^\dagger(\mathbf{x},t),\hat{V}(t)\right] \\ &= \frac{1}{2}\int d\mathbf{y}\int d\mathbf{y}'\,\hat{\psi}_H^\dagger(\mathbf{y},t)\hat{\psi}_H^\dagger(\mathbf{y}',t)\left[\delta^{(3)}(\mathbf{x}-\mathbf{y}')\hat{\psi}_H(\mathbf{y},t)-\hat{\psi}_H(\mathbf{y}',t)\delta^{(3)}(\mathbf{x}-\mathbf{y})\right]v(\mathbf{r}_{\mathbf{y}},\mathbf{r}_{\mathbf{y}'},t) \\ &= \frac{1}{2}\int d\mathbf{y}\,v(\mathbf{r}_{\mathbf{y}},\mathbf{r},t)\underbrace{\hat{\psi}_H^\dagger(\mathbf{y},t)\hat{\psi}_H^\dagger(\mathbf{x},t)}_{=-\hat{\psi}_H^\dagger(\mathbf{x},t)\hat{\psi}_H^\dagger(\mathbf{y},t)}\hat{\psi}_H(\mathbf{y},t)-\frac{1}{2}\int d\mathbf{y}'\,v(\mathbf{r},\mathbf{r}_{\mathbf{y}'},t)\hat{\psi}_H^\dagger(\mathbf{x},t)\hat{\psi}_H^\dagger(\mathbf{y}',t)\hat{\psi}_H(\mathbf{y}',t) \\ &= -\int d\mathbf{x}'\,v(\mathbf{r},\mathbf{r}',t)\hat{\psi}_H^\dagger(\mathbf{x},t)\hat{\psi}_H^\dagger(\mathbf{x}',t)\hat{\psi}_H(\mathbf{x}',t)\ . \qquad (2.63)\end{aligned}$$

Overall, we have for the equation of motion for the field operator $\hat{\psi}_H^\dagger$ from Eqs. (2.55), (2.59) and (2.63)

$$\begin{aligned} -\mathrm{i}\hbar\partial_t\hat{\psi}_H^\dagger(\mathbf{x},t) &= \left[\hat{\psi}_H^\dagger(\mathbf{x},t),\hat{H}(t)\right] \\ &= \left[-\frac{\hbar^2}{2m}\nabla^2+u(\mathbf{r},t)\right]\hat{\psi}_H^\dagger(\mathbf{x},t)+\int\mathrm{d}\mathbf{x}'\,v(\mathbf{r},\mathbf{r}')\hat{\psi}_H^\dagger(\mathbf{x},t)\hat{\psi}_H^\dagger(\mathbf{x}',t)\hat{\psi}_H(\mathbf{x}',t)\,. \quad (2.64)\end{aligned}$$

The adjoint of Eq. (2.64), i.e., the equation of motion for the field operator $\hat{\psi}_H$ can be derived similarly, and for that we have

$$\mathrm{i}\hbar\partial_t\hat{\psi}_H(\mathbf{x},t)=\left[-\frac{\hbar^2}{2m}\nabla^2+u(\mathbf{r},t)\right]\hat{\psi}_H(\mathbf{x},t)+\int\mathrm{d}\mathbf{x}'\,v(\mathbf{r},\mathbf{r}')\hat{\psi}_H^\dagger(\mathbf{x}',t)\hat{\psi}_H(\mathbf{x}',t)\hat{\psi}_H(\mathbf{x},t)\,. \quad (2.65)$$

The equations of motion for the field operators in Eqs. (2.64) and (2.65) turn out to be useful when we consider many-particle dynamics in the next chapter.

### 2.1.4 Hubbard model

We now introduce some simple models with second quantized Hamiltonians for electrons. The Hubbard model, named after John Hubbard [16], is a model of interacting electrons in a lattice. The Hubbard-model Hamiltonian contains only two terms: a kinetic term allowing for hopping of electrons between different sites of the lattice and a potential term consisting of an on-site interaction. Hubbard-model Hamiltonian can therefore be written as $\hat{H}=\hat{H}_0+\hat{U}$ with

$$\begin{aligned} \hat{H}_0 &= \sum_{i,j,\sigma} t_{ij}\hat{a}_{i,\sigma}^\dagger\hat{a}_{j,\sigma} \quad (2.66)\\ \hat{U} &= \sum_i u_i\hat{n}_{i,+}\hat{n}_{i,-}\,, \quad (2.67)\end{aligned}$$

where $\hat{n}_{i,\sigma}=\hat{a}_{i,\sigma}^\dagger\hat{a}_{i,\sigma}$ with $\sigma\in\{+,-\}$. The matrix element $t_{ij}$ is the hopping probability between different sites. We consider hoppings only between sequential sites, i.e., the hopping probability is taken to be $t_{ij}=-t$ for nearest neighbours (for which $|i-j|=1$) and $t_{ij}=0$ otherwise. We will then, as an example, restrict ourselves to a molecule with two sites. These sites are described in energy eigenbasis as the highest occupied molecular orbital (HOMO) and the lowest unoccupied molecular orbital (LUMO). The expression for the non-interacting part of the Hamiltonian in Eq. (2.66) is in so-called site basis, i.e., we are adding (removing) electrons to (from) a particular site of a lattice. We would like the Hamiltonian to be of the form that we add and remove electrons to and from a corresponding energy level. For this purpose, we write the non-interacting part of the Hamiltonian $\hat{H}_0$ as

$$\hat{H}_0=-t\sum_\sigma\left(\hat{a}_{1,\sigma}^\dagger\hat{a}_{2,\sigma}+\hat{a}_{2,\sigma}^\dagger\hat{a}_{1,\sigma}\right)\,. \quad (2.68)$$

In matrix form Eq. (2.68) is

$$\left(\hat{H}_0\right)_{ij}=\begin{pmatrix}0 & -t\\ -t & 0\end{pmatrix}\,, \quad (2.69)$$

for which we have eigenvalues and the corresponding eigenvectors

$$\epsilon_{1,2}=\pm t \qquad \varphi_{1,2}=\frac{1}{\sqrt{2}}(1,\pm 1)\,. \quad (2.70)$$

From the eigenvectors in Eq. (2.70) we can construct a unitary matrix which has the eigenvectors as column vectors

$$U_{ij} = \frac{1}{\sqrt{2}} \begin{pmatrix} 1 & 1 \\ 1 & -1 \end{pmatrix} . \tag{2.71}$$

This transformation now takes us from the site basis to the energy eigenbasis by

$$\hat{b}^{\dagger}_{i,\sigma} = \sum_{j=1}^{2} U_{ij} \hat{a}^{\dagger}_{j,\sigma} \tag{2.72}$$

$$\hat{b}_{i,\sigma} = \sum_{j=1}^{2} U_{ji} \hat{a}_{j,\sigma} , \tag{2.73}$$

where the new creation and annihilation operators ($\hat{b}^{\dagger}$ and $\hat{b}$) now add and remove electrons to and from the corresponding energy levels, and we furthermore have $i \in \{H, L\}$. We will then take the energy gap between the HOMO and the LUMO levels to be $\Delta_0$, i.e., we have the energies

$$\epsilon_1 = \xi_H \qquad \epsilon_2 = \xi_H + \Delta_0 . \tag{2.74}$$

The non-interacting part of the Hubbard-model Hamiltonian in energy eigenbasis is then

$$\begin{aligned} \hat{H}_0 &= \xi_H \hat{b}^{\dagger}_H \hat{b}_H + (\xi_H + \Delta_0) \hat{b}^{\dagger}_L \hat{b}_L \\ &= \xi_H \hat{n}_H + (\xi_H + \Delta_0) \hat{n}_L , \end{aligned} \tag{2.75}$$

where we have $\hat{b}^{(\dagger)}_{H/L} = \hat{b}^{(\dagger)}_{H/L,+} + \hat{b}^{(\dagger)}_{H/L,-}$. The interacting part of the Hubbard-model Hamiltonian can also be expressed in the energy eigenbasis. We only need to consider the interactions between the electrons that occupy the molecular orbitals. We take the interaction between the electrons within the same molecular orbital to be $U_0$, and the interaction between the electrons in different molecular orbitals to be $U_{HL}$. With these values, we can write the interacting part as

$$\begin{aligned} \hat{U} &= U_0 \left( \hat{b}^{\dagger}_{H,+} \hat{b}_{H,+} \hat{b}^{\dagger}_{H,-} \hat{b}_{H,-} + \hat{b}^{\dagger}_{L,+} \hat{b}_{L,+} \hat{b}^{\dagger}_{L,-} \hat{b}_{L,-} \right) + U_{HL} \hat{b}^{\dagger}_H \hat{b}_H \hat{b}^{\dagger}_L \hat{b}_L \\ &= U_0 \left( \hat{n}_H + \hat{n}_L \right) + U_{HL} \hat{n}_H \hat{n}_L . \end{aligned} \tag{2.76}$$

It is essential to note that, as

$$\hat{b}^{(\dagger)}_{H/L,\sigma} = \frac{1}{\sqrt{2}} \left( \hat{a}^{(\dagger)}_{1,\sigma} \pm \hat{a}^{(\dagger)}_{2,\sigma} \right) , \tag{2.77}$$

also the operators in the energy eigenbasis obey the fermionic operator algebra. With this information we see that it is not possible to have two identical electrons occupying the same energy level: their spin must be different at least.

### 2.1.5 Tight-binding approximation

The model of tight binding (TB) is actually a generalization of the non-interacting part of the Hubbard model in the previous section. TB approximation is mainly used to calculate the electronic band structures by using an approximate set of wave functions. These wave functions are constructed by superposition princinple from isolated atoms located at each atomic site.

For the TB approximation we do not take any interactions between the atomic sites into account but consider only the hopping term. We are also consdering hoppings between nearest neighbours, and then the TB hamiltonian reads

$$\hat{H} = -t \sum_{\sigma} \sum_{j=1}^{N-1} \left( \hat{c}^{\dagger}_{j,\sigma} \hat{c}_{j+1,\sigma} + \hat{c}^{\dagger}_{j+1,\sigma} \hat{c}_{j,\sigma} \right) , \tag{2.78}$$

where the creation and annihilation operators $\hat{c}^{\dagger}$ and $\hat{c}$ are represented in the site basis. As we did for the Hubbard model earlier, also these operators can be expressed in the energy eigenbasis (with operators $\hat{d}$). For an $N$-site TB chain, this calculation is done later in Chap. 5.

## 2.2 Propagators

We introduce the concept of propagators, i.e., Green's functions by considering a concrete example.

Let us study a free (non-relativistic) particle located in $\mathbf{x} = \mathbf{x}_i$ at time $t = t_i$. The mass of the particle is assumed to be constant $m$. The wavefunction corresponding to this particle, in position representation, is

$$\psi(\mathbf{x}_i, t_i) = \langle \mathbf{x} | \psi(t_i) \rangle = \delta^{(3)}(\mathbf{x} - \mathbf{x}_i) . \tag{2.79}$$

Then we try to find the time evolution of the wavefunction $\psi$ for $t_f > t_i$, i.e., compute $\langle \mathbf{x} | \psi(t_f) \rangle$. We have an operation which transforms the initial state at $t_i$ to a final state at time $t_f$

$$|\psi(t_f)\rangle = \mathrm{e}^{-\frac{\mathrm{i}}{\hbar}\hat{H}(t_f - t_i)} |\psi(\mathbf{x}_i, t_i)\rangle , \tag{2.80}$$

which is called time-evolution operator. We will give a proper introduction later, and now we will simply use it as a tool. We may take a projection of Eq. (2.80) to a final state in position space as

$$\langle \mathbf{x}_f | \psi(t_f) \rangle = \langle \mathbf{x}_f | \mathrm{e}^{-\frac{\mathrm{i}}{\hbar}\hat{H}(t_f - t_i)} | \psi(\mathbf{x}_i, t_i) \rangle . \tag{2.81}$$

Since we know the expression for a free-particle's Hamiltonian in momentum space, we perform a change of basis by inserting a unit operator in the following form

$$\mathbb{1} = \int \mathrm{d}\mathbf{p} \, |\mathbf{p}\rangle\langle\mathbf{p}| . \tag{2.82}$$

We also know the relation between position space and momentum space vectors to be

$$\langle \mathbf{x} | \mathbf{p} \rangle = \frac{1}{(2\pi\hbar)^{3/2}} \mathrm{e}^{\frac{\mathrm{i}}{\hbar}\mathbf{p}\cdot\mathbf{x}} , \tag{2.83}$$

and the complex conjugate of Eq. (2.83) simply gives the inner product the other way around. With this information we can rewrite Eq. (2.81) as

$$\begin{aligned} \langle \mathbf{x}_f | \psi(t_f) \rangle &= \int \mathrm{d}\mathbf{p} \, \langle \mathbf{x}_f | \mathbf{p} \rangle \langle \mathbf{p} | \mathrm{e}^{-\frac{\mathrm{i}}{\hbar}\hat{H}(t_f - t_i)} | \psi(\mathbf{x}_i, t_i) \rangle \\ &= \int \mathrm{d}\mathbf{p} \, \frac{1}{(2\pi\hbar)^{3/2}} \mathrm{e}^{\frac{\mathrm{i}}{\hbar}\mathbf{p}\cdot\mathbf{x}_f} \mathrm{e}^{-\frac{\mathrm{i}}{\hbar}\frac{\mathbf{p}^2}{2m}(t_f - t_i)} \langle \mathbf{p} | \psi(\mathbf{x}_i, t_i) \rangle . \end{aligned} \tag{2.84}$$

Then we, in turn, insert a unit operator in terms of the position space vectors in order to use the deltafunction in Eq. (2.79) (notice that we already have **x** reserved, so we use **y** instead)

$$\begin{aligned}\langle \mathbf{x}_f|\psi(t_f)\rangle &= \int \mathrm{d}\mathbf{p} \int \mathrm{d}\mathbf{y}\, \frac{1}{(2\pi\hbar)^{3/2}} \mathrm{e}^{\frac{\mathrm{i}}{\hbar}\mathbf{p}\cdot\mathbf{x}_f} \mathrm{e}^{-\frac{\mathrm{i}}{\hbar}\frac{\mathbf{p}^2}{2m}(t_f-t_i)} \langle \mathbf{p}|\mathbf{y}\rangle\langle \mathbf{y}|\psi(\mathbf{x}_i,t_i)\rangle \\ &= \int \mathrm{d}\mathbf{p} \int \mathrm{d}\mathbf{y}\, \frac{1}{(2\pi\hbar)^{3/2}} \mathrm{e}^{\frac{\mathrm{i}}{\hbar}\mathbf{p}\cdot\mathbf{x}_f} \mathrm{e}^{-\frac{\mathrm{i}}{\hbar}\frac{\mathbf{p}^2}{2m}(t_f-t_i)} \frac{1}{(2\pi\hbar)^{3/2}} \mathrm{e}^{-\frac{\mathrm{i}}{\hbar}\mathbf{p}\cdot\mathbf{y}} \delta^{(3)}(\mathbf{y}-\mathbf{x}_i) \\ &= \int \mathrm{d}\mathbf{p}\, \frac{1}{(2\pi\hbar)^{3/2}} \mathrm{e}^{\frac{\mathrm{i}}{\hbar}\mathbf{p}\cdot\mathbf{x}_f} \mathrm{e}^{-\frac{\mathrm{i}}{\hbar}\frac{\mathbf{p}^2}{2m}(t_f-t_i)} \frac{1}{(2\pi\hbar)^{3/2}} \mathrm{e}^{-\frac{\mathrm{i}}{\hbar}\mathbf{p}\cdot\mathbf{x}_i} \\ &= \frac{1}{(2\pi\hbar)^3} \int \mathrm{d}\mathbf{p}\, \mathrm{e}^{-\left[\frac{\mathrm{i}(t_f-t_i)}{2\hbar m}\mathbf{p}^2 - \frac{\mathrm{i}}{\hbar}\mathbf{p}\cdot(\mathbf{x}_f-\mathbf{x}_i)\right]} . \end{aligned} \tag{2.85}$$

The integral in Eq. (2.85) is of the Gaussian type, and it can be evaluated by completing the square in the exponent. The integration variable **p**, however, is three-dimensional, and so is the integral itself. It however turns out, that the one-dimensional Gaussian integral

$$\int_{-\infty}^{\infty} \mathrm{e}^{-(ax^2-bx)}\mathrm{d}x = \sqrt{\frac{\pi}{a}}\,\mathrm{e}^{\frac{b^2}{4a}} \tag{2.86}$$

can be used here with the exception for the normalization factor; it needs to be expanded to include all the three dimensions we are working with, i.e., the exponent should be 3/2 instead of 1/2 by the squareroot. We stress here that we are not after a rigorous derivation for the propagator but rather an outlook how it looks like. This way we have for the propagator

$$\begin{aligned}\langle \mathbf{x}_f|\psi(t_f)\rangle &= \frac{1}{(2\pi\hbar)^3}\left[\frac{\pi}{\frac{\mathrm{i}(t_f-t_i)}{2\hbar m}}\right]^{3/2} \mathrm{e}^{\frac{\left(\frac{\mathrm{i}}{\hbar}(\mathbf{x}_f-\mathbf{x}_i)\right)^2}{4\left(\frac{\mathrm{i}(t_f-t_i)}{2\hbar m}\right)}} \\ &= \left[\frac{m}{2\pi\mathrm{i}\hbar(t_f-t_i)}\right]^{3/2} \mathrm{e}^{\frac{\mathrm{i}m(\mathbf{x}_f-\mathbf{x}_i)^2}{2\hbar(t_f-t_i)}} . \end{aligned} \tag{2.87}$$

This result if known as the *free-particle propagator*, and it sets the base for the so-called *path-integral formalism* of quantum mechanics. This point of view was introduced by R. Feynman in 1942 [9]. On a fundamental level, the action principle of classical mechanics is generalized. The path-integral formalism replaces the classical idea of a point particle in a single, unique trajectory with a sum[4] over an infinite possible trajectories.

The propagator $G(\mathbf{x}_f,t_f;\mathbf{x}_i,t_i) = \langle \mathbf{x}_f,t_f|\mathbf{x}_i,t_i\rangle$ "knows" how a wavefunction propagates in time. We may, in fact write the wavefunction as

$$\begin{aligned}\psi(\mathbf{x}_f,t_f) &= \langle \mathbf{x}_f,t_f|\psi\rangle \\ &= \int \mathrm{d}\mathbf{x}_i\, \langle \mathbf{x}_f,t_f|\mathbf{x}_i,t_i\rangle\langle \mathbf{x}_i,t_i|\psi\rangle \\ &= \int \mathrm{d}\mathbf{x}_i\, G(\mathbf{x}_f,t_f;\mathbf{x}_i,t_i)\psi(\mathbf{x}_i,t_i) , \end{aligned} \tag{2.88}$$

which is exactly the Green's function of the Schrödinger equation. As we know the solution of a

---

[4] or rather a functional integral

time-dependent Schrödinger equation by heart, we may put the idea of a propagator also as

$$\begin{aligned} G(\mathbf{x}_f, t_f; \mathbf{x}_i, t_i) &= \langle \mathbf{x}_f | \mathrm{e}^{-\frac{\mathrm{i}}{\hbar}\hat{H}(t_f - t_i)} | \mathbf{x}_i \rangle \\ &= \sum_n \langle \mathbf{x}_f | n \rangle \mathrm{e}^{-\frac{\mathrm{i}}{\hbar}E_n(t_f - t_i)} \langle n | \mathbf{x}_i \rangle \\ &= \sum_n \mathrm{e}^{-\frac{\mathrm{i}}{\hbar}E_n(t_f - t_i)} \psi_n^*(\mathbf{x}_f) \psi_n(\mathbf{x}_i) \, . \end{aligned} \tag{2.89}$$

From Eq. (2.89) we may deduce that the Fourier analysis of the propagator gives all energy eigenvalues and eigenfunctions. In fact, also all the dynamical information about the quantum system is packed within the propagator. We will be dealing with many-particle propagators in detail in the next chapter.

## 2.3 Vacuum amplitude

In the previous section we presented the idea of a particle propagator. The vacuum amplitude could be realized as a 'no-particle propagator'. Let us investigate this statement more thoroughly.

Let $\Phi_0$ be the initial ground state of an unperturbed $N$-particle system, i.e., the vacuum presented in Sec. 2.1.2. Some external potential or internal interactions of the system are then allowed to act. The vacuum amplitude, $R(t)$, is a probability amplitude that the system is found in the same initial state $\Phi_0$ also after time $t$ has passed. Thus, $R(t)$ is the transition amplitude from vacuum to vacuum, and since no particles were added nor removed, it is realized as a 'no-particle propagator'.

Then suppose that there is no interaction after $t = 0$. Then the wavefunction after time $t$ is given by

$$\Psi(t) = \mathrm{e}^{-\frac{\mathrm{i}}{\hbar}\epsilon_0 t} \Phi_0 \, , \tag{2.90}$$

where $\epsilon_0$ is the ground state energy of the non-interacting system. If, however, the interactions were switched on after $t = 0$, the system would start to make transitions from $\Phi_0$ to all possible $N$-particle states. Now we are after the probability amplitude for which the system is found, after time $t$, in a non-interacting state $\mathrm{e}^{-\frac{\mathrm{i}}{\hbar}\epsilon_0 t}\Phi_0$. We must have some operation that takes the initial state to the desired final state, i.e.,

$$\Psi(t) = \hat{U}(t)\Phi_0 \, , \tag{2.91}$$

where $\hat{U}(t)$ is regarded as a time-evolution operator, which will be discussed more in detail in the next chapter. The probability amplitude $R(t)$ is now found simply as a scalar product

$$\begin{aligned} R(t) &= \langle \mathrm{e}^{-\frac{\mathrm{i}}{\hbar}\epsilon_0 t}\Phi_0 | \Psi(t) \rangle \\ &= \int \mathrm{d}\mathbf{x}_1 \cdots \int \mathrm{d}\mathbf{x}_N \, \Phi_0^* \mathrm{e}^{\frac{\mathrm{i}}{\hbar}\epsilon_0 t} \hat{U}(t) \Phi_0 \\ &= \langle \Phi_0 | \hat{U}(t) | \Phi_0 \rangle \mathrm{e}^{\frac{\mathrm{i}}{\hbar}\epsilon_0 t} \, . \end{aligned} \tag{2.92}$$

This is an important quantity as the ground state energy $E_0$ of the interacting system may be obtained provided that we have an expression for the vacuum amplitude. Let us see how. The vacuum amplitude in Eq. (2.92) may be written as

$$\begin{aligned} R(t) &= \mathrm{e}^{\frac{\mathrm{i}}{\hbar}\epsilon_0 t} \langle \Phi_0 | \hat{U}(t) | \Phi_0 \rangle \\ &= \mathrm{e}^{\frac{\mathrm{i}}{\hbar}\epsilon_0 t} \langle \Phi_0 | \mathrm{e}^{-\frac{\mathrm{i}}{\hbar}\hat{H}t} | \Phi_0 \rangle \, , \end{aligned} \tag{2.93}$$

where we inserted an expression for the time-evolution operator which is found as a solution to the time-dependent Schrödinger equation. The expression in Eq. (2.93) can be expanded in terms of the eigenstates of the Hamiltonian $\hat{H}$:

$$\begin{aligned} R(t) &= \mathrm{e}^{\frac{\mathrm{i}}{\hbar}\epsilon_0 t}\sum_n \langle\Phi_0|\Psi_n\rangle\langle\Psi_n|\mathrm{e}^{-\frac{\mathrm{i}}{\hbar}\hat{H}t}|\Phi_0\rangle \\ &= \mathrm{e}^{\frac{\mathrm{i}}{\hbar}\epsilon_0 t}\sum_n \langle\Phi_0|\Psi_n\rangle\langle\Psi_n|\Phi_0\rangle\mathrm{e}^{-\frac{\mathrm{i}}{\hbar}E_n t}\,, \end{aligned} \tag{2.94}$$

where $E_n$ is an energy eigenvalue corresponding to the Hamiltonian $\hat{H}$. Taking logarithms on both sides of Eq. (2.94) yields

$$\begin{aligned} \ln R(t) &= \ln\left[\mathrm{e}^{\frac{\mathrm{i}}{\hbar}\epsilon_0 t}\sum_n |\langle\Phi_0|\Psi_n\rangle|^2\mathrm{e}^{-\frac{\mathrm{i}}{\hbar}E_n t}\right] \\ &= \ln(\mathrm{e}^{\frac{\mathrm{i}}{\hbar}\epsilon_0 t}) + \ln\left[\sum_n |\langle\Phi_0|\Psi_n\rangle|^2\mathrm{e}^{-\frac{\mathrm{i}}{\hbar}E_n t}\right] \\ &= \frac{\mathrm{i}}{\hbar}\epsilon_0 t + \ln\left[\sum_n |\langle\Phi_0|\Psi_n\rangle|^2\mathrm{e}^{-\frac{\mathrm{i}}{\hbar}E_n t}\right]. \end{aligned} \tag{2.95}$$

Then by taking derivatives with respect to time on both sides we obtain

$$\partial_t \ln R(t) = \frac{\mathrm{i}}{\hbar}\epsilon_0 + \left[\frac{\sum_n |\langle\Phi_0|\Psi_n\rangle|^2\mathrm{e}^{-\frac{\mathrm{i}}{\hbar}E_n t}(-\frac{\mathrm{i}}{\hbar}E_n)}{\sum_n |\langle\Phi_0|\Psi_n\rangle|^2\mathrm{e}^{-\frac{\mathrm{i}}{\hbar}E_n t}}\right]. \tag{2.96}$$

Then we make use of a trick: $t = T(1-\mathrm{i}\eta)$ with $\eta$ being a positive infinitesimal number such that $\eta\cdot\infty = \infty$, and take $T \to \infty$. We are then able to rewrite Eq. (2.96) as

$$\begin{aligned} \lim_{T\to\infty}\left[\partial_t \ln R(t)\right]_{t=T(1-\mathrm{i}\eta)} &= \frac{\mathrm{i}}{\hbar}\epsilon_0 + \lim_{T\to\infty}\left[\frac{\sum_n |\langle\Phi_0|\Psi_n\rangle|^2(-\frac{\mathrm{i}}{\hbar}E_n)\mathrm{e}^{-\frac{\mathrm{i}}{\hbar}E_n T-\frac{1}{\hbar}E_n\eta T}}{\sum_n |\langle\Phi_0|\Psi_n\rangle|^2\mathrm{e}^{-\frac{\mathrm{i}}{\hbar}E_n T-\frac{1}{\hbar}E_n\eta T}}\right] \\ &= \frac{\mathrm{i}}{\hbar}\epsilon_0 + \left[\frac{\langle\Phi_0|\Psi_0\rangle|^2(-\frac{\mathrm{i}}{\hbar}E_0)\mathrm{e}^{-\frac{\mathrm{i}}{\hbar}E_0\cdot\infty}\mathrm{e}^{-\frac{1}{\hbar}E_0\eta\cdot\infty}}{|\langle\Phi_0|\Psi_0\rangle|^2\mathrm{e}^{-\frac{\mathrm{i}}{\hbar}E_0\cdot\infty}\mathrm{e}^{-\frac{1}{\hbar}E_0\eta\cdot\infty}}\right] \\ &= \frac{\mathrm{i}}{\hbar}(\epsilon_0 - E_0)\,, \end{aligned} \tag{2.97}$$

where, on the second line, we noticed that the exponentials with the smallest energy $E_n$ will decay the slowest, and furthermore, the only term in the sums that will be important, when taking the limit $T \to \infty$, is $n = 0$. From Eq. (2.97) we can solve for the ground state energy of the interacting system $E_0$

$$E_0 = \epsilon_0 + \mathrm{i}\hbar\lim_{T\to\infty}\left[\partial_t \ln R(t)\right]_{t=T(1-\mathrm{i}\eta)}\,. \tag{2.98}$$

Now we are left with determining the vacuum amplitude $R(t)$. This can be done by field-theoretical diagram techniques which will be introduced in the next chapter. As the form of Eq. (2.98) suggests (cf. energy corrections via Rayleigh-Schrödinger perturbation series[5]), the vacuum amplitude will have a perturbative expansion which will be expressed in terms of Feynman diagrams.

---

[5] see e.g. [26]

# Chapter 3

# Many-particle perturbation theory

In this chapter we consider the many-particle quantum mechanics in detail by, e.g., discussing the Feynman rules. Most of the ideas presented in this chapter follow from Refs. [1,3,5,8,14,21], from the lecture notes of an advanced level course in quantum mechanics by Kimmo Tuominen, and from the lecture notes of a course in many-particle quantum mechanics by Robert van Leeuwen.

## 3.1 Green's functions and statistical physics

Consider a non-relativistic system with a second quantized Hamiltonian in Eq. (2.51), derived in the previous chapter. Then let us take a system at an initial time $t_0$, specified with a density operator $\hat{\rho}$, and study the evolution of the system. We may study the evolution by introducing a one-particle Green's function

$$G^{<}_{(1)}(\mathbf{x}_1, t_1; \mathbf{x}_2, t_2) = \mathrm{i}\langle \hat{\psi}^{\dagger}_{H}(\mathbf{x}_2, t_2)\hat{\psi}_{H}(\mathbf{x}_1, t_1)\rangle \,, \tag{3.1}$$

where the bracket $\langle\rangle$ refers to an expectation value with respect to the initial state. The subscripts '$H$' within the field operators announce that these operators are in Heisenberg picture for which the meaning will be discussed later. The superscript '$<$' for the Green's function denotes the so-called lesser Green's function, which means that we have the field operators inside the expectation value in particular oder, i.e., $t_1 < t_2$. Before going any further, let us take a look at the initial state, with respect to the expectation value is to be taken. The density matrix operator $\hat{\rho}$, in terms of a complete orthonormal set of states $\{|n\rangle\}$, can be expressed as

$$\hat{\rho} = \sum_n p_n |n\rangle\langle n| \,, \tag{3.2}$$

where $p_n$ is the probability of finding the system in state $|n\rangle$. We can then express an expectation value of an operator $\hat{A}$ with respect to the states $|n\rangle$ as

$$\langle \hat{A} \rangle = \sum_n p_n \langle n|\hat{A}|n\rangle \,. \tag{3.3}$$

The expression in Eq. (3.3) can be rewritten, with $\{|\Psi_k\rangle\}$ being a complete orthonormal set, as

$$\begin{aligned}\langle\hat{A}\rangle &= \sum_{n,k} p_n\langle n|\hat{A}|\Psi_k\rangle\langle\Psi_k|n\rangle \\ &= \sum_{n,k}\langle\Psi_k|n\rangle p_n\langle n|\hat{A}|\Psi_k\rangle \\ &= \sum_k\langle\Psi_k|\hat{\rho}\hat{A}|\Psi_k\rangle \\ &= \mathrm{Tr}\{\hat{\rho}\hat{A}\}\,, \end{aligned} \tag{3.4}$$

where we used Eq. (3.2) on the third line, and on the last line introduced the *trace of a matrix* as the sum of the diagonal elements. What about the probability $p_n$ then? Suppose we have a bunch of systems that are described with identical Hamiltonians, and let there be $M$ such systems, called an *ensemble*. Then we perform a measurement on each of the systems in the ensemble and find that $M_n$ of them are in state $|n\rangle$. Then the probability of finding a system in state $|n\rangle$ would be

$$p_n = \frac{M_n}{M}\,. \tag{3.5}$$

Consider then the evolution of a system in this ensemble. If the system we are studying was initially at state $|n, t_0\rangle$, then we have for later time $t$ the evolved state as

$$|n,t\rangle = \hat{U}(t,t_0)|n,t_0\rangle\,, \tag{3.6}$$

where $\hat{U}(t,t_0)$ is the time-evolution operator of the system. We would then like to have a definition for a time-dependent density matrix operator $\hat{\rho}(t)$ as

$$\hat{\rho}(t) = \sum_n p_n|n,t\rangle\langle n,t|\,. \tag{3.7}$$

If the probability of finding the system in state $|n,t_0\rangle$ was $p_n$ then the system would have the same probability to be found with the same particles $n$, i.e., in state $|n,t\rangle$ at a later time $t$. Therefore we may write the expectation value of an operator $\hat{A}$ at time $t$ as

$$\begin{aligned}\langle\hat{A}(t)\rangle &= \sum_n p_n\langle n,t|\hat{A}(t)|n,t\rangle \\ &= \sum_n p_n\langle n,t_0|\hat{U}(t_0,t)\hat{A}(t)\hat{U}(t,t_0)|n,t_0\rangle \\ &= \sum_{n,k} p_n\langle n,t_0|\hat{U}(t_0,t)\hat{A}(t)\hat{U}(t,t_0)|\Psi_k\rangle\langle\Psi_k|n,t_0\rangle \\ &= \sum_{n,k}\langle\Psi_k|n,t_0\rangle p_n\langle n,t_0|\hat{U}(t_0,t)\hat{A}(t)\hat{U}(t,t_0)|\Psi_k\rangle \\ &= \sum_k\langle\Psi_k|\hat{\rho}(t_0)\hat{U}(t_0,t)\hat{A}(t)\hat{U}(t,t_0)|\Psi_k\rangle \\ &= \mathrm{Tr}\{\hat{\rho}(t_0)\hat{U}(t_0,t)\hat{A}(t)\hat{U}(t,t_0)\} \\ &= \mathrm{Tr}\{\hat{\rho}(t_0)\hat{A}_H(t)\}\,, \end{aligned} \tag{3.8}$$

where, on the fifth line, we used Eq. (3.7), and on the last line we expressed the operator $\hat{A}$ in Heisenberg picture. From Eq. (3.8) we may deduce that if we know the initial density matrix of the system, we are able to calculate the time-dependent expectation value of any operator $\hat{A}$.

Logically, the next task would be to determine an expression for the density matrix operator $\hat{\rho}(t_0)$ for equilibrium systems.

For this task, we consider an ensemble of $M$ identical systems in equlibrium and in weak contact with each other. We assume that our ensemble has fixed total energy $E$ and particle number $N$. After a measurement we find $M_r$ systems to be in energy eigenstate $|r\rangle$ with energy $E_r$ and particle number $N_r$. Then, by assuming that the coupling between systems is weak, we have from statistical physics[1] that

$$E = \sum_r M_r E_r \tag{3.9}$$

$$N = \sum_r M_r N_r \,. \tag{3.10}$$

The degeneracy of the level $E$, $\Omega_E$, is then obtained by studying the ensemble combinatorically. This procedure is a standard problem in statistical physics, and involves, e.g., *Stirling's approximation*. The result of the degeneracy is usually expressed in logarithmic form as

$$\ln \Omega_E = -M \sum_r p_r \ln(p_r) \,, \tag{3.11}$$

where $p_r$ is the probability of finding the system in state $|r\rangle$, as in Eq. (3.5). Eq. (3.11) is often rewritten by defining the entropy associated with each system in the ensemble as

$$S = -\sum_r p_r \ln(p_r) \,. \tag{3.12}$$

Then we have the degeneracy of level $E$ as $\Omega_E = MS$. Then we see that by maximizing the degeneracy of the level $E$ we get the most likely configuration for our system in Eqs. (3.9) and (3.10). Furthermore, we need to find the extremum of the entropy in Eq. (3.12) with the conditions in Eqs. (3.9) and (3.10) for each of the systems in the ensemble, i.e.,

$$E_S = \frac{E}{M} = \frac{1}{M}\sum_r M_r E_r = \sum_r p_r E_r \tag{3.13}$$

$$N_S = \frac{N}{M} = \frac{1}{M}\sum_r M_r N_r = \sum_r p_r N_r \,, \tag{3.14}$$

where $E_S$ and $N_S$ correspond to each system. We then have to maximize the function

$$f(p_r) = -\sum_r p_r \ln(p_r) - \alpha \sum_r p_r N_r - \beta \sum_r p_r E_r - \gamma \sum_r p_r \,. \tag{3.15}$$

The last term on the right-hand side in Eq. (3.15) comes from an obvious constraint for the probabilities $\sum_r p_r \equiv 1$. By differentiating Eq. (3.15) with respect to $p_r$ and then finding the zeros of the derivative, we obtain

$$p_r = \frac{1}{e^{\gamma - 1}} e^{\beta E_r - \alpha N_r} \,. \tag{3.16}$$

---

[1] see e.g. [22]

By using the constraint for the probabilities, that they must sum to one, we get

$$\begin{aligned}
\frac{1}{\mathrm{e}^{\gamma-1}} \underbrace{\sum_r \mathrm{e}^{\beta E_r - \alpha N_r}}_{\overset{\text{def.}}{=}\,\mathcal{Z}} &= 1 \\
\Rightarrow \qquad \frac{1}{\mathrm{e}^{\gamma-1}} &= \frac{1}{\mathcal{Z}} \\
\Rightarrow \qquad p_r &= \frac{1}{\mathcal{Z}} \mathrm{e}^{\beta E_r - \alpha N_r} \,, \qquad (3.17)
\end{aligned}$$

where, on the second line, we introduced the so-called *partition function* $\mathcal{Z}$. The parameters $\alpha$ and $\beta$ are now functions of $E$ and $N$, and, again referring to statistical physics, it is straightforward to show that the parameters are given by

$$\beta = \frac{1}{T} \qquad \text{and} \qquad \alpha = -\beta\mu \,, \qquad (3.18)$$

where $T = \partial_E S$ is the temperature of the system and $\mu = -T\partial_N S$ is the chemical potential. We hereby have

$$p_r = \frac{1}{\mathcal{Z}} \mathrm{e}^{-\beta(E_r - \mu N_r)} \,, \qquad (3.19)$$

which can now be inserted into Eq. (3.2) to get

$$\begin{aligned}
\hat{\rho} &= \frac{1}{\mathcal{Z}} \sum_r \mathrm{e}^{-\beta(E_r - \mu N_r)} |r\rangle\langle r| \qquad\qquad | \leftarrow |r\rangle \\
\Rightarrow \hat{\rho}|r\rangle &= \frac{1}{\mathcal{Z}} \sum_r \mathrm{e}^{-\beta(E_r - \mu N_r)} |r\rangle \,. \qquad (3.20)
\end{aligned}$$

By noticing how the eigenvalues of energy $E_r$ and particle number $N_r$ appear in Eq. (3.20), we finally have for the density operator

$$\hat{\rho} = \frac{1}{\mathcal{Z}} \sum_r \mathrm{e}^{-\beta(\hat{H} - \mu\hat{N})} \,, \qquad (3.21)$$

where $\hat{H}$ is the total Hamiltonian of the system and $\hat{N}$ the total particle number operator. Here the number of particles does not have to be fixed, and the quantum states with indefinite particle number span the Fock space introduced earlier in Chap. 2, Eq. (2.4). This concept is called the *Grand canonical ensemble*. For the partition function $\mathcal{Z}$ we have

$$\begin{aligned}
\mathcal{Z} &= \sum_r \mathrm{e}^{-\beta(E_r - \mu N_r)} \\
&= \sum_r \langle r| \mathrm{e}^{-\beta(\hat{H} - \mu\hat{N})} |r\rangle \\
&= \mathrm{Tr}\{\mathrm{e}^{-\beta(\hat{H} - \mu\hat{N})}\} \,. \qquad (3.22)
\end{aligned}$$

We can now insert Eq. (3.21) with Eq. (3.22) into Eq. (3.8) in order to obtain the final result for an expectation value of any time-dependent operator $\hat{A}(t)$

$$\begin{aligned}
\langle \hat{A}(t) \rangle &= \mathrm{Tr}\{\hat{\rho}(t_0) \hat{A}_H(t)\} \\
&= \mathrm{Tr}\{\frac{\mathrm{e}^{-\beta(\hat{H} - \mu\hat{N})}}{\mathrm{Tr}\{\mathrm{e}^{-\beta(\hat{H} - \mu N)}\}} \hat{A}_H(t)\} \\
&= \frac{\mathrm{Tr}\{\mathrm{e}^{-\beta(\hat{H} - \mu\hat{N})} \hat{A}_H(t)\}}{\mathrm{Tr}\{\mathrm{e}^{-\beta(\hat{H} - \mu\hat{N})}\}} \,, \qquad (3.23)
\end{aligned}$$

where, on the last line, we used a property of a trace that it can be moved out from another trace as it is simply a number. This statement is readily seen when the traces are expanded as in Eq. (3.4).

As we see, the quantum-mechanical description of statistical physics can take us quite far from our original problems. In fact, Ludwig Boltzmann ended up hanging himself after dedicating his life to statistical physics [4], and we do not want that happening to us, do we? Instead, let us get back to beginning, to the Green's function.

In Eq. (3.1) we had the lesser Green's function $G^{<}_{(1)}(\mathbf{x}_1, t_1; \mathbf{x}_2, t_2)$ which was defined with the field operators $\hat{\psi}$ being in the Heisenberg picture. We might as well give a definition for the so-called *greater* Green's function as

$$G^{>}_{(1)}(\mathbf{x}_1, t_1; \mathbf{x}_2, t_2) = -\mathrm{i}\langle \hat{\psi}_H(\mathbf{x}_1, t_1)\hat{\psi}^{\dagger}_H(\mathbf{x}_2, t_2)\rangle \,. \tag{3.24}$$

If we take $t_1 = t_2 = t$ and $\mathbf{x}_1 = \mathbf{x}_2 = \mathbf{x}$ in Eqs. (3.1) and (3.24) we have a one-particle density matrix inside the expectation value. We then see that the spatial density of particles is given by

$$n(\mathbf{x}, t) = \langle \hat{n}_H(\mathbf{x}, t)\rangle = \mathrm{i}G^{<}_{(1)}(\mathbf{x}, t; \mathbf{x}, t) \,. \tag{3.25}$$

On the other hand, the density of holes is given similarly by the greater component. The physical meaning of a Green's function is starting to come clearer: for $t_1 > t_2$ the Green's function in Eq. (3.24) describes a propagation of a state containing an additional partile. Similarly, for $t_1 < t_2$ in Eq. (3.1), the field operator first removes a particle (creates a hole) and the system is then propagating in time. These holes then seem to be propagating backwards in time, as Feynman suggested in his famous articles in 1949 [10, 11].

For us, it would be easier to handle the Green's functions for both lesser and greater component simultaneously. As we see from the definitions of the Green's functions, the time parameter must have something to do with distinguishing between one and the other. Let us then study the meaning of time more carefully, i.e., the time evolution of many-particle systems.

## 3.2 Time evolution and equations of motion

Time evolution of quantum systems is connected with various pictures. Earlier in Eq. (3.1) we had our operators in the so-called Heisenberg picture. Usually, in elementary quantum mechanics, the framework is the so-called Schrödinger picture. The difference between these two is that while the state vectors are time-dependent and the operators time-independent in the Schrödinger picture, their time-dependence is exactly the opposite in the Heisenberg picture. In the Heisenberg picture all the time-dependence is in operators

$$\hat{A}_H(t) = \hat{U}^{\dagger}_S(t, t_0)\hat{A}_S\hat{U}_S(t_0, t) \,, \tag{3.26}$$

where we denoted the Schrödinger operators with a subscript '*S*' for clarity. From this on, we omit the notation '*S*' and use only '*H*' for Heisenberg operators. If there is no subscript, the operator is in the Schrödinger picture. The time-evolution operators in Eq. (3.26) are determined from the time-dependent Schrödinger equation

$$\mathrm{i}\hbar\partial_t|\Psi(t)\rangle = \hat{H}(t)|\Psi(t)\rangle \tag{3.27}$$

with initial condition $|\Psi(t_0)\rangle = |\Phi_0\rangle$. In Eq. (3.27) we also allow the Hamiltonian to be time-dependent. If, however, the Hamiltonian is constant in all times, the solution to the Eq. (3.27) is

$$|\Psi(t)\rangle = \mathrm{e}^{-\frac{\mathrm{i}}{\hbar}\hat{H}(t-t_0)}|\Phi_0\rangle \,. \tag{3.28}$$

We therefore have that an operator

$$\hat{U}(t,t_0) = \mathrm{e}^{-\frac{\mathrm{i}}{\hbar}\hat{H}(t-t_0)} \tag{3.29}$$

evolves the initial state $|\Phi_0\rangle$ to $|\Psi(t)\rangle$. The operator in Eq. (3.29) is, because of this, called the time-evolution operator which can be checked to be unitary. We are then able to rewrite the Heisenberg operators in Eq. (3.26) as

$$\hat{A}_H(t) = \mathrm{e}^{\frac{\mathrm{i}}{\hbar}\hat{H}(t-t_0)}\hat{A}\mathrm{e}^{-\frac{\mathrm{i}}{\hbar}\hat{H}(t-t_0)} \,, \tag{3.30}$$

and with this expression we can rewrite the expectation value of an operator $\hat{A}$ in Eq. (3.23) as

$$\langle\hat{A}(t)\rangle = \frac{\mathrm{Tr}\{\mathrm{e}^{-\beta(\hat{H}-\mu\hat{N})}\hat{U}(t_0,t)\hat{A}(t)\hat{U}(t,t_0)\}}{\mathrm{Tr}\{\mathrm{e}^{-\beta(\hat{H}-\mu\hat{N})}\}} \,. \tag{3.31}$$

If we denote $\hat{H}_{\mathrm{eq}} = \hat{H} - \mu\hat{N}$, we have for the exponential term in Eq. (3.31)

$$\begin{aligned} \mathrm{e}^{-\beta(\hat{H}-\mu\hat{N})} &= \mathrm{e}^{-\beta\hat{H}_{\mathrm{eq}}} \\ &= \mathrm{e}^{-\frac{\mathrm{i}}{\hbar}[(t_0-\mathrm{i}\beta\hbar)-t_0]\hat{H}_{\mathrm{eq}}} \\ &= \hat{U}(t_0-\mathrm{i}\beta\hbar,t_0) \,, \end{aligned} \tag{3.32}$$

which can be thought as an evolution operator from time $t_0$ to complex time $t_0 - \mathrm{i}\beta\hbar$. The numerator in Eq. (3.31) therefore has the following structure

$$\langle\Psi_0|\underbrace{\hat{U}(t_0-\mathrm{i}\beta\hbar,t_0)}_{4.}\underbrace{\hat{U}(t_0,t)}_{3.}\underbrace{\hat{A}(t)}_{2.}\underbrace{\hat{U}(t,t_0)|\Psi_0\rangle}_{1.} \tag{3.33}$$

1. time propagation from initial state at $t_0$ to evolved state at time $t$ ;
2. acting with an operator $\hat{A}$ at time $t$ ;
3. time propagation back to time $t_0$ ;
4. time propagation to a complex time $t_0 - \mathrm{i}\beta\hbar$ ;

which can be viewed as the so-called *Keldysh contour* [18] in complex time plane as shown in Fig. 3.1.

Consider then a Hamiltonian that is piecewise constant in time

$$\hat{H}(t) = \hat{H}(t_i) \,, \qquad t_i \in [t_1, t_{n+1}[ \,, \qquad t_{n+1} = t \,, \tag{3.34}$$

which can be viewed schematically as in Fig. 3.2. The time-evolution between the time steps is then given by

$$\hat{U}(t_1,t_2) = \mathrm{e}^{-\frac{\mathrm{i}}{\hbar}\hat{H}(t_1-t_2)} \,. \tag{3.35}$$

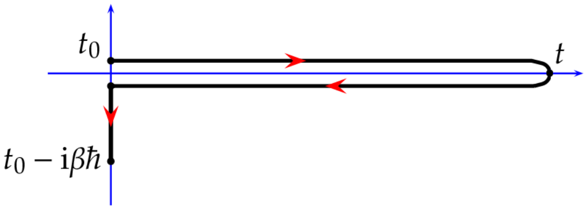

Figure 3.1: Keldysh contour in complex time plane. The contour line is, for the sake of clarity, drawn slightly above and below the real-time axis to distinguish the different parts.

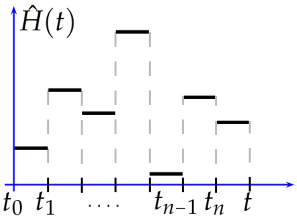

Figure 3.2: Piecewise constant Hamiltonian with respect to time $t$.

The total time-evolution operator from $t_0$ to $t$ is then a product of all the steps

$$\begin{aligned}\hat{U}(t,t_0) &= \hat{U}(t,t_n)\hat{U}(t_n,t_{n-1})\cdots\hat{U}(t_2,t_1)\hat{U}(t_1,t_0)\\ &= \mathrm{e}^{-\frac{\mathrm{i}}{\hbar}\hat{H}(t_n)(t-t_n)}\mathrm{e}^{-\frac{\mathrm{i}}{\hbar}\hat{H}(t_{n-1})(t_n-t_{n-1})}\ldots\mathrm{e}^{-\frac{\mathrm{i}}{\hbar}\hat{H}(t_1)(t_2-t_1)}\mathrm{e}^{-\frac{\mathrm{i}}{\hbar}\hat{H}(t_0)(t_1-t_0)}\,,\end{aligned}\tag{3.36}$$

and similarly from $t$ to $t_0$

$$\begin{aligned}\hat{U}(t_0,t) &= \hat{U}(t_0,t_1)\hat{U}(t_1,t_2)\cdots\hat{U}(t_{n-1},t_n)\hat{U}(t_n,t)\\ &= \mathrm{e}^{-\frac{\mathrm{i}}{\hbar}\hat{H}(t_0)(t_0-t_1)}\mathrm{e}^{-\frac{\mathrm{i}}{\hbar}\hat{H}(t_1)(t_1-t_2)}\ldots\mathrm{e}^{-\frac{\mathrm{i}}{\hbar}\hat{H}(t_{n-1})(t_{n-1}-t_n)}\mathrm{e}^{-\frac{\mathrm{i}}{\hbar}\hat{H}(t_n)(t_n-t)}\,.\end{aligned}\tag{3.37}$$

We will then relabel the times along the horizontal track of the Keldysh contour, starting from initial time $z_i = z_0$ and ending to final time $z_f = z_{2n+2}$, as in Fig. 3.3 and Eq. (3.38).

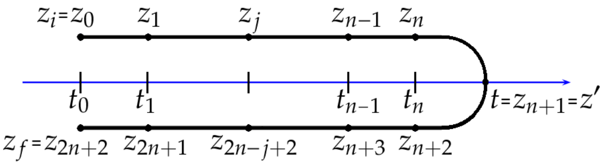

Figure 3.3: Relabeled times along the horizontal track of Keldysh contour.

$$\begin{cases} z_j = t_j & \text{when } j = 0,1,\ldots,n \\ z' = t & \\ z_{2n-j+2} = t_j & \text{when } j = 0,1,\ldots,n \end{cases}\tag{3.38}$$

Eqs. (3.36) and (3.37) can, with this relabeling, be written as

$$\begin{aligned}\hat{U}(t,t_0) &= \hat{U}(z',z_i)\\ &= \mathrm{e}^{-\frac{\mathrm{i}}{\hbar}\hat{H}(z_n)(z'-z_n)}\mathrm{e}^{-\frac{\mathrm{i}}{\hbar}\hat{H}(z_{n-1})(z_n-z_{n-1})}\ldots\mathrm{e}^{-\frac{\mathrm{i}}{\hbar}\hat{H}(z_1)(z_2-z_1)}\mathrm{e}^{-\frac{\mathrm{i}}{\hbar}\hat{H}(z_0)(z_1-z_0)}\,,\end{aligned}\tag{3.39}$$

and

$$\begin{aligned}
\hat{U}(t_0,t) &= \hat{U}(z_f,z') \\
&= \mathrm{e}^{-\frac{\mathrm{i}}{\hbar}\hat{H}(z_{2n+2})(z_{2n+2}-z_{2n+1})}\mathrm{e}^{-\frac{\mathrm{i}}{\hbar}\hat{H}(z_{2n+1})(z_{2n+1}-z_{2n})}\dots\times \\
&\times\ \mathrm{e}^{-\frac{\mathrm{i}}{\hbar}\hat{H}(z_{n+2})(z_{n+2}-z_{n+1})}\mathrm{e}^{-\frac{\mathrm{i}}{\hbar}\hat{H}(z_{n+1})(z_{n+1}-z')}\,. \qquad (3.40)
\end{aligned}$$

With Eqs. (3.39) and (3.40) we may write the operators on the horizontal part of Eq. (3.31) as

$$\begin{aligned}
\hat{U}(t_0,t)\hat{A}(t)\hat{U}(t,t_0) &= \hat{U}(z_f,z')\hat{A}(z')\hat{U}(z',z_i) \\
&= \mathrm{e}^{-\frac{\mathrm{i}}{\hbar}\hat{H}(z_f)(z_f-z_{2n+1})}\dots\mathrm{e}^{-\frac{\mathrm{i}}{\hbar}\hat{H}(z_{n+1})(z_{n+1}-z')}\hat{A}(z')\times \\
&\times\ \mathrm{e}^{-\frac{\mathrm{i}}{\hbar}\hat{H}(z_n)(z'-z_n)}\dots\mathrm{e}^{-\frac{\mathrm{i}}{\hbar}\hat{H}(z_i)(z_1-z_i)}\,. \qquad (3.41)
\end{aligned}$$

A quick review of Eq. (3.41) shows that the operators are ordered along the contour, i.e., the ones furthest away from the starting point appear on the left whereas the ones closest to the starting point appear on the right. With this information we may define the so-called *contour-ordered product* and rewrite Eq. (3.41) as

$$\begin{aligned}
\hat{U}(t_0,t)\hat{A}(t)\hat{U}(t,t_0) &= \mathcal{T}_C[\mathrm{e}^{-\frac{\mathrm{i}}{\hbar}\hat{H}(z_f)(z_f-z_{2n+1})}\dots\mathrm{e}^{-\frac{\mathrm{i}}{\hbar}\hat{H}(z_{n+1})(z_{n+1}-z')}\hat{A}(z')\times \\
&\times\ \mathrm{e}^{-\frac{\mathrm{i}}{\hbar}\hat{H}(z_n)(z'-z_n)}\dots\mathrm{e}^{-\frac{\mathrm{i}}{\hbar}\hat{H}(z_i)(z_1-z_i)}]\,. \qquad (3.42)
\end{aligned}$$

The contour-ordering operator $\mathcal{T}_C$ does nothing but arranges the operators within its argument to the correct order. The cleverness of introducing such operator[2] is that the operators inside it commute, i.e., we have for the operator exponentials

$$\mathcal{T}_C[\mathrm{e}^{\hat{A}(z)}\mathrm{e}^{\hat{B}(z')}] = \mathcal{T}_C[\mathrm{e}^{\hat{A}(z)+\hat{B}(z')}]\,. \qquad (3.43)$$

The statement in Eq. (3.43) can be proven by expanding the exponents as

$$\begin{aligned}
\mathcal{T}_C[\mathrm{e}^{\hat{A}(z)+\hat{B}(z')}] &= \sum_{k=0}^{\infty}\frac{1}{k!}\mathcal{T}_C[(\hat{A}(z)+\hat{B}(z'))^k] \\
&= \sum_{k=0}^{\infty}\frac{1}{k!}\sum_{n=0}^{k}\binom{k}{n}\mathcal{T}_C[\hat{A}(z)^n\hat{B}(z')^{k-n}] \\
&= \sum_{k=0}^{\infty}\sum_{n=0}^{k}\frac{1}{\cancel{k!}}\frac{\cancel{k!}}{n!(k-n)!}\mathcal{T}_C[\hat{A}(z)^n\hat{B}(z')^{k-n}] \\
&= \sum_{k=0}^{\infty}\sum_{n=0}^{\infty}\sum_{m=0}^{\infty}\frac{\delta_{k-n,m}}{n!m!}\mathcal{T}_C[\hat{A}(z)^n\hat{B}(z')^{m}] \\
&= \sum_{n=0}^{\infty}\sum_{m=0}^{\infty}\frac{1}{n!m!}\mathcal{T}_C[\hat{A}(z)^n\hat{B}(z')^{m}] \\
&= \mathcal{T}_C[\mathrm{e}^{\hat{A}(z)}\mathrm{e}^{\hat{B}(z')}]\,, \qquad (3.44)
\end{aligned}$$

where, on the second line, we used the *binomial theorem*[3]

$$(a+b)^k = \sum_{n=0}^{k}\binom{k}{n}a^n b^{k-n}\,. \qquad (3.45)$$

---

[2] which, in fact, is not an operator in a mathematical sense, but rather an operation.

[3] see e.g. [2]

On the third line of Eq. (3.44) we introduced a third sum over $m$ which has only one term because of the Kronecker delta. With this trick, we may extend the sum over $n$ up to infinity, because for the terms $n > k$ the delta gives zero contribution. With the knowledge of operators commuting inside the contour-ordered product we may proceed with our expression in Eq. (3.42) and combine the operators as

$$\hat{U}(t_0,t)\hat{A}(t)\hat{U}(t,t_0) = \mathcal{T}_C[\mathrm{e}^{-\frac{\mathrm{i}}{\hbar}\{\sum_{j=1}^{n}\hat{H}(z_j)(z_{j+1}-z_j)+\sum_{j=n+1}^{2n+2}\hat{H}(z_{j+1})(z_{j+1}-z_j)\}}\hat{A}(z')] \,. \tag{3.46}$$

By decreasing the time step, i.e., taking eventually $n \to \infty$, the expression in Eq. (3.46) becomes a contour integral. This, in turn, leads to

$$\hat{U}(t_0,t)\hat{A}(t)\hat{U}(t,t_0) = \hat{U}(z_f,z')\hat{A}(z')\hat{U}(z',z_i) = \mathcal{T}_C[\mathrm{e}^{-\frac{\mathrm{i}}{\hbar}\int_C \mathrm{d}z\,\hat{H}(z)}\hat{A}(z')] \,, \tag{3.47}$$

where the contour $C$ runs from $z_i = t_0$ to $z' = t$ and back to $z_f = t_0$. We can similarly discretize the vertical track of the Keldysh contour in Eq. (3.33) and add this contribution to the one obtained in Eq. (3.47). All in all, we finally have for the expectation value in Eq. (3.31)

$$\langle\hat{A}(t)\rangle = \frac{\mathrm{Tr}\{\mathcal{T}_C[\mathrm{e}^{-\frac{\mathrm{i}}{\hbar}\int_C \mathrm{d}z\,\hat{H}(z)}\hat{A}(t)]\}}{\mathrm{Tr}\{\mathrm{e}^{-\frac{\mathrm{i}}{\hbar}\int_C \mathrm{d}z\,\hat{H}(z)}\}} \,. \tag{3.48}$$

Then recall the definition for the one-particle Green's function in Eqs. (3.1) and (3.24). The field operators inside the expectation values can now be viewed as one operator $\hat{A}$ in Eq. (3.48). Because of the time-ordering, we may now combine our results for a general Green's function

$$\begin{aligned} G_{(1)}(\mathbf{x}_1,t_1;\mathbf{x}_2,t_2) &= \theta(z_1,z_2)G^{>}_{(1)}(\mathbf{x}_1,z_1;\mathbf{x}_2,z_2) + \theta(z_2,z_1)G^{<}_{(1)}(\mathbf{x}_1,z_1;\mathbf{x}_2,z_2) \\ &= -\mathrm{i}\theta(z_1,z_2)\langle\hat{\psi}_H(\mathbf{x}_1,z_1)\hat{\psi}^\dagger_H(\mathbf{x}_2,z_2)\rangle + \mathrm{i}\theta(z_2,z_1)\langle\hat{\psi}^\dagger_H(\mathbf{x}_2,z_2)\hat{\psi}_H(\mathbf{x}_1,z_1)\rangle \\ &= -\mathrm{i}\langle\mathcal{T}_C[\hat{\psi}_H(\mathbf{x}_1,z_1)\hat{\psi}^\dagger_H(\mathbf{x}_2,z_2)]\rangle \\ &= -\mathrm{i}\frac{\mathrm{Tr}\{\mathcal{T}_C[\mathrm{e}^{-\frac{\mathrm{i}}{\hbar}\int_C \mathrm{d}z\,\hat{H}(z)}\hat{\psi}(\mathbf{x}_1,z_1)\hat{\psi}^\dagger(\mathbf{x}_2,z_2)]\}}{\mathrm{Tr}\{\mathrm{e}^{-\frac{\mathrm{i}}{\hbar}\int_C \mathrm{d}z\,\hat{H}(z)}\}} \,, \end{aligned} \tag{3.49}$$

which is usually cut shorter by combining the coordinates for space and time as

$$G_{(1)}(1;2) = -\mathrm{i}\frac{\mathrm{Tr}\{\mathcal{T}_C[\mathrm{e}^{-\frac{\mathrm{i}}{\hbar}\int_C \mathrm{d}z\,\hat{H}(z)}\hat{\psi}(1)\hat{\psi}^\dagger(2)]\}}{\mathrm{Tr}\{\mathrm{e}^{-\frac{\mathrm{i}}{\hbar}\int_C \mathrm{d}z\,\hat{H}(z)}\}} \,. \tag{3.50}$$

It is worth noticing that the field operators in Eq. (3.50) are in Schrödinger picture as the time-evolution is included in the exponential term. Also, the "time" coordinate $z$ is to be understood as a position on the Keldysh contour.

Next thing to consider is the equations of motion for the one-particle Green's function. We now, however, wish to study an isolated system, i.e., taking the system to be in zero temperature. Taking the limit $\beta \to \infty$ justifies us to consider only the horizontal track of Keldysh contour (see. e.g. [5]), and with the time-ordering $\mathcal{T}_C$ we may write the one-particle Green's function in the following form

$$G_{(1)}(1;1') = -\mathrm{i}\langle\Psi_0|\mathcal{T}_C[\hat{\psi}_H(1)\hat{\psi}^\dagger_H(1')]|\Psi_0\rangle \,. \tag{3.51}$$

The equations of motion for the field operators $\hat{\psi}_H$ were derived in Eqs. (2.64) and (2.65) of the previous chapter. We will rewrite these equations here using the notation in Eq. (3.51):

$$\begin{cases} \mathrm{i}\hbar\partial_{t_1}\hat{\psi}_H(1) = \hat{h}(1)\hat{\psi}_H(1) + \int \mathrm{d}1'\,v(1,1')\hat{\psi}^\dagger_H(1')\hat{\psi}_H(1')\hat{\psi}_H(1) \\ \mathrm{i}\hbar\partial_{t_{1'}}\hat{\psi}^\dagger_H(1') = -\hat{h}(1')\hat{\psi}^\dagger_H(1') - \int \mathrm{d}1\,v(1,1')\hat{\psi}^\dagger_H(1')\hat{\psi}^\dagger_H(1)\hat{\psi}_H(1) \,, \end{cases} \tag{3.52}$$

where $\hat{h}$ is the one-particle part of the Hamiltonian, and $v(1,1') = \delta(t_1, t_{1'})/|\mathbf{r}_1 - \mathbf{r}_{1'}|$ is the Coulomb interaction. Taking a derivative with respect to time $t_1$ of the Green's function in Eq. (3.51) yields

$$\begin{aligned}
\mathrm{i}\hbar\partial_{t_1} G_{(1)}(1;1') &= \mathrm{i}\hbar\partial_{t_1}\Big[-\mathrm{i}\langle\Psi_0|\mathcal{T}_C[\hat{\psi}_H(1)\hat{\psi}^\dagger_H(1')]|\Psi_0\rangle\Big] \\
&= \mathrm{i}\hbar\partial_{t_1}\Big[-\mathrm{i}\theta(t_1 - t_{1'})\langle\Psi_0|\hat{\psi}_H(1)\hat{\psi}^\dagger_H(1')|\Psi_0\rangle \\
&\qquad + \mathrm{i}\theta(t_{1'} - t_1)\langle\Psi_0|\hat{\psi}^\dagger_H(1')\hat{\psi}_H(1)|\Psi_0\rangle\Big] . \qquad (3.53)
\end{aligned}$$

The derivatives of the step functions give deltafunctions as $\partial_x\theta(x) = \delta(x)$, and this way we can expand the derivatives of the products as

$$\begin{aligned}
\mathrm{i}\hbar\partial_{t_1} G_{(1)}(1;1') &= \hbar\delta(t_1 - t_{1'})\langle\Psi_0|\hat{\psi}_H(1)\hat{\psi}^\dagger_H(1')|\Psi_0\rangle \\
&- \mathrm{i}\theta(t_1 - t_{1'})\langle\Psi_0|\mathrm{i}\hbar\partial_{t_1}\hat{\psi}_H(1)\hat{\psi}^\dagger_H(1')|\Psi_0\rangle \\
&+ \hbar\delta(t_{1'} - t_1)\langle\Psi_0|\hat{\psi}^\dagger_H(1')\hat{\psi}_H(1)|\Psi_0\rangle \\
&+ \mathrm{i}\theta(t_{1'} - t_1)\langle\Psi_0|\hat{\psi}^\dagger_H(1')\mathrm{i}\hbar\partial_{t_1}\hat{\psi}_H(1)|\Psi_0\rangle . \qquad (3.54)
\end{aligned}$$

The deltafunction in the third term is symmetric, i.e., it is the same as in the first term. Hence, we can combine these two terms, which in turn leads to having an anticommutator inside the matrix element. This anticommutator, $\left\{\hat{\psi}_H(1), \hat{\psi}^\dagger_H(1')\right\}$, will then give a deltafunction over the spatial coordinates, and we may combine the deltafunctions of time and space. Also, the time-derivatives of the field operators inside the matrix element are then expanded as in Eq. (3.52), and by this manner we have

$$\begin{aligned}
\mathrm{i}\hbar\partial_{t_1} G_{(1)}(1;1') &= \underbrace{\hbar\delta(t_1 - t_{1'})\delta^{(3)}(\mathbf{x}_1 - \mathbf{x}_{1'})}_{=\delta(1-1')}\underbrace{\langle\Psi_0|\Psi_0\rangle}_{=1} \\
&- \mathrm{i}\theta(t_1 - t_{1'})\langle\Psi_0|\Bigg[\hat{h}(1)\hat{\psi}_H(1) \\
&\qquad + \int \mathrm{d}2\, v(1,2)\hat{\psi}^\dagger_H(2)\hat{\psi}_H(2)\hat{\psi}_H(1)\Bigg]\hat{\psi}^\dagger_H(1')|\Psi_0\rangle \\
&+ \mathrm{i}\theta(t_{1'} - t_1)\langle\Psi_0|\hat{\psi}^\dagger_H(1')\Bigg[\hat{h}(1)\hat{\psi}_H(1) \\
&\qquad + \int \mathrm{d}2\, v(1,2)\hat{\psi}^\dagger_H(2)\hat{\psi}_H(2)\hat{\psi}_H(1)\Bigg]|\Psi_0\rangle . \qquad (3.55)
\end{aligned}$$

From the last two terms of Eq. (3.55) we get altogether four terms. The ones with the one-particle Hamiltonian $\hat{h}$ can be combined as we notice that the field operators with the step functions give back exactly the one-particle Green's function in Eq. (3.50). The two terms with four field operators can also be combined together by using the step functions and the time-ordering operator. This operation gives rise to a definition for the two-particle Green's function

$$G_{(2)}(1,2;2,1^+) = (-\mathrm{i})^2\langle\Psi_0|\mathcal{T}_C[\hat{\psi}_H(1)\hat{\psi}^\dagger_H(1^+)\hat{\psi}^\dagger_H(2)\hat{\psi}_H(2)]|\Psi_0\rangle , \qquad (3.56)$$

where the notation $t^+ \equiv t + \epsilon \quad (\epsilon \to 0)$ stands for equal time limit for the field operators. The operator with $+$ acts slightly after the one without $+$, and after the operation, the small time interval between the operations ($\epsilon$) is taken to be zero. Afterall, we have for the time-derivative with respect to $t_1$

$$\mathrm{i}\hbar\partial_{t_1} G_{(1)}(1;1') = \hbar\delta(1-1') + \hat{h}(1)G(1,1') + \int \mathrm{d}2\, v(1^+,2)G_{(2)}(1,2;2^+,1') . \qquad (3.57)$$

We can similarly evaluate the derivative with respect to time $t_{1'}$, and finally combine our results for the equations of motion for the one-particle Green's function

$$\begin{cases}[\mathrm{i}\hbar\partial_{t_1} - \hat{h}(1)]G_{(1)}(1;1') = \hbar\delta(1-1') - \mathrm{i}\int \mathrm{d}2\, v(1^+,2)G_{(2)}(1,2;2^+,1') \\ [-\mathrm{i}\hbar\partial_{t_{1'}} - \hat{h}(1')]G_{(1)}(1;1') = \hbar\delta(1-1') - \mathrm{i}\int \mathrm{d}2\, v(1,2^+)G_{(2)}(1,2;2^+,1')\,. \end{cases} \tag{3.58}$$

These equations relate the one- and two-particle Green's functions together. The equations of motion can also be generalized up to $N$-particle Green's functions, which in turn will lead to the so-called *Martin–Schwinger hierarchy equations* [23]

$$\begin{aligned} & [\mathrm{i}\hbar\partial_{t_k} - \hat{h}(k)]G_{(N)}(1,\ldots,N;N',\ldots,1') \\ = \; & \sum_{j=1}^{N} (-1)^{k+j}\hbar\delta(k-j')G_{(N-1)}(1,\ldots,k-1,k+1,\ldots,N;N',\ldots,j'+1,j'-1,\ldots,1') \\ - \; & \mathrm{i}\int \mathrm{d}(N+1)\, v(k^+,N+1)G_{(N+1)}(1,\ldots,(N+1);(N'+1)^+,\ldots,1') \end{aligned} \tag{3.59}$$

and

$$\begin{aligned} & [-\mathrm{i}\hbar\partial_{t_{k'}} - \hat{h}(k')]G_{(N)}(1,\ldots,N;N',\ldots,1') \\ = \; & \sum_{j=1}^{N} (-1)^{k+j}\hbar\delta(j-k')G_{(N-1)}(1,\ldots,j-1,j+1,\ldots,N;N',\ldots,k'+1,k'-1,\ldots,1') \\ - \; & \mathrm{i}\int \mathrm{d}(N+1)\, v(k',(N+1)^+)G_{(N+1)}(1,\ldots,(N+1);(N'+1)^+,\ldots,1')\,. \end{aligned} \tag{3.60}$$

All in all, the equations of motion for the Green's functions relate the $N$-particle case to the cases of $N \pm 1$ particles. This is a general nature of the Green's functions: If we study a system of $N$ particles, we get information from the $N \pm 1$-particle systems as well, without even considering them separately.

As an example we consider a non-interacting approximation for the two-particle Green's function

$$G_{(2)}(1,2;2',1') = G_{(1)}(1;1')G_{(1)}(2;2') - G_{(1)}(1;2')G_{(1)}(2;1')\,, \tag{3.61}$$

which follows from the hierarchy equation by setting $v = 0$. With Eq. (3.61) we have from Eq. (3.58) that

$$\begin{aligned} & [\mathrm{i}\hbar\partial_{t_1} - \hat{h}(1)]G_{(1)}(1;1') \\ = \; & \hbar\delta(1-1') - \mathrm{i}\int \mathrm{d}2\, v(1,2^+)[G_{(1)}(1;2^+)G_{(1)}(2;1') - G_{(1)}(1;1')G_{(1)}(2;2^+)] \\ = \; & \hbar\delta(1-1') - \mathrm{i}\int \mathrm{d}2\, v(1,2^+)G_{(1)}(1;2^+)G_{(1)}(2;1') + \mathrm{i}\int \mathrm{d}2\, v(1,2^+)G_{(1)}(1;1')G_{(1)}(2;2^+) \\ = \; & \hbar\delta(1-1') - \mathrm{i}\int \mathrm{d}2\left[v(1^+,2)G_{(1)}(1;2^+) - \delta(1,2)\int \mathrm{d}3\, v(1,3)G_{(1)}(3;3^+)\right]G_{(1)}(2;1^+) \\ = \; & \hbar\delta(1-1') - \mathrm{i}\int \mathrm{d}2\, \Sigma(1,2)G_{(1)}(2;1')\,, \end{aligned} \tag{3.62}$$

where, on the last line, we introduced the *self-energy* $\Sigma$ as

$$\Sigma(1,2) = -\mathrm{i}v(1^+,2)G_{(1)}(1;2^+) + \mathrm{i}\delta(1,2)\int \mathrm{d}3\, v(1^+,3)G_{(1)}(3;3^+)\,. \tag{3.63}$$

As we see from Eqs. (3.62) and (3.63), all the interaction terms are included into self-energy. This, in fact, is the main concept of introducing such quantity as self-energy, because with it we are able to keep track of all the interactions within our many-particle system under consideration. Similarly we have

$$[\mathrm{i}\hbar\partial_{t_{1'}} - \hat{h}(1')]G_{(1)}(1;1') = \hbar\delta(1-1') - \mathrm{i}\int \mathrm{d}2\, G_{(1)}(1;2)\Sigma(2,1') \,. \tag{3.64}$$

If we define pictorial representations such as

$$G_{(1)}(1;1') \quad = \tag{3.65}$$

$$v(1,2) \quad = \tag{3.66}$$

,

we may write the self-energy as

$$\Sigma(1,2) \quad = \tag{3.67}$$

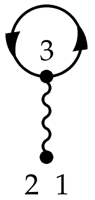

$$+$$

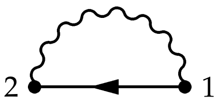

,

where an integration over an internal point 3 is to be understood. We can also express the two-particle Green's function in Eq. (3.61) pictorially.

$$G_{(2)}(1,2;2',1') = \tag{3.68}$$

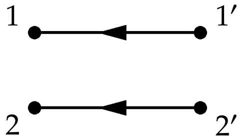

$$-$$

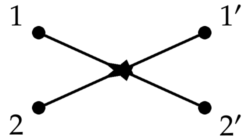

.

The Green's function $G_{(2)}(1,2;2',1')$ then describes the propagation of a pair of particles from space-time points $(1',2')$ to space-time points $(1,2)$. In Eq. (3.68) it is essential to note that in the second term the particles only pass by each other without any interaction.

The pictorial representations of the terms in Eqs. (3.67) and (3.68) are called *Feynman diagrams*. We will now construct the diagrammatic structure of many-particle theory, which ultimately boils down to the hierarchy equations in Eqs. (3.59) and (3.60).

## 3.3 Perturbative expansion

We now wish to add a small perturbation to the Hamiltonian

$$\hat{H}(z) \rightarrow \hat{H}(z) + \delta\hat{V}(z) \,, \tag{3.69}$$

and see how an expectation value of an operator would change in this process. We consider a contour from $z_i$ to $z_f$ and the following quantity

$$\begin{aligned} a(z_1,\ldots,z_f) &= \hat{U}(z_f,z_i)\mathcal{T}_C[\hat{A}_{1,H}(z_1)\cdots\hat{A}_{n,H}(z_n)] \\ &= \mathcal{T}_C[\mathrm{e}^{-\frac{\mathrm{i}}{\hbar}\int_C \mathrm{d}z\,\hat{H}(z)}\hat{A}_1(z_1)\cdots\hat{A}_n(z_n)] \,. \end{aligned} \tag{3.70}$$

We will give a certain form for the operators $\hat{A}$ later when we apply the expansion for the Green's function. Now transforming the Hamiltonian as in Eq. (3.69) we have

$$a(z_1,\ldots,z_f)+\delta a(z_1,\ldots,z_f)=\mathcal{T}_C[\mathrm{e}^{-\frac{\mathrm{i}}{\hbar}\int_C \mathrm{d}z\,\hat{H}(z)-\frac{\mathrm{i}}{\hbar}\int_C \mathrm{d}z'\,\delta V(z')}\hat{A}_1(z_1)\cdots\hat{A}_n(z_n)]\,. \tag{3.71}$$

On the other hand, we have an expression for $a(z_1,\ldots,z_f)$ in Eq. (3.70), and hence, we can insert it into Eq. (3.71) and then substract it from both sides to obtain

$$\begin{aligned}\delta a(z_1,\ldots,z_f) &= \mathcal{T}_C[\mathrm{e}^{-\frac{\mathrm{i}}{\hbar}\int_C \mathrm{d}z\,\hat{H}(z)-\frac{\mathrm{i}}{\hbar}\int_C \mathrm{d}z'\,\delta V(z')}\hat{A}_1(z_1)\cdots\hat{A}_n(z_n)]\\ &- \mathcal{T}_C[\mathrm{e}^{-\frac{\mathrm{i}}{\hbar}\int_C \mathrm{d}z\,\hat{H}(z)}\hat{A}_1(z_1)\cdots\hat{A}_n(z_n)]\,.\end{aligned} \tag{3.72}$$

Since we are dealing with small perturbation $\delta\hat{V}(z)$, we may expand the exponential as $\mathrm{e}^x \approx 1+x$, and by this manner we have

$$\begin{aligned}\delta a(z_1,\ldots,z_f) &= \mathcal{T}_C[\mathrm{e}^{-\frac{\mathrm{i}}{\hbar}\int_C \mathrm{d}z\,\hat{H}(z)}\mathrm{e}^{-\frac{\mathrm{i}}{\hbar}\int_C \mathrm{d}z'\,\delta V(z')}\hat{A}_1(z_1)\cdots\hat{A}_n(z_n)]\\ &- \mathcal{T}_C[\mathrm{e}^{-\frac{\mathrm{i}}{\hbar}\int_C \mathrm{d}z\,\hat{H}(z)}\hat{A}_1(z_1\cdots\hat{A}_n(z_n))]\\ &\approx \mathcal{T}_C[\mathrm{e}^{-\frac{\mathrm{i}}{\hbar}\int_C \mathrm{d}z\,\hat{H}(z)}\Big(1-\frac{\mathrm{i}}{\hbar}\int_C \mathrm{d}z'\,\delta V(z')\Big)\hat{A}_1(z_1)\cdots\hat{A}_n(z_n)]\\ &- \mathcal{T}_C[\mathrm{e}^{-\frac{\mathrm{i}}{\hbar}\int_C \mathrm{d}z\,\hat{H}(z)}\hat{A}_1(z_1)\cdots\hat{A}_n(z_n)]\\ &= -\frac{\mathrm{i}}{\hbar}\int_C \mathrm{d}z'\,\mathcal{T}_C[\mathrm{e}^{-\frac{\mathrm{i}}{\hbar}\int_C \mathrm{d}z\,\hat{H}(z)}\delta\hat{V}(z')\hat{A}_1(z_1)\cdots\hat{A}_n(z_n)]\\ &= -\frac{\mathrm{i}}{\hbar}\int_C \mathrm{d}z'\,\hat{U}(z_f,z_i)\mathcal{T}_C[\delta\hat{V}(z')\hat{A}_1(z_1)\cdots\hat{A}_n(z_n)]\,,\end{aligned} \tag{3.73}$$

where on the last but one line we noticed that two terms cancel each other. Then we take the perturbation to be of the form

$$\delta\hat{V}(z)=\lambda(z)\hat{A}\,, \tag{3.74}$$

where $\lambda(z)$ is a "well-behaving" function of $z$, and $\hat{A}$ is an operator independent of $z$. It is possible to show that by considering functional derivatives of Eq. (3.73) we have for the derivative of order $k$

$$\left.\frac{\delta^{(k)}a(z_1,\ldots,z_n)}{\delta\lambda(z'_1)\ldots\delta\lambda(z'_k)}\right|_{\lambda=0}=\Big(-\frac{\mathrm{i}}{\hbar}\Big)^k\hat{U}(z_f,z_i)\mathcal{T}_C[\hat{A}_H(z'_1)\cdots\hat{A}_H(z'_k)\hat{A}_{1,H}(z_1)\cdots\hat{A}_{n,H}(z_n)]\,, \tag{3.75}$$

and with Eq. (3.75) we have the perturbative expansion

$$\begin{aligned}a(z_1,\ldots,z_n) &= \sum_{k=0}^{\infty}\frac{1}{k!}\Big(-\frac{\mathrm{i}}{\hbar}\Big)^k\int_C \mathrm{d}z'_1\cdots\int_C \mathrm{d}z'_k\,\lambda(z'_1)\cdots\lambda(z'_k)\\ &\times\ \hat{U}(z_f,z_i)\mathcal{T}_C[\hat{A}_H(z'_1)\cdots\hat{A}_H(z'_k)\hat{A}_{1,H}(z_1)\cdots\hat{A}_{n,H}(z_n)]\,.\end{aligned} \tag{3.76}$$

This is a general expression which we will now use to derive the perturbative expansion for the Green's function.

We take the Hamiltonian to be

$$\hat{H}'_\lambda(z)=\hat{H}(z)+\lambda(z)\hat{V}\,, \tag{3.77}$$

with

$$\hat{H}(z) = \int \mathrm{d}\mathbf{x}\,\hat{\psi}^\dagger(\mathbf{x})\hat{h}(\mathbf{r},z)\hat{\psi}(\mathbf{x}) \tag{3.78}$$

$$\hat{V} = \int \mathrm{d}\mathbf{x}\int \mathrm{d}\mathbf{x}'\,v(\mathbf{r},\mathbf{r}')\hat{\psi}^\dagger(\mathbf{x})\hat{\psi}^\dagger(\mathbf{x}')\hat{\psi}(\mathbf{x}')\hat{\psi}(\mathbf{x})\,. \tag{3.79}$$

The function $\lambda(z)$ accounts for the powers of the interaction $\hat{V}$ which is the quantity with respect to the expansion is to be made. After the expansion we will set $\lambda(z) = 1$. Now we take the one-particle Green's function in Eq. (3.49)

$$G^{\lambda}_{(1)}(\mathbf{x},z;\mathbf{x}',z') = -\mathrm{i}\frac{\mathrm{Tr}\{\mathcal{T}_C[\mathrm{e}^{-\frac{\mathrm{i}}{\hbar}\int_C \mathrm{d}\zeta\, \hat{H}'_{\lambda}(\zeta)}\hat{\psi}(\mathbf{x},z)\hat{\psi}^{\dagger}(\mathbf{x}',z')]\}}{\mathrm{Tr}\{\mathrm{e}^{-\frac{\mathrm{i}}{\hbar}\int_C \mathrm{d}\zeta\, \hat{H}'_{\lambda}(\zeta)}\}}\,. \tag{3.80}$$

The numerator of Eq. (3.80) can be expanded by using the formula in Eq. (3.76), and we obtain

$$\begin{aligned} &\sum_{k=0}^{\infty}\frac{1}{k!}\left(-\frac{\mathrm{i}}{\hbar}\right)^k\int_C \mathrm{d}z_1\cdots\int_C \mathrm{d}z_k\,\lambda(z_1)\cdots\lambda(z_k) \\ \times\quad &\mathrm{Tr}\{\hat{U}(z_f,z_i)\mathcal{T}_C[\hat{V}_H(z_1)\cdots\hat{V}_H(z_k)\hat{\psi}_H(\mathbf{x},z)\hat{\psi}^{\dagger}_H(\mathbf{x}',z')]\}\,. \end{aligned} \tag{3.81}$$

The denominator of Eq. (3.80) is the same as Eq. (3.70) with $\hat{A}_k = 1$ for all $k$, i.e., we have similarly for the denominator

$$\sum_{k=0}^{\infty}\frac{1}{k!}\left(-\frac{\mathrm{i}}{\hbar}\right)^k\int_C \mathrm{d}z_1\cdots\int_C \mathrm{d}z_k\,\lambda(z_1)\cdots\lambda(z_k)\mathrm{Tr}\{\hat{U}(z_f,z_i)\mathcal{T}_C[\hat{V}_H(z_1)\cdots\hat{V}_H(z_k)]\}\,. \tag{3.82}$$

Then we put $\lambda = 1$ in Eqs. (3.81) and (3.82) and divide to obtain a perturbative expansion for the Green's function

$$\begin{aligned} &G_{(1)}(\mathbf{x},z;\mathbf{x}',z') \\ = \quad &-\mathrm{i}\left[\sum_{k=0}^{\infty}\frac{1}{k!}\left(-\frac{\mathrm{i}}{\hbar}\right)^k\int_C \mathrm{d}z_1\cdots\int_C \mathrm{d}z_k\,\mathrm{Tr}\{\hat{U}(z_f,z_i)\mathcal{T}_C[\hat{V}_H(z_1)\cdots\hat{V}_H(z_k)\hat{\psi}_H(\mathbf{x},z)\hat{\psi}^{\dagger}_H(\mathbf{x}',z')]\}\right] \\ &\times\left[\sum_{k=0}^{\infty}\frac{1}{k!}\left(-\frac{\mathrm{i}}{\hbar}\right)^k\int_C \mathrm{d}z_1\cdots\int_C \mathrm{d}z_k\,\mathrm{Tr}\{\hat{U}(z_f,z_i)\mathcal{T}_C[\hat{V}_H(z_1)\cdots\hat{V}_H(z_k)]\}\right]^{-1}\,. \end{aligned} \tag{3.83}$$

Next thing to do is to insert the operators $\hat{V}$ for the two-particle interactions. This procedure involves careful calculations with the time-ordering operator $\mathcal{T}_C$. It also turns out that the integrands both in the numerator and in the denominator can be expressed using non-interacting Green's functions $G^0$. The non-interacting Green's functions are then found from the hierarchy equations by using the so-called Wick's theorem, which produces determinant-form solutions for the $N$-particle Green's function. We will not go through this calculation due to limited space *and time*, but we state the final result which ultimately completes the many-particle perturbation theory:

$$\begin{aligned} &G_{(1)}(\mathbf{x},z;\mathbf{x}',z') = \\ &\left[\sum_{k=0}^{\infty}\frac{1}{k!}\left(\frac{\mathrm{i}}{2\hbar}\right)^k\int_C \mathrm{d}1\int_C \mathrm{d}1'\cdots\int_C \mathrm{d}k\int_C \mathrm{d}k'\,v_{11'}\cdots v_{kk'}\begin{vmatrix} G^0_{(1)}(\mathbf{x},z;\mathbf{x}',z') & G^0_{(1)}(\mathbf{x},z;1'') & \cdots & G^0_{(1)}(\mathbf{x},z;k'') \\ G^0_{(1)}(1;\mathbf{x}',z') & G^0_{(1)}(1;1'') & \cdots & G^0_{(1)}(1;k'') \\ \vdots & \vdots & \ddots & \vdots \\ G^0_{(1)}(k';\mathbf{x}',z') & G^0_{(1)}(k';1'') & \cdots & G^0_{(1)}(k';k'') \end{vmatrix}\right] \\ \times&\left[\sum_{k=0}^{\infty}\frac{1}{k!}\left(\frac{\mathrm{i}}{2\hbar}\right)^k\int_C \mathrm{d}1\int_C \mathrm{d}1'\cdots\int_C \mathrm{d}k\int_C \mathrm{d}k'\,v_{11'}\cdots v_{kk'}\begin{vmatrix} G^0_{(1)}(1;1'') & G^0_{(1)}(1;1'^{+}) & \cdots & G^0_{(1)}(1;k'^{+}) \\ G^0_{(1)}(1';1'') & G^0_{(1)}(1';1'^{+}) & \cdots & G^0_{(1)}(1';k'^{+}) \\ \vdots & \vdots & \ddots & \vdots \\ G^0_{(1)}(k';1'') & G^0_{(1)}(k';1'^{+}) & \cdots & G^0_{(1)}(k';k'^{+}) \end{vmatrix}\right]^{-1}\,. \end{aligned} \tag{3.84}$$

In Eq. (3.84) we have expressed the "full" one-particle Green's function $G$ as an infinite sum of non-interacting one-particle Green's functions $G^0$. For the two-particle interactions we used notation $v_{kk'} = v(k^+, k')$, where the superscript $+$ denotes the equal time limit: $k^+ = k + \epsilon$ , $\epsilon \to 0$.

We admit it; the "magic" equation (3.84) seems like a tall order. To lighten the mathematics a little, the terms of the infinite sum are often expressed not by horrible equations but rather intuitive pictures called Feynman diagrams. For instance, let us take a first order approximation, i.e., we take only the terms up to linear order in $v$. For the numerator we have

$$\begin{aligned} &\frac{1}{0!}\left(\frac{\mathrm{i}}{2\hbar}\right)^0 G^0_{(1)}(\mathbf{x},z;\mathbf{x}',z') \\ +\ &\frac{1}{1!}\left(\frac{\mathrm{i}}{2\hbar}\right)^1 \int_C \mathrm{d}1 \int_C \mathrm{d}1'\, v_{11'} \begin{vmatrix} G^0_{(1)}(\mathbf{x},z;\mathbf{x}',z') & G^0_{(1)}(\mathbf{x},z;1'') & G^0_{(1)}(\mathbf{x},z;1'^+) \\ G^0_{(1)}(1;\mathbf{x}',z') & G^0_{(1)}(1;1'') & G^0_{(1)}(1;1'^+) \\ G^0_{(1)}(1';\mathbf{x}',z') & G^0_{(1)}(1';1'') & G^0_{(1)}(1';1'^+) \end{vmatrix} . \end{aligned} \tag{3.85}$$

Expanding the determinant gives six terms, and all in all we have seven terms for the numerator up to first order

$$\begin{aligned} &G^0_{(1)}(\mathbf{x},z;\mathbf{x}',z') \\ +\ &\frac{\mathrm{i}}{2\hbar} G^0_{(1)}(\mathbf{x},z;\mathbf{x}',z') \int \mathrm{d}1 \int \mathrm{d}1'\, v_{11'} \left[ G^0_{(1)}(1;1'') G^0_{(1)}(1';1'^+) - G^0_{(1)}(1;1'^+) G^0_{(1)}(1';1'') \right] \\ -\ &\frac{\mathrm{i}}{2\hbar} \int \mathrm{d}1 \int \mathrm{d}1'\, v_{11'} G^0_{(1)}(1;\mathbf{x}',z') \left[ G^0_{(1)}(\mathbf{x},z;1'') G^0_{(1)}(1';1'^+) - G^0_{(1)}(\mathbf{x},z;1'^+) G^0_{(1)}(1';1'') \right] \\ +\ &\frac{\mathrm{i}}{2\hbar} \int \mathrm{d}1 \int \mathrm{d}1'\, v_{11'} G^0_{(1)}(1';\mathbf{x}',z') \left[ G^0_{(1)}(\mathbf{x},z;1'') G^0_{(1)}(1;1'^+) - G^0_{(1)}(\mathbf{x},z;1'^+) G^0_{(1)}(1;1'') \right] . \end{aligned} \tag{3.86}$$

Now using the diagrammatic expressions in Eq. (3.65) we may write Eq. (3.86) as

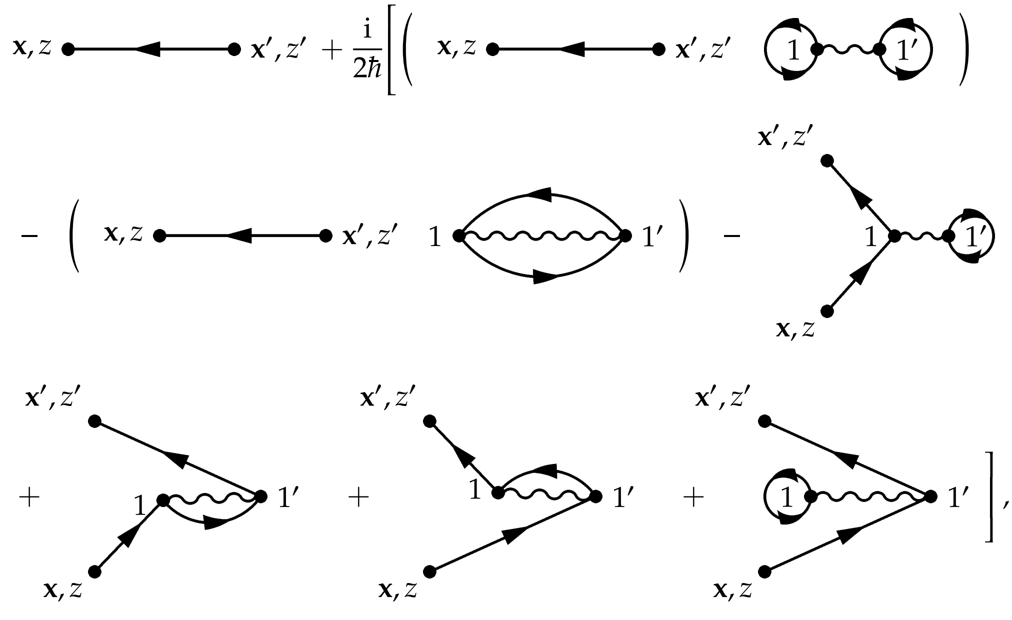

(3.87)

where in the first two terms inside the square brackets a product is to be understood between the two disconnected diagrams. Similarly for the denominator we have up to first order

$$
\begin{aligned}
&\frac{1}{0!}\left(\frac{\mathrm{i}}{2\hbar}\right)^0+\frac{1}{1!}\left(\frac{\mathrm{i}}{2\hbar}\right)\int \mathrm{d}1 \int \mathrm{d}1'\, v_{11'}\begin{vmatrix} G^0_{(1)}(1;1'') & G^0_{(1)}(1;1'^+) \\ G^0_{(1)}(1';1'') & G^0_{(1)}(1';1'^+) \end{vmatrix} \\
= \;& 1+\frac{\mathrm{i}}{2\hbar}\int \mathrm{d}1 \int \mathrm{d}1'\, v_{11'}\left[G^0_{(1)}(1;1'')G^0_{(1)}(1';1'^+)-G^0_{(1)}(1;1'^+)G^0_{(1)}(1';1'')\right]
\end{aligned}
$$

$= 1+\frac{\mathrm{i}}{2\hbar}\Big[$ 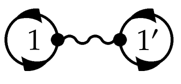 $-\; 1$ 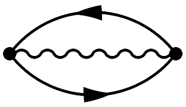 $1' \Big].$ (3.88)

The denominator of the Green's function, i.e., Eq. (3.88) is, in fact, the so-called vacuum amplitude which was discussed in the previous chapter. This quantity is the probability amplitude for the transition from the vacuum state back to the same vacuum state. Illustrating this property, all the $G^0$-lines in Eq. (3.88) begin and end on the endpoints of interaction lines. It is, however, essential to notice that these diagrams are only in the first order, and there are lots of diagrams left in higher orders which also contribute to the vacuum amplitude.

From Eqs. (3.87) and (3.88) we can calculate the full Green's function for single-particle propagation from spacetime point $\mathbf{x}', z'$ to $\mathbf{x}, z$. We also see that if we set $v = 0$, i.e., all the terms with wiggly lines vanish, we have $G = G^0$. As we are evaluating a ratio between two large sums, it is a good assumption that some terms will cancel. If we look carefully to Eqs. (3.87) and (3.88) we see that the first two terms inside the square brackets can be combined as they have common multiplier. This common multiplier happens to be exactly the denominator, hence, we have a cancellation of diagrams. The first two terms inside the square brackets are called *disconnected* diagrams, as they are composed of two different diagrams. It can, in fact, be proven that all the disconnected diagrams cancel with the denominator in every order. This leads to great reduction of diagrams to be considered. Also what we see immediately, is that the diagrams in the numerator are all the possibilities of connecting four spacetime points with one wiggly line and three solid lines. All the other combinations (other than these) do not give any more information about the propagation, and all diagrams that are necessary to consider are exactly only these *topologically inequivalent* ones.

## 3.4 Dyson equation

By considering only the connected and topologically inequivalent diagrams, we may introduce an expression for the full Green's function

$$
G = G^0 + G^0\Sigma G^0 + G^0\Sigma G^0\Sigma G^0 + G^0\Sigma G^0\Sigma G^0\Sigma G^0 + \ldots
$$

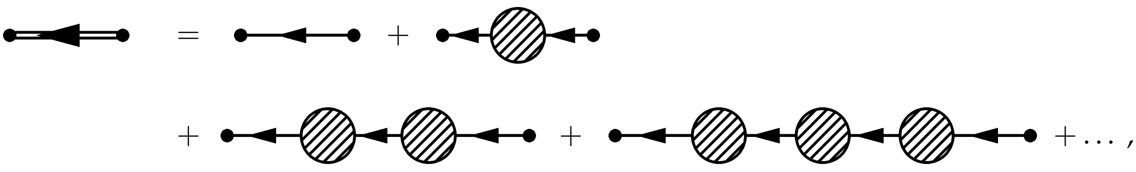

(3.89)

where the self-energy insertions $\Sigma$ (shaded blobs) contain all the so-called *irreducible* diagrams, i.e., all the diagrams that do not break up into two disjoint parts by cutting a single $G^0$ line:

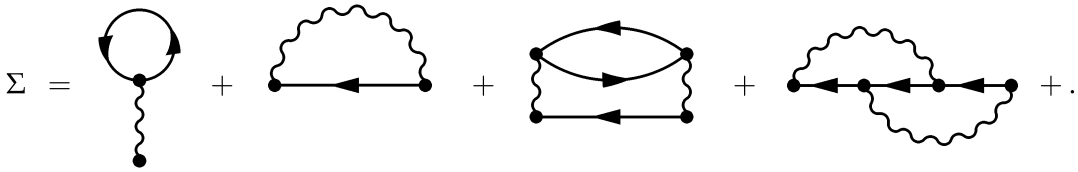

(3.90)

In Eq. (3.89) we denoted the full Green's function by double line, and with this notation we may also write the infinite sum as

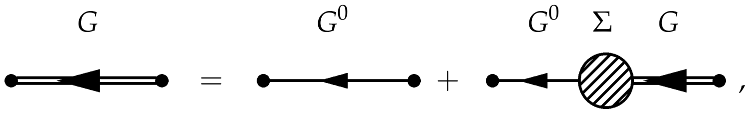

(3.91)

or as

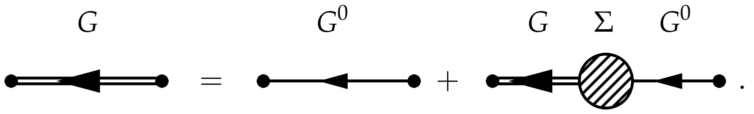

(3.92)

By reverting our pictorial expressions in Eqs. (3.91) and (3.92) we may write the full Green's functions explicitly as

$$G_{(1)}(1;1') = \begin{cases} G^0_{(1)}(1;1') + \int \mathrm{d}2 \int \mathrm{d}2' \, G^0_{(1)}(1;2)\Sigma(2,2')G_{(1)}(2';1') \\ \\ G^0_{(1)}(1;1') + \int \mathrm{d}2 \int \mathrm{d}2' \, G_{(1)}(1;2)\Sigma(2,2')G^0_{(1)}(2';1') \, . \end{cases} \tag{3.93}$$

These are known as the Dyson equation, which is a solution to the equation of motion for the Green's function – the hierarchy equation. From the Dyson equation we see, provided that we know the self-energy, that the full Green's function is obtained by solving an integral equation *self-consistently*, i.e., we solve for the Green's function $G$ first by inserting $G = G^0$ to the integrand, and then inserting these solutions back to the integral equation iteratively. Eventually we will obtain the converged result.

We may manipulate the expression in the Dyson equation as (with the shorthand notation)

$$G = G^0 + G^0\Sigma G \tag{3.94}$$

can be inverted by multiplying from the right by $(G^0)^{-1}$, and then combining the terms with $G$ as a common multiplier. We then have

$$\left[(G^0)^{-1} - \Sigma\right] G = \mathbb{1}, \tag{3.95}$$

from where we can solve for the full Green's function

$$G = \left[(G^0)^{-1} - \Sigma\right]^{-1} \, . \tag{3.96}$$

The formula in Eq. (3.96) is, for us, the most essential tool for studying the many-particle systems in Chap. 5. We first need to obtain an expression for the self-energy $\Sigma$ by expanding the non-interacting Green's function in terms of the interaction $v$. Then we insert both the non-interacting Green's function and the self-energy into the Dyson equation (3.96) and we have our result. We still need to evaluate the self-energy $\Sigma$, and for this task we need to consider some rules for the diagrammatic calculations.

## 3.5 Feynman rules

We have already seen some rules that give explicit prescriptions to evaluate certain physical quantities that are expressed in terms of Feynman diagrams. For instance, from (3.87) and (3.88) we see that the sign in front of a diagram varies. In fact, the prefactor is proportional to $(-1)^l$, where $l$ is the number of fermion loops within a diagram. This is one example of the rules regarding how to do calculations with the diagrams.

So far, we have been working in spacetime $(\mathbf{r}, t)$, but in the remainder of this thesis we will consider the equilibrium case in which the Hamiltonian is time-independent. In that case the Green's function depends only on the difference of its time-arguments and it will be convenient to go to frequency space by defining the non-interacting Green's function via Fourier transform

$$G^0(\mathbf{x},\mathbf{x}';\omega) = \int_{-\infty}^{\infty} \mathrm{d}\tau\, \mathrm{e}^{\mathrm{i}\omega\tau} G^0(\mathbf{x},\mathbf{x}';\tau)\,, \tag{3.97}$$

where $\tau = t - t'$. Furthermore, in a general basis $\{\varphi_n\}$ [see Eqs. (2.30) and (2.31)] we can write

$$\begin{aligned} G^0(\mathbf{x},t;\mathbf{x}',t') &= -\mathrm{i}\left\langle \mathcal{T}_C[\hat{\psi}_H(\mathbf{x},t)\hat{\psi}^\dagger_H(\mathbf{x}',t')]\right\rangle \\ &= \sum_{i,j} \varphi_i(\mathbf{r})\varphi^*_j(\mathbf{r}')G^0_{ij}(t,t')\,, \end{aligned} \tag{3.98}$$

where $G^0_{ij}(t,t') = -\mathrm{i}\langle \mathcal{T}_C[\hat{a}_{i,H}(t)\hat{a}^\dagger_{j,H}(t')]\rangle$. Hence, Eq. (3.97) is of the form

$$G^0(\mathbf{x},\mathbf{x}';\omega) = \sum_{i,j} \varphi_i(\mathbf{r})\varphi^*_j(\mathbf{r}')G^0_{ij}(\omega) \tag{3.99}$$

with

$$G^0_{ij}(\omega) = \int_{-\infty}^{\infty} \mathrm{d}\tau\, \mathrm{e}^{\mathrm{i}\omega\tau} G^0_{ij}(\tau)\,. \tag{3.100}$$

We will give the Feynman rules for this representation. From the diagrammatic analysis of the Green's function in frequency space we easily get information about the energies in a system under consideration (as discussed earlier within the topic of propagators in general). The frequency $\omega$ will be a conserved quantity in dynamical processes, and the energy via relation $E = \hbar\omega$, is readily obtained. Also, as stated earlier, we are interested in the self-energy calculations since the full Green's function is obtained from the self-energy and from the non-interacting Green's function by using the Dyson equation. We will therefore introduce nothing more than the Feynman rules for the self-energy $\Sigma$.

1. Draw all connected and topologically inequivalent Feynman diagrams, which contribute to the self-energy, i.e., the ones that are *irreducible*.

2. Assign a direction to each Green's function line $G^0$ and each interaction line $v$, and conserve the frequency at each vertex. An integration is to be performed over all internal frequencies, and a summing over all internal indices as

$$\sum_{kl} \int \frac{\mathrm{d}\omega}{2\pi}\,.$$

3. For every diagram assign a prefactor

$$(-1)^l \left(\frac{\mathrm{i}}{\hbar}\right)^n ,$$

where $l$ is the number of closed $G^0$ loops, and $n$ is the number of interaction lines.

4. When a Green's function line closes on itself or is joined by the same interaction line, insert a convergence factor $\mathrm{e}^{\mathrm{i}\omega\eta}$ and take the limit $\eta \to 0$ after the calculation.

As an example we draw here not all but one irreducible diagram – the so-called *tadpole* diagram

$$\Sigma_{ij}(\omega) \quad =$$

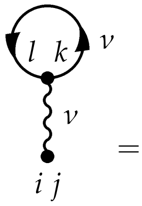

$$= \quad (-1)\left(\frac{\mathrm{i}}{\hbar}\right)\sum_{kl}\int \frac{\mathrm{d}\nu}{2\pi}\mathrm{e}^{\mathrm{i}\nu\eta}G^0_{lk}(\nu)v_{ikjl} \qquad (\eta \to 0)\,. \tag{3.101}$$

We see that in Eq. (3.101) there is one closed fermion loop, which gives the factor $-1$ and the rest of the prefactor is of order 1 because of the one interaction line. We have an internal frequency $\nu$ which is integrated over, and internal indices $k$ and $l$ which are summed over. Also, the Green's function line closes on itself, and we must insert the convergence factor stated by the 4th rule. For the non-interacting Green's function $G^0_{lk}$ and for the interaction between indices $i, j, k$ and $l$ we have not yet introduced any explicit forms, and we will leave them as they are. As this diagram contributes to the self-energy, we must assume that a Green's function line with frequency $\omega$ is joined to point $j$ and is left from point $i$.

The nature of Feynman diagrams and especially the calculations regarding them will become much clearer when we consider some concrete examples in Chap. 5. There we will also pay more attention to the actual form of the non-interacting Green's function $G^0$. Before these calculations, there seems to be at least one barrier in front of us – how to evaluate the integrals in Eq. (3.101)?

# Chapter 4

# Mathematical tools

The ideas presented in this chapter are mainly based upon the lecture notes of an advanced course in mathematical methods in physics by Markku Lehto, and Ref. [2].

## 4.1 Complex contour integrals

When we consider complex numbers instead of real numbers, the usual integral calculus differs remarkably because of the extra degree of freedom of the studied number — the imaginary part. Following the variation of a complex number $z \in \mathbb{C}$ takes us to a path in the complex plane. As the complex number varies along a path, one thing springing to our mind is that the integral of a complex-variable function $f(z)$ is a line integral:

$$\int_C f(z)\mathrm{d}z \qquad \text{or} \qquad \oint_C f(z)\mathrm{d}z \,. \tag{4.1}$$

This integral is, in complex analysis, called a contour integral as the integration path $C$ is called a contour. There are several strategies to evaluate these contour integrals. The simplest case arises when we can express the contour $C$ in terms of a real parameter $t$, and in this case we can perform the integration as we would do in the case of a real line integral. Another simple case is when the function of a complex variable can be split into real and imaginary part

$$f(z) = u(x, y) + \mathrm{i}v(x, y) \,. \tag{4.2}$$

In this case, as a reduction, only two real line integrals appear. More complicated cases involve keeping the contour integral as such, and developing some results that allow us to evaluate it directly. These results are mostly invented single-handedly by Augustin-Louis Cauchy in the 19th century [29].

### 4.1.1 Cauchy's integral theorem

Before we get to the integral calculus of complex functions, we first need to study the nature of such functions. A way to evaluate a complex number $w$ from the complex number $z = x + \mathrm{i}y$, where $x$ and $y$ are real numbers, as $w = f(z)$, is called a function of the complex variable. The function $w = f(z)$ is called a *single-valued* function if $w$ is determined uniquely by $z$, otherwise the function is called *multiple-valued*. However, we may consider a multiple-valued function to consist of a set of single-valued functions. We will concentrate on the single-valued functions here.

The complex-variable function $w = f(z)$ can be imagined as a mapping of a set of points in one complex plane to a new set of points in another complex plane. (See Fig. 4.1.)

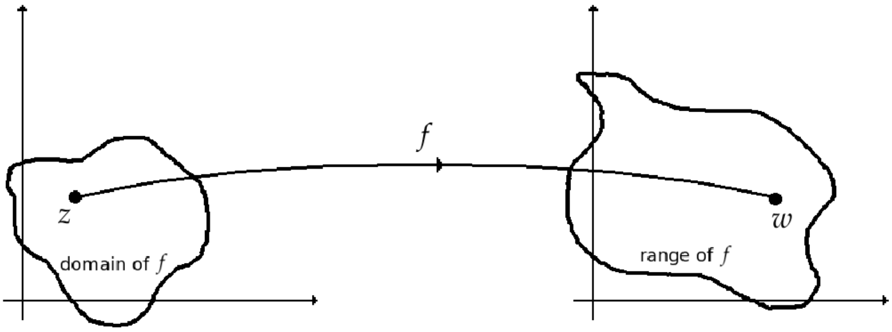

Figure 4.1: Visualization of a function of complex variable $w = f(z)$.

We then discuss shortly the topic of complex differentiation as this relates strongly to complex integration. For the complex differentiation we take the idea from the calculus of real functions. We claim the real-kind definition of differentiation for $w = f(z)$ through the *mean-value theorem*:

$$\frac{\mathrm{d}w}{\mathrm{d}z} = \lim_{\Delta z \to 0} \left[ \frac{f(z + \Delta z) - f(z)}{\Delta z} \right] \tag{4.3}$$

which leads, for $z = x + \mathrm{i}y$ and $f(z) = u(x, y) + \mathrm{i}v(x, y)$, to

$$\frac{\mathrm{d}w}{\mathrm{d}z} = \lim_{\substack{\Delta x \to 0 \\ \Delta y \to 0}} \left[ \frac{u(x + \Delta x, y + \Delta y) - u(x, y) + \mathrm{i}v(x + \Delta x, y + \Delta y) - \mathrm{i}v(x, y)}{\Delta x + \mathrm{i}\Delta y} \right] . \tag{4.4}$$

This limit must then exist uniquely, no matter how $\Delta z$ tends to zero. Although there is an infinite number of paths to approach a point in the complex plane, there still are only two *independent* paths, say parallel to the $x$-axis ($\Delta y = 0$) and parallel to the $y$-axis ($\Delta x = 0$). Inserting these conditions into Eq. (4.4) we find that

$$\frac{\mathrm{d}w}{\mathrm{d}z} = \frac{\partial u}{\partial x} + \mathrm{i}\frac{\partial v}{\partial x} \tag{4.5}$$

and

$$\frac{\mathrm{d}w}{\mathrm{d}z} = \frac{\partial v}{\partial y} - \mathrm{i}\frac{\partial u}{\partial y} . \tag{4.6}$$

A derivative exists and it is unique if $\frac{\partial u}{\partial x} = \frac{\partial v}{\partial y}$ and $\frac{\partial v}{\partial x} = -\frac{\partial u}{\partial y}$. These relations, called the *Cauchy-Riemann* equations, provide (the necessary and sufficient) conditions for differentiability: $u, v$ and their partial derivatives must be continuous. We can now use any of the four equivalent expressions: if $f(z)$ is differentiable, then $\frac{\mathrm{d}f}{\mathrm{d}z}$ is given by

$$\frac{\mathrm{d}f}{\mathrm{d}z} = \frac{\partial u}{\partial x} + \mathrm{i}\frac{\partial v}{\partial x} = \frac{\partial v}{\partial y} - \mathrm{i}\frac{\partial u}{\partial y} = \frac{\partial u}{\partial x} - \mathrm{i}\frac{\partial u}{\partial y} = \frac{\partial v}{\partial y} + \mathrm{i}\frac{\partial v}{\partial x} . \tag{4.7}$$

**Definition.** *A single-valued function $w = f(z)$ that possesses a unique and finite derivative $\frac{\mathrm{d}f}{\mathrm{d}z}$ at every point in a region $\mathcal{R}$ of the complex plane, is said to be analytic in $\mathcal{R}$.*

The analyticity of functions of a complex variable can therefore be tested by the Cauchy-Riemann equations. Although functions of a complex variable have fairly simple forms in regions where they are analytic, we often end up studying points where complex functions are not analytic in order to obtain deeper understanding about these functions.

If the function $w = f(z)$ is analytic in a certain point, the point is called a *regular point* of the function, whereas the points where the function is not analytic are called *singular points*, or singularities of the function. If the function is analytic in a punctured neighbourhood of a singularity, then the singular point is an isolated singularity. Usually, functions become unbounded at singular points, and by a concept of *pole* we can classify the meaning of a singularity conveniently.

**Definition.** *If in a small neighbourhood of an isolated singularity $z = z_0$ the function $f(z)$ behaves like $(z - z_0)^{-n}$, where $n \in \mathbb{Z}_+$, then $z = z_0$ is a pole of order $n$. If $n = 1$, the point $z = z_0$ is called a simple pole.*

One final remark concerning the integration path and the region in the complex plane before stating the famous integral theorem.

**Definition.** *A curve is piecewise smooth (PWS) if it is made up of finite number of pieces, each of which is smooth. A simple closed curve does not intersect or touch itself. A simply-connected region is bounded by a single closed curve, i.e., it is a region with no holes in it.*

**Theorem** (Cauchy's integral theorem)**.** *For a PWS simple closed curve $C$, and $f(z)$ analytic in a simply-connected region containing $C$ we have*

$$\oint_C f(z)\mathrm{d}z = 0\,. \tag{4.8}$$

*Proof.* Start with $z = x + \mathrm{i}y$ and expand the function as $f(z) = u(x,y) + \mathrm{i}v(x,y)$:

$$\oint_C f(z)\mathrm{d}z = \oint_C (u + \mathrm{i}v)\,(\mathrm{d}x + \mathrm{i}\mathrm{d}y) = \oint_C (u\mathrm{d}x - v\mathrm{d}y) + \mathrm{i}\oint_C (v\mathrm{d}x + u\mathrm{d}y)\ .$$

Then by introducing vectors $\mathbf{w_1} = (u, -v, 0)$, $\mathbf{w_2} = (v, u, 0)$ and $\mathrm{d}\mathbf{r} = (\mathrm{d}x, \mathrm{d}y, 0)$, we obtain

$$\oint_C f(z)\mathrm{d}z = \oint_C \mathbf{w_1}\cdot\mathrm{d}\mathbf{r} + \mathrm{i}\oint_C \mathbf{w_2}\cdot\mathrm{d}\mathbf{r}\,.$$

We can now use *Stokes' theorem* (see, e.g., Ref. [2, p. 65]) to rewrite the line integrals as surface integrals

$$\oint_C f(z)\mathrm{d}z = \iint_S (\nabla\times\mathbf{w_1} + \mathrm{i}\nabla\times\mathbf{w_2})\cdot\mathrm{d}\mathbf{S}\,.$$

Here $S$ is an open surface in 3-dimensional euclidean space bounded by the path $C$. Expanding the curls inside the integrand gives

$$\begin{aligned}\nabla\times\mathbf{w_1} &= \left(0, 0, -\frac{\partial v}{\partial x} - \frac{\partial u}{\partial y}\right)\\ \nabla\times\mathbf{w_2} &= \left(0, 0, \frac{\partial u}{\partial x} - \frac{\partial v}{\partial y}\right),\end{aligned}$$

and both these give exactly null vectors due to the Cauchy-Riemann equations. Therefore we have proven the theorem (4.8). □

One important corollary of Cauchy's integral theorem is the so-called *path deformation*. We can deform closed contour across any region of the complex plane over which $f(z)$ is analytic without changing the value of the integral $\oint_C f(z)\mathrm{d}z$. Although the contour cannot be moved across singularities, it can be made to collapse around them.

For instance, consider a doubly-connected region $\mathcal{R}$, encircled counter-clockwise (CCW) with a contour $C$, with two isolated singularities ('is') in Fig. 4.2. We can, without changing the value of the integral, deform the contour $C$ into $C'$. To think this statement more carefully, consider the contour $C'$ inside $C$, and connect the contours from one point as in Fig. 4.3. The opposing lines between $C$ and $C'$ cancel each other due to an elementary property of line integrals. (We consider those lines the same except for the orientation.) The doubly-connected region now becomes simply connected and we can use Cauchy's integral theorem as follows

Figure 4.2: Doubly-connected region $\mathcal{R}$ with two isolated singularities.

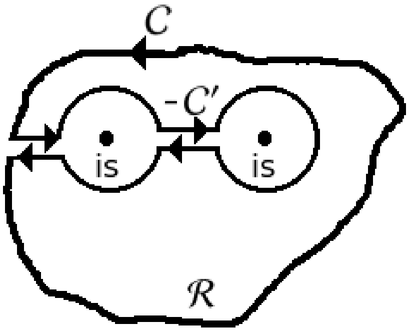

Figure 4.3: Doubly-connected region becomes simply-connected.

$$
\begin{aligned}
\oint_C f(z)\mathrm{d}z \;&+\; \oint_{-C'} f(z)\mathrm{d}z \;=\; 0\\
\oint_C f(z)\mathrm{d}z \;&-\; \oint_{C'} f(z)\mathrm{d}z \;=\; 0\\
\Rightarrow \qquad \oint_C f(z)\mathrm{d}z \;&=\; \oint_{C'} f(z)\mathrm{d}z\,. \qquad (4.9)
\end{aligned}
$$

Also, the opposing lines of the contour $C'$ between the singularities cancel each other. Hence, we are left with two contours, both encircling one singularity CCW. Generally this means that a closed contour $C$ enclosing $n$ singularities can be replaced by separately closed contours $C_i$ ($i \in [0, n]$), each of which is enclosing one singularity, i.e.,

$$\oint_C f(z)\mathrm{d}z = \sum_{i=1}^{n} \oint_{C_i} f(z)\mathrm{d}z\,. \tag{4.10}$$

As an example, consider an integral

$$\oint_C f(z)\mathrm{d}z = \oint_C \frac{\mathrm{d}z}{(z-z_0)^n} \tag{4.11}$$

with the point $z_0$ being inside the contour $C$. We can now deform the contour $C$ into a small circular contour around the point $z_0$. We can also express the complex number $z - z_0$ in a polar form $z - z_0 = \rho \mathrm{e}^{\mathrm{i}\theta}$, where $\rho$ is the radius of the small circle around $z_0$. Now we have

$$\begin{aligned}
\oint_C \frac{\mathrm{d}z}{(z-z_0)^n} &= \oint_{|z-z_0|=\rho} \frac{\mathrm{d}z}{(z-z_0)^n}\\
&= \mathrm{i}\rho^{1-n} \int_0^{2\pi} \mathrm{e}^{\mathrm{i}(1-n)\theta}\mathrm{d}\theta\\
&= \begin{cases} 0 & \text{for } n \neq 1\\ 2\pi\mathrm{i} & \text{for } n = 1\,. \end{cases}
\end{aligned} \tag{4.12}$$

### 4.1.2 Cauchy's integral formula

To this end, we simply introduce a powerful tool for evaluating complex contour integrals.

**Theorem** (Cauchy's integral formula). *Assume that $f(z)$ is analytic in a simply-connected region $\mathcal{R}$, $C$ is a PWS simple closed contour in $\mathcal{R}$, oriented CCW, and $z$ is any point lying inside $C$. Then*

$$f(z) = \frac{1}{2\pi\mathrm{i}} \oint_C \frac{f(\zeta)\mathrm{d}\zeta}{\zeta - z}\,. \tag{4.13}$$

*Proof.* The proof of this theorem is actually a fairly simple calculation, as follows

$$\begin{aligned}
\frac{1}{2\pi\mathrm{i}} \oint_C \frac{f(\zeta)\mathrm{d}\zeta}{\zeta - z} &\overset{\text{add zero}}{=} \frac{1}{2\pi\mathrm{i}} \oint_C \frac{f(\zeta) - f(z) + f(z)}{\zeta - z}\mathrm{d}\zeta\\
&= \frac{1}{2\pi\mathrm{i}} \oint_C \frac{f(\zeta) - f(z)}{\zeta - z}\mathrm{d}\zeta + \frac{f(z)}{2\pi\mathrm{i}} \oint_C \frac{\mathrm{d}\zeta}{\zeta - z}\\
&\overset{\text{path deform.}}{=} \frac{1}{2\pi\mathrm{i}} \oint_{|\zeta-z|=\rho} \underbrace{\frac{f(\zeta) - f(z)}{\zeta - z}}_{=\frac{\mathrm{d}f(\zeta)}{\mathrm{d}\zeta}\text{ , when } \rho\to 0} \mathrm{d}\zeta + \frac{f(z)}{2\pi\mathrm{i}} \underbrace{\oint_{|\zeta-z|=\rho} \frac{\mathrm{d}\zeta}{\zeta - z}}_{=2\pi\mathrm{i}\text{ , see Eq. (4.12)}}\\
&= \frac{1}{2\pi\mathrm{i}} \underbrace{\oint_{|\zeta-z|=\rho} \overbrace{\mathrm{d}f(\zeta)}^{\text{total differential}}}_{=0} + \frac{f(z)}{\cancel{2\pi\mathrm{i}}}\cancel{2\pi\mathrm{i}}\\
&= f(z)\,,
\end{aligned}$$

which gives the desired result. □

With this result we can determine $f(z)$ throughout the entire region enclosed by $C$ if we only know $f(z)$ on $C$. It also turns out that an analytic function is infinitely differentiable, i.e., all the derivatives of an analytic function are analytic. To see this, we differentiate both sides of Eq. (4.13), assuming that we are allowed to differentiate under the integral sign:

$$\begin{aligned}
\frac{\mathrm{d}f}{\mathrm{d}z} &= \frac{1}{2\pi\mathrm{i}}\oint_C \frac{f(\zeta)}{(\zeta-z)^2} \\
\frac{\mathrm{d}^2 f}{\mathrm{d}z^2} &= \frac{2}{2\pi\mathrm{i}}\oint_C \frac{f(\zeta)}{(\zeta-z)^3} \\
&\vdots \\
\frac{\mathrm{d}^n f}{\mathrm{d}z^n} &= \frac{n!}{2\pi\mathrm{i}}\oint_C \frac{f(\zeta)}{(\zeta-z)^{n+1}}\,, \qquad (4.14)
\end{aligned}$$

for all $n \in \mathbb{N}$. Note how the minus signs vanish when taking derivatives with respect to $z$. This general result in Eq. (4.14), for the integrands with higher order poles, is called Cauchy's *extended* integral formula.

### 4.1.3 Important improper integrals

Consider a contour integral as in Eq. (4.13)

$$\oint_C \frac{f(\zeta)}{\zeta-z}\mathrm{d}\zeta = 2\pi\mathrm{i}f(z)\,, \qquad (4.15)$$

where the contour $C$ consists of an interval $[-\rho,\rho]$ on the real axis and a semicircular arc $C_\rho$ of radius $\rho$ in the upper half plane (UHP), see Fig. 4.4.

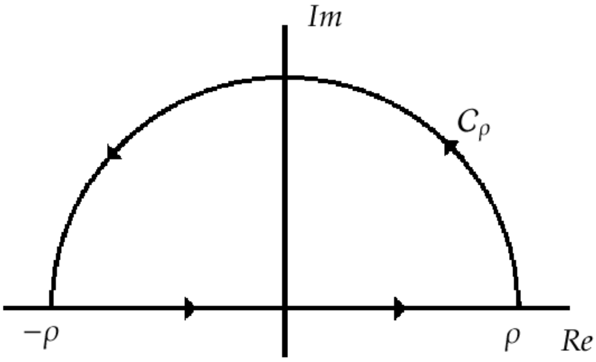

Figure 4.4: Contour $C$ that consists of two parts: an interval on the real axis and a semicircular arc in the UHP.

The integral in Eq. (4.15) can now be calculated in parts

$$\oint_C \frac{f(\zeta)}{\zeta-z}\mathrm{d}\zeta = \int_{-\rho}^{\rho} \frac{f(\zeta)}{\zeta-z}\mathrm{d}\zeta + \int_{C_\rho} \frac{f(\zeta)}{\zeta-z}\mathrm{d}\zeta\,. \qquad (4.16)$$

If we now take the limit $\rho \to \infty$ we get:

1. $C$ encloses all the $n$ singularities in the UHP, and due to Eq. (4.10) and Cauchy's integral formula we get
$$\oint_C \frac{f(\zeta)}{\zeta - z} \mathrm{d}\zeta = \sum_{j=1}^{n} \oint_{C_j} \frac{f(\zeta)}{\zeta - z} \mathrm{d}\zeta = 2\pi\mathrm{i} \sum_{j=1}^{n} f(z_j) \, .$$
2. denoting $\frac{f(\zeta)}{\zeta - z}$ as $g(\zeta)$ we get
$$\begin{aligned} \lim_{\rho\to\infty} \int_{C_\rho} \frac{f(\zeta)}{\zeta - z} \mathrm{d}\zeta &= \lim_{\rho\to\infty} \int_{C_\rho} g(\zeta) \mathrm{d}\zeta \\ &= \lim_{\rho\to\infty} \int_0^{\pi} g\left(\mathrm{e}^{\mathrm{i}\rho\theta}\right) \mathrm{i}\rho \mathrm{e}^{\mathrm{i}\rho\theta} \mathrm{d}\theta \\ &= 0 \, , \end{aligned}$$
provided that, when $|\zeta| \to \infty$, $\left|g(\zeta)\right| = \left|g\left(\mathrm{e}^{\mathrm{i}\rho\theta}\right)\right|$ decays at least as rapidly as $|\zeta|^{-2} = \rho^{-2}$ in the UHP.

Thus, as the integral over the semicircular path vanishes, we obtain
$$\int_{-\infty}^{\infty} \frac{f(\zeta)}{\zeta - z} \mathrm{d}\zeta = 2\pi\mathrm{i} \sum_{j=1}^{n} f(z_j) \, , \tag{4.17}$$
where the $n$ singularities are enclosed in the UHP. If we had completed the closed contour via lower half plane (LHP), we would have got an extra minus sign in front of the result because of the angular part of the integral. In this case the singularities are, naturally, to be handled in the LHP.

As an example we consider an integral
$$\int_{-\infty}^{\infty} \frac{1}{x - \mathrm{i}a} \frac{1}{x + \mathrm{i}a} \mathrm{d}x \, , \tag{4.18}$$
where $a \in \mathbb{R}$. We can now add zero to this integral as follows
$$\int_{-\infty}^{\infty} \frac{1}{x - \mathrm{i}a} \frac{1}{x + \mathrm{i}a} \mathrm{d}x + \int_{C_\rho} \frac{1}{z - \mathrm{i}a} \frac{1}{z + \mathrm{i}a} \mathrm{d}z = \oint_C \frac{1}{z - \mathrm{i}a} \frac{1}{z + \mathrm{i}a} \mathrm{d}z \, , \tag{4.19}$$
where $C_\rho$ is a semicircular countour from $\infty$ to $-\infty$ in the UHP, and $C$ a closed contour containing all the singularities in the UHP. The function
$$f(z) = \frac{1}{z - \mathrm{i}a} \frac{1}{z + \mathrm{i}a} \tag{4.20}$$
has one simple pole in the UHP at $z = \mathrm{i}a$. Therefore, the integral is readily evaluated as
$$\begin{aligned} \int_{-\infty}^{\infty} \frac{1}{x - \mathrm{i}a} \frac{1}{x + \mathrm{i}a} \mathrm{d}x &= \oint_C \frac{1/(z + \mathrm{i}a)}{z - \mathrm{i}a} \mathrm{d}z \\ &= 2\pi\mathrm{i} \left[\frac{1}{z + \mathrm{i}a}\right]_{z=\mathrm{i}a} \\ &= 2\pi\mathrm{i} \left[\frac{1}{2\mathrm{i}a}\right] \\ &= \frac{\pi}{a} \, . \end{aligned} \tag{4.21}$$

We could have also chosen to integrate via LHP, and considered the simple pole at $z = -\mathrm{i}a$, and eventually got the same answer.

Consider then an integral of the Fourier form

$$\int_{-\infty}^{\infty} \mathrm{e}^{\mathrm{i}\lambda x} f(x)\mathrm{d}x\,, \tag{4.22}$$

with $\lambda \in \mathbb{R}$ being a constant. For $\lambda \neq 0$, the function $f(z)$ is allowed to obey a less restrictive condition because of the behaviour of $\mathrm{e}^{\mathrm{i}\lambda z}$ in the complex plane, than in case $\lambda = 0$. More precisely, if $\left|f(z)\right| \to 0$ as $|z| \to \infty$ (or, $\left|f(z)\right|$ decays as $|z|^{-p}$, $p > 0$), the integration contour can be closed by a semicircle in the UHP for $\lambda > 0$, and in the LHP for $\lambda < 0$. Then

$$\lim_{\rho\to\infty} \int_{C_\rho:\ |z|=\rho} \mathrm{e}^{\mathrm{i}\lambda z} f(z)\mathrm{d}z = 0\,. \tag{4.23}$$

This result in Eq. (4.23) is called *Jordan's lemma*. Notice that on the semicircle $C_\rho$, where (in polar form) $z = \rho\mathrm{e}^{\mathrm{i}\theta} = \rho\,(\cos\theta + \mathrm{i}\sin\theta)$, we have

$$\begin{aligned}
\left|\mathrm{e}^{\mathrm{i}\lambda z}\right| &= \left|\mathrm{e}^{\mathrm{i}\lambda\rho(\cos\theta+\mathrm{i}\sin\theta)}\right| = \left|\mathrm{e}^{\mathrm{i}\lambda\rho\cos\theta-\lambda\rho\sin\theta}\right| \\
&= \left[\mathrm{e}^{\cancel{\mathrm{i}\lambda\rho\cos\theta}-\lambda\rho\sin\theta}\mathrm{e}^{\cancel{-\mathrm{i}\lambda\rho\cos\theta}-\lambda\rho\sin\theta}\right]^{1/2} \\
&= \left[\mathrm{e}^{-2\lambda\rho\sin\theta}\right]^{1/2} \\
&= \mathrm{e}^{-\lambda\rho\sin\theta}\,.
\end{aligned} \tag{4.24}$$

If $\lambda > 0$ and $\sin\theta \geq 0$, then $\mathrm{e}^{-\lambda\rho\sin\theta} \to 0$ as $\rho \to \infty$ in the UHP for which $0 \leq \theta \leq \pi$. On the other hand, if $\lambda < 0$ we must have $\sin\theta \leq 0$, which is what happens when $\pi \leq \theta \leq 2\pi$, i.e., in the LHP. Thus, when we convert integrals, such as in Eq. (4.22), into closed-contour integrals (in order to use Cauchy's integral formula), the poles need to be considered *only* in either half of the complex plane.

### 4.1.4 Cauchy's principal value

We consider an improper integral

$$\int_a^b f(x)\mathrm{d}x \tag{4.25}$$

with the function $f(x)$ having a singular point $x_0 \in [a,b]$, i.e.,

$$\lim_{x\to x_0} \left|f(x)\right| = \infty\,. \tag{4.26}$$

If the function is integrable over every portion of the interval $[a,b]$ without the point $x_0$ then we define

$$\int_a^b f(x)\mathrm{d}x = \lim_{\delta\to 0}\int_a^{x_0-\delta} f(x)\mathrm{d}x + \lim_{\epsilon\to 0}\int_{x_0+\epsilon}^b f(x)\mathrm{d}x\,, \tag{4.27}$$

when the limit exists as $\delta$ and $\epsilon$ tend to zero *independently*. Otherwise the integral is said to diverge. However, if we have $\delta = \epsilon$, we define the integral in Eq. (4.27) as the *Cauchy's principal value* ("valeur principale")

$$\lim_{\delta\to 0}\left[\int_a^{x_0-\delta} f(x)\mathrm{d}x + \int_{x_0+\delta}^b f(x)\mathrm{d}x\right] =: \mathcal{VP}\!\int_a^b f(x)\mathrm{d}x\,. \tag{4.28}$$

This means that if the integral as such diverges, but the principal value exists, the integral is defined as its principal value.

And how exactly does the principal value defined above relate to complex integrals studied in this section? In the next chapter we will study the following type of integral

$$\lim_{\eta\to 0}\int_{-\infty}^{\infty}\frac{g(x)\mathrm{d}x}{x-a\pm\mathrm{i}\eta}\,. \tag{4.29}$$

We may rewrite the integrand without the function $g(x)$ as follows

$$\begin{aligned}\frac{1}{x-a\pm\mathrm{i}\eta} &= \frac{x-a\mp\mathrm{i}\eta}{(x-a\pm\mathrm{i}\eta)(x-a\mp\mathrm{i}\eta)}\\ &= \frac{x-a\mp\eta}{x^2-xa\mp x\mathrm{i}\eta-xa+a^2\pm a\mathrm{i}\eta\pm x\mathrm{i}\eta\mp a\mathrm{i}\eta+\eta^2}\\ &= \frac{x-a\mp\mathrm{i}\eta}{x^2-2xa+a^2+\eta^2}\\ &= \frac{x-a}{(x-a)^2+\eta^2}\mp\mathrm{i}\frac{\eta}{(x-a)^2+\eta^2}\,. \end{aligned}\tag{4.30}$$

We also introduce a form of the deltafunction

$$\delta(x-a)=\lim_{\eta\to 0}\left[\frac{1}{\pi}\frac{\eta}{(x-a)^2+\eta^2}\right]. \tag{4.31}$$

Then we get back to the integral in Eq. (4.29) and obtain

$$\begin{aligned}\lim_{\eta\to 0}\int_{-\infty}^{\infty}\frac{g(x)\mathrm{d}x}{x-a\pm\mathrm{i}\eta} &= \lim_{\eta\to 0}\int_{-\infty}^{\infty}\left[\frac{x-a}{(x-a)^2+\eta^2}\mp\mathrm{i}\frac{\eta}{(x-a)^2+\eta^2}\right]g(x)\mathrm{d}x\\ &= \mathcal{VP}\int_{-\infty}^{\infty}\frac{g(x)\mathrm{d}x}{x-a}\mp\mathrm{i}\pi\int_{-\infty}^{\infty}\delta(x-a)g(x)\mathrm{d}x\\ &= \mathcal{VP}\int_{-\infty}^{\infty}\frac{g(x)\mathrm{d}x}{x-a}\mp\mathrm{i}\pi g(a)\,. \end{aligned}\tag{4.32}$$

## 4.2 Integral transforms

This section is a very brief one as we only state the definitions for the used methods within the field of integral transforms.

### 4.2.1 Fourier transform

For $f\in S(\mathbb{R}^n)$, where $S(\mathbb{R}^n)$ is an $n$-dimensional *Schwartz space*, the Fourier transform is a bijection $\mathcal{F}:S(\mathbb{R}^n)\to S(\mathbb{R}^n)$ with

$$\mathcal{F}\left[f(\mathbf{x})\right]=\frac{1}{(2\pi)^{n/2}}\int_{\mathbb{R}^n}\mathrm{d}\mathbf{x}\,\mathrm{e}^{-\mathrm{i}\mathbf{p}\cdot\mathbf{x}}f(\mathbf{x})\,, \tag{4.33}$$

and the inverse transform is

$$\mathcal{F}^{-1}\left[f(\mathbf{p})\right]=\frac{1}{(2\pi)^{n/2}}\int_{\mathbb{R}^n}\mathrm{d}\mathbf{p}\,\mathrm{e}^{\mathrm{i}\mathbf{p}\cdot\mathbf{x}}f(\mathbf{p})\,. \tag{4.34}$$

### 4.2.2 Hilbert transform

The Hilbert transform of a real function $f(t)$ is defined as a convolution with the function $h(t-\tau) = [\pi(t-\tau)]^{-1}$

$$\mathcal{H}\left[f(t)\right] = \frac{1}{\pi}\mathcal{VP}\int_{-\infty}^{\infty} \mathrm{d}\tau\, \frac{f(\tau)}{t-\tau}\,. \tag{4.35}$$

Because of the possible singularity at $\tau = t$, the integral is considered as a Cauchy's principal value integral, introduced in the previous section.

# Chapter 5

# Model system: molecule and chain

In this chapter, we consider a physical model that can be studied by using the formalism introduced in Chaps. 2 and 3.

## 5.1 Preliminaries

Consider a model with a two-site molecule and an $N$-site tight-binding (TB) chain. The Hamiltonian describing the model system is constructed from three different parts, viz.

$$\hat{H}_{\rm tot} = \hat{H}_{\rm ch} + \hat{H}_{\rm mol} + \hat{V} \ , \tag{5.1}$$

where $\hat{H}_{\rm ch}$ is the TB Hamiltonian for the chain, $\hat{H}_{\rm mol}$ is the Hamiltonian for the molecule, and the operator $\hat{V}$ stands for the interaction between the molecule and the terminal (1st) site of the chain. The interacting electrons of the molecule are allowed to be located either on the lowest unoccupied molecular orbital (LUMO) or on the highest occupied molecular orbital (HOMO). The hopping probabilities between the sites of the chain are assumed to be the same, $t$, with all the sites, and the hopping probability between the terminal site of the chain and the molecular orbitals is $t_{\rm hyb}$. The interaction strengths between the electrons are $U_0$ and $U_{HL}$ on and between the LUMO and HOMO levels, respectively, and $U_{\rm ext}$ between the terminal site of the chain and the molecular orbitals. The model is shown schematically in Fig. 5.1.

With these definitions the different parts of the Hamiltonian in Eq. (5.1) become

$$\begin{aligned}
\hat{H}_{\rm ch} &= -t \sum_{\sigma} \sum_{j=1}^{N-1} \left( \hat{c}^{\dagger}_{j,\sigma} \hat{c}_{j+1,\sigma} + \hat{c}^{\dagger}_{j+1,\sigma} \hat{c}_{j,\sigma} \right) && (5.2)\\
\hat{H}_{\rm mol} &= \xi_H \hat{n}_H + (\xi_H + \Delta_0)\, \hat{n}_L + U_0 \hat{n}_{H,+} \hat{n}_{H,-} + U_0 \hat{n}_{L,+} \hat{n}_{L,-} + U_{HL} \hat{n}_H \hat{n}_L && (5.3)\\
\hat{V} &= t_{\rm hyb} \sum_{\alpha=H,L} \sum_{\sigma} \left( \hat{c}^{\dagger}_{1,\sigma} \hat{b}_{\alpha,\sigma} + \hat{b}^{\dagger}_{\alpha,\sigma} \hat{c}_{1,\sigma} \right) + U_{\rm ext} \left( \hat{n}_{\rm ch} - 1 \right) \left( \hat{n}_{\rm mol} - 2 \right) \ , && (5.4)
\end{aligned}$$

where the operators $\hat{c}^{\dagger}$ and $\hat{c}$ correspond to the creation and annihilation operators on the chain, respectively, whereas the operators $\hat{b}^{\dagger}$ and $\hat{b}$ are the creation and annihilation operators,

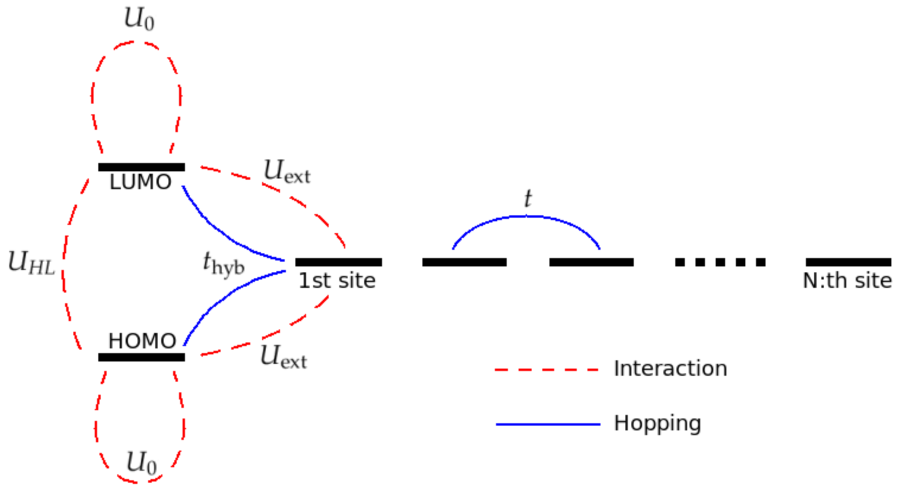

Figure 5.1: Schematic figure of the studied model

respectively, corresponding to the molecule.[1] The spin labels $\sigma$ are denoted so that $+$ corresponds to a "spin up" electron and $-$ corresponds to a "spin down" electron. The number operators $\hat{n}$ are all of the same form, e.g. $\hat{n}_{L,-} = \hat{b}^\dagger_{L,-}\hat{b}_{L,-}$. The constants $\xi_H$ and $\Delta_0$ are the energy level of the HOMO state and the energy gap between the molecular orbitals, respectively. The last term in Eq. (5.4) represents the excess charge on the chain's terminal site and on the molecule, i.e., $\hat{n}_{\rm ch}$ is a number operator only on the terminal site of the chain. It is essential to note that in this model the interactions within the TB chain are neglected. As well as for the molecule, there is interaction only with the terminal site of the chain, not with the interior sites. We also take the hopping probability $t$ to be negative. This choice is argued in a while, when we solve the eigenvalue problem. The model introduced here is similar to the one studied in Refs. [13,30].

## 5.2 Solving the eigenvalue problem

The exact solution of the presented problem involves diagonalization of the Hamiltonian in Eq. (5.1). For this task we need to find all the possible electron configurations on the molecule and on the chain, and thereafter operate with $\hat{H}_{\rm tot}$ to these states. Projections to the all other possible states give the matrix elements $\langle i|\hat{H}_{\rm tot}|j\rangle$ for the Hamiltonian matrix. Finding the eigenenergies and the corresponding eigenstates requires then diagonalization of this matrix. We now discuss the solution of the different parts of the total Hamiltonian $\hat{H}_{\rm tot}$ separately.

### 5.2.1 Tight-binding chain

For the $N$-site TB chain we have the Hamiltonian in Eq. (5.2), where $t$ is the hopping matrix element $t_{ij}$ between the neighbouring sites $i$ and $j$, the operator $\hat{c}^\dagger_{k,\sigma}$ creates a fermion with spin $\sigma$ to the site $k$, the operator $\hat{c}_{k,\sigma}$ removes a fermion with spin $\sigma$ from the site $k$, and these operators obey the canonical anticommutation relations for fermionic operators. The Hamiltonian for the

---

[1] As we did in Chap. 2, also in here the operators $\hat{a}$ and $\hat{b}$ correspond to the molecule's site and energy eigenbasis, respectively. The operators for the TB chain are $\hat{c}$ in site basis and $\hat{d}$ in energy eigenbasis.

TB chain can be diagonalized by a linear transformation having the form

$$\begin{aligned}\hat{d}_{k,\sigma} &= \sum_{j=1}^{N} \varphi_k(j)\hat{c}_{j,\sigma} && (5.5)\\ \hat{d}^{\dagger}_{k,\sigma} &= \sum_{j=1}^{N} \varphi^*_k(j)\hat{c}^{\dagger}_{j,\sigma}\,, && (5.6)\end{aligned}$$

where the orbitals $\varphi$ have the form

$$\varphi_k(j) = \sqrt{\frac{2}{N+1}}\sin\left(\frac{\pi k j}{N+1}\right)\,. \tag{5.7}$$

We then have $\varphi^*_k(j) = \varphi_k(j)$ and

$$\begin{aligned}\sum_{j=1}^{N} \varphi^*_k(j)\varphi_{k'}(j) &= \delta_{k,k'} && (5.8)\\ \sum_{k=1}^{N} \varphi^*_k(i)\varphi_k(j) &= \delta_{i,j}\,, && (5.9)\end{aligned}$$

since $\varphi_k(j) = \varphi_j(k)$. We can then check that the new operators $\hat{d}_{k,\sigma}$ obey the usual anticommutator algebra:

$$\begin{aligned}\left\{\hat{d}_{k,\sigma}, \hat{d}^{\dagger}_{k',\sigma'}\right\} &= \sum_{j,j'}\left[\varphi_k(j)\varphi^*_{k'}(j')\hat{c}_{j,\sigma}\hat{c}^{\dagger}_{j',\sigma'} + \varphi^*_{k'}(j')\varphi_k(j)\hat{c}^{\dagger}_{j',\sigma'}\hat{c}_{j,\sigma}\right]\\ &= \sum_{j,j'}\varphi_k(j)\varphi^*_{k'}(j')\left\{\hat{c}_{j,\sigma}, \hat{c}^{\dagger}_{j',\sigma'}\right\}\\ &= \sum_{j,j'}\varphi_k(j)\varphi^*_{k'}(j')\delta_{j,j'}\delta_{\sigma,\sigma'}\\ &= \sum_{j=1}^{N}\varphi_k(j)\varphi^*_{k'}(j)\delta_{\sigma,\sigma'}\\ &= \delta_{k,k'}\delta_{\sigma,\sigma'}\,. && (5.10)\end{aligned}$$

From Eqs. (5.5) and (5.6) we get by inversion

$$\begin{aligned} && \hat{d}_{k,\sigma} &= \sum_{j=1}^{N}\varphi_k(j)\hat{c}_{j,\sigma} \qquad \mid\cdot\varphi^*_k(i)\ \&\ \sum_{k=1}^{N}\\ \Rightarrow && \sum_{k=1}^{N}\varphi^*_k(i)\hat{d}_{k,\sigma} &= \sum_{j,k}\varphi_k(j)\varphi^*_k(i)\hat{c}_{j,\sigma}\\ \Rightarrow && \sum_{k=1}^{N}\varphi^*_k(i)\hat{d}_{k,\sigma} &= \sum_{j=1}^{N}\delta_{i,j}\hat{c}_{j,\sigma}\\ \Rightarrow && \hat{c}_{i,\sigma} &= \sum_{k=1}^{N}\varphi^*_k(i)\hat{d}_{k,\sigma}\,. && (5.11)\end{aligned}$$

and

$$
\begin{aligned}
& \hat{d}^{\dagger}_{k,\sigma} &=& \sum_{j=1}^{N} \varphi^{*}_{k}(j)\hat{c}^{\dagger}_{j,\sigma} \qquad\qquad | \cdot \varphi_k(i) \;\&\; \sum_{k=1}^{N} \\
\Rightarrow\quad & \sum_{k=1}^{N} \varphi_k(i)\hat{d}^{\dagger}_{k,\sigma} &=& \sum_{j,k} \varphi^{*}_{k}(j)\varphi_k(i)\hat{c}^{\dagger}_{j,\sigma} \\
\Rightarrow\quad & \sum_{k=1}^{N} \varphi_k(i)\hat{d}^{\dagger}_{k,\sigma} &=& \sum_{j=1}^{N} \delta_{i,j}\hat{c}^{\dagger}_{j,\sigma} \\
\Rightarrow\quad & \hat{c}^{\dagger}_{i,\sigma} &=& \sum_{k=1}^{N} \varphi_k(i)\hat{d}^{\dagger}_{k,\sigma} \,. \qquad (5.12)
\end{aligned}
$$

We can now insert Eqs. (5.11) and (5.12) into Eq. (5.2) as follows

$$
\begin{aligned}
\hat{H}_{\text{ch}} &= t\sum_{\sigma}\sum_{j=1}^{N-1}\sum_{k,k'}\left[\varphi_k(j)\varphi^{*}_{k'}(j+1)\hat{d}^{\dagger}_{k,\sigma}\hat{d}_{k',\sigma} + \varphi_k(j+1)\varphi^{*}_{k'}(j)\hat{d}^{\dagger}_{k,\sigma}\hat{d}_{k',\sigma}\right] \\
&= t\sum_{\sigma}\sum_{j=1}^{N-1}\sum_{k,k'}\left[\varphi_k(j)\varphi^{*}_{k'}(j+1) + \varphi_k(j+1)\varphi^{*}_{k'}(j)\right]\hat{d}^{\dagger}_{k,\sigma}\hat{d}_{k',\sigma} \,.
\end{aligned}
$$

The part inside the square brackets contains only real functions and we can rewrite it by expanding the sine functions as

$$
\begin{aligned}
[\ldots] &= \varphi_k(j)\sqrt{\frac{2}{N+1}}\sin\left[\frac{\pi k'(j+1)}{N+1}\right] + \varphi_{k'}(j)\sqrt{\frac{2}{N+1}}\sin\left[\frac{\pi k(j+1)}{N+1}\right] \\
&= \sqrt{\frac{2}{N+1}}\left\{\varphi_k(j)\left[\sin\left(\frac{\pi k' j}{N+1}\right)\cos\left(\frac{\pi k'}{N+1}\right) + \cos\left(\frac{\pi k' j}{N+1}\right)\sin\left(\frac{\pi k'}{N+1}\right)\right]\right. \\
&\quad + \left.\varphi_{k'}(j)\left[\sin\left(\frac{\pi k j}{N+1}\right)\cos\left(\frac{\pi k}{N+1}\right) + \cos\left(\frac{\pi k j}{N+1}\right)\sin\left(\frac{\pi k}{N+1}\right)\right]\right\} \,. \qquad (5.13)
\end{aligned}
$$

For $j = N$ Eq. (5.13) is zero, hence we can extend the sum over $j$ in Eq. (5.13) from $N - 1$ to $N$. With this trick we can then rewrite Eq. (5.13) as

$$\begin{aligned}
\hat{H}_{\mathrm{ch}} &= t\sum_{\sigma}\sum_{j,k,k'}[\ldots]\,\hat{d}^{\dagger}_{k,\sigma}\hat{d}_{k',\sigma} \\
&= t\sum_{\sigma}\sum_{j,k,k'}\left[\varphi_k(j)\sqrt{\frac{2}{N+1}}\sin\left(\frac{\pi k' j}{N+1}\right)\cos\left(\frac{\pi k'}{N+1}\right)\right. \\
&\qquad \left. +\ \varphi_{k'}(j)\sqrt{\frac{2}{N+1}}\sin\left(\frac{\pi k j}{N+1}\right)\cos\left(\frac{\pi k}{N+1}\right)\right]\hat{d}^{\dagger}_{k,\sigma}\hat{d}_{k',\sigma} \\
&+\ t\sum_{\sigma}\sum_{k,k'}\sqrt{\frac{2}{N+1}}\ \times \\
&\times\ \underbrace{\sum_{j=1}^{N}\left[\varphi_k(j)\cos\left(\frac{\pi k' j}{N+1}\right)\sin\left(\frac{\pi k'}{N+1}\right)+\varphi_{k'}(j)\cos\left(\frac{\pi k j}{N+1}\right)\sin\left(\frac{\pi k}{N+1}\right)\right]\hat{d}^{\dagger}_{k,\sigma}\hat{d}_{k',\sigma}}_{=0} \\
&= t\sum_{\sigma}\sum_{j,k,k'}\left[\overbrace{\varphi_k(j)\varphi_{k'}(j)}^{\sum_j \to\ \delta_{k,k'}}\cos\left(\frac{\pi k'}{N+1}\right)+\underbrace{\varphi_{k'}(j)\varphi_k(j)}_{\sum_j \to\ \delta_{k,k'}}\cos\left(\frac{\pi k}{N+1}\right)\right]\hat{d}^{\dagger}_{k,\sigma}\hat{d}_{k',\sigma} \\
&= \sum_{\sigma}\sum_{k=1}^{N}2t\cos\left(\frac{\pi k}{N+1}\right)\hat{d}^{\dagger}_{k,\sigma}\hat{d}_{k,\sigma} \\
&= \sum_{\sigma}\sum_{k=1}^{N}\epsilon_k\hat{d}^{\dagger}_{k,\sigma}\hat{d}_{k,\sigma}\ .
\end{aligned} \tag{5.14}$$

On the second line we noticed that the second term vanishes as the summing of sines and cosines over $j$, fortunately, gives zero.

Let us now concentrate a little on the sign of the hopping probability $t$. From Eq. (5.14) we see that the eigenenergy corresponding to the diagonal Hamiltonian is

$$\epsilon_k = 2t\cos\left(\frac{\pi k}{N+1}\right)\ . \tag{5.15}$$

In Fig. 5.2 we have a plot of the energy $\epsilon_k$ against $k$ with the hopping probability $t$ being negative. We see that by taking $t < 0$ the lowest energy is obtained with $k = 1$. We may then see how the ground-state wavefunction looks like, by substituting $k = 1$ into Eq. (5.7)

$$\varphi_1(j) = \sqrt{\frac{2}{N+1}}\sin\left(\frac{\pi j}{N+1}\right)\ , \tag{5.16}$$

which has no nodes and is spread along the whole $N$-site chain. This kind of smooth behaviour for the ground-state wavefunction is naturally desired, and it would be a good choice to take $t < 0$ to attain this particular behaviour. The choice for the sign of the hopping probability $t$ therefore arises from the choice of orbitals with respect to we are expanding our Hamiltonian. If, however, we chose $t > 0$ then the cosine curve in Fig. 5.2 would be the other way around, and

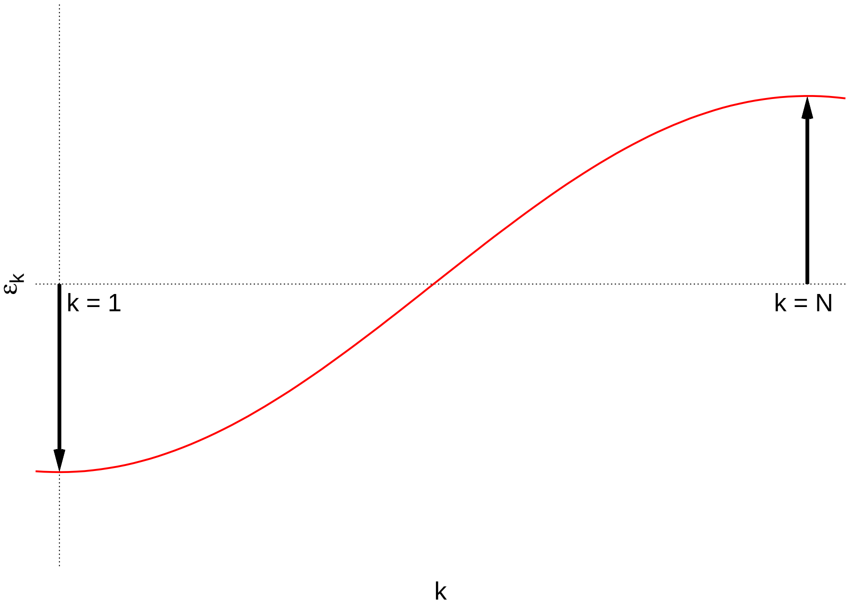

Figure 5.2: Energy eigenvalue $\epsilon_k$ for the diagonal Hamiltonian with respect to $k$ with the hopping probability $t$ being negative.

then the lowest-energy state is obtained when $k = N$. With $k = N$ the ground-state wavefunction would, in contrast, have $N$ nodes between the first and the last site of the chain.

All in all, we have obtained a Hamiltonian for the TB chain that is diagonal, and that the operator $\hat{d}^\dagger_{k,\sigma}$ is a "ladder" operator that maps an eigenstate of $\hat{H}_\text{ch}$ with energy $E$ onto another eigenstate with energy $E + \epsilon_k$. This statement is easily verified: If $\hat{H}_\text{ch}|E\rangle = E|E\rangle$, then

$$\begin{aligned} \hat{H}_\text{ch}\hat{d}^\dagger_{k,\sigma}|E\rangle &= \Big(\hat{H}_\text{ch}\hat{d}^\dagger_{k,\sigma} \overbrace{-\hat{d}^\dagger_{k,\sigma}\hat{H}_\text{ch} + \hat{d}^\dagger_{k,\sigma}\hat{H}_\text{ch}}^{=0}\Big)|E\rangle \\ &= \Big(\Big[\hat{H}_\text{ch}, \hat{d}^\dagger_{k,\sigma}\Big] + \hat{d}^\dagger_{k,\sigma}\hat{H}_\text{ch}\Big)|E\rangle \\ &= \Big(\epsilon_k\hat{d}^\dagger_{k,\sigma} + E\hat{d}^\dagger_{k,\sigma}\Big)|E\rangle \\ &= (E + \epsilon_k)\,\hat{d}^\dagger_{k,\sigma}|E\rangle \\ \Rightarrow \qquad \hat{d}^\dagger_{k,\sigma}|E\rangle &= |E + \epsilon_k\rangle\,. \end{aligned} \tag{5.17}$$

For the vacuum state $|0\rangle$ we have $\hat{d}_{k,\sigma}|0\rangle = 0,\ \forall k, \sigma$. The general form of the eigenstate of $\hat{H}_\text{ch}$ therefore reads

$$|E\rangle = \mathcal{N}\sum_\sigma\sum_{\{n_{k_1},\dots\}}\left(\hat{d}^\dagger_{k_1,\sigma}\right)^{n_{k_1}}\left(\hat{d}^\dagger_{k_2,\sigma}\right)^{n_{k_2}}\dots|0\rangle\,, \tag{5.18}$$

where $\mathcal{N}$ is a normalization factor, and the energy of this state is $E = \sum_k n_k\epsilon_k$ with $n_k = \{0, 1\}$ (since we are studying fermions).

So far, we have considered the case with $N$-site chain, and obtained a diagonal Hamiltonian in Eq. (5.14). For small systems this can be solved analytically by pen and paper, and for this purpose we consider a truncated chain with only two sites. Now that $N = 2$ we have

$\epsilon_k = 2t\cos\left(\frac{\pi}{3}k\right)$. Then we have for the Hamiltonian

$$\begin{aligned}\hat{H}_{\mathrm{ch}} &= \sum_\sigma \sum_{k=1}^{2} \epsilon_k \hat{d}^\dagger_{k,\sigma}\hat{d}_{k,\sigma} \\ &= 2t\underbrace{\cos\left(\frac{\pi}{3}\right)}_{=1/2}\left(\hat{d}^\dagger_{1,+}\hat{d}_{1,+} + \hat{d}^\dagger_{1,-}\hat{d}_{1,-}\right) + 2t\underbrace{\cos\left(\frac{2\pi}{3}\right)}_{=-1/2}\left(\hat{d}^\dagger_{2,+}\hat{d}_{2,+} + \hat{d}^\dagger_{2,-}\hat{d}_{2,-}\right) \\ &= t\left(\hat{n}_{2,+} + \hat{n}_{2,-} - \hat{n}_{1,+} - \hat{n}_{1,-}\right) . \qquad (5.19)\end{aligned}$$

Then we need to construct all the possible states for two electrons occupying the two sites, i.e., the eigenstates

$$|1\rangle = \hat{d}^\dagger_{1,+}\hat{d}^\dagger_{1,-}|0\rangle\,, \quad |2\rangle = \hat{d}^\dagger_{1,+}\hat{d}^\dagger_{2,-}|0\rangle\,, \quad |3\rangle = \hat{d}^\dagger_{1,-}\hat{d}^\dagger_{2,+}|0\rangle\,, \quad |4\rangle = \hat{d}^\dagger_{2,+}\hat{d}^\dagger_{2,-}|0\rangle\,. \qquad (5.20)$$

Because the Hamiltonian is diagonal, we get the corresponding eigenenergies simply as $\langle i|\hat{H}_{\mathrm{ch}}|i\rangle$ with $i \in [1,4]$:

$$\langle 1|\hat{H}_{\mathrm{ch}}|1\rangle = 2t\,, \quad \langle 2|\hat{H}_{\mathrm{ch}}|2\rangle = 0\,, \quad \langle 3|\hat{H}_{\mathrm{ch}}|3\rangle = 0\,, \quad \langle 4|\hat{H}_{\mathrm{ch}}|4\rangle = -2t\,. \qquad (5.21)$$

### 5.2.2 Two-site molecule

For the molecule we have the (diagonal) Hamiltonian in Eq. (5.3). The creation and annihilation operators for the electrons on the molecular orbitals are $\hat{b}^\dagger$ and $\hat{b}$, respectively. The number of electrons on the LUMO and HOMO levels is essential. Because there is two states for the electrons to be located, the number of interacting electrons can be from one to four. These four cases need to be considered separately.

For the one-electron case there is only two different configurations:

$$|1\rangle = \hat{b}^\dagger_{H,+}|0\rangle\,, \quad |2\rangle = \hat{b}^\dagger_{L,+}|0\rangle\,. \qquad (5.22)$$

The other possibilities with "spin down" electrons are essentially the same because the physical properties of the system do not change by choosing the direction of the spin. This is of course different when there is more than one electron to be considered. When operating with $\hat{H}_{\mathrm{mol}}$ to the states in Eq. (5.22) we get the eigenenergies

$$\langle 1|\hat{H}_{\mathrm{mol}}|1\rangle = \xi_H\,, \quad \langle 2|\hat{H}_{\mathrm{mol}}|2\rangle = \xi_H + \Delta_0\,. \qquad (5.23)$$

For the two-electron case there is four different configurations:

$$|1\rangle = \hat{b}^\dagger_{H,+}\hat{b}^\dagger_{H,-}|0\rangle\,, \quad |2\rangle = \hat{b}^\dagger_{H,+}\hat{b}^\dagger_{L,-}|0\rangle\,, \quad |3\rangle = \hat{b}^\dagger_{H,-}\hat{b}^\dagger_{L,+}|0\rangle\,, \quad |4\rangle = \hat{b}^\dagger_{L,+}\hat{b}^\dagger_{L,-}|0\rangle\,. \qquad (5.24)$$

Now the physical situation between the second and the third ket would change when interchanging the spin labels. This is due to the fact that the direction for the spin needs to be fixed (although it can be chosen arbitrarily) whereas in the one-electron case the spins were pointing only in one direction. The corresponding eigenenergies are readily calculated (note, however, that the energies of the second and the third state are the same)

$$\begin{aligned}\langle 1|\hat{H}_{\mathrm{mol}}|1\rangle &= 2\xi_H + U_0\,, \quad \langle 2|\hat{H}_{\mathrm{mol}}|2\rangle = 2\xi_H + \Delta_0 + U_{HL}\,, \\ \langle 3|\hat{H}_{\mathrm{mol}}|3\rangle &= 2\xi_H + \Delta_0 + U_{HL}\,, \quad \langle 4|\hat{H}_{\mathrm{mol}}|4\rangle = 2\xi_H + 2\Delta_0 + U_0\,. \qquad (5.25)\end{aligned}$$

The calculation for the three-electron case goes identically as above but now we have only two different states:

$$|1\rangle = \hat{b}^{\dagger}_{H,+}\hat{b}^{\dagger}_{H,-}\hat{b}^{\dagger}_{L,+}|0\rangle\,, \quad |2\rangle = \hat{b}^{\dagger}_{H,+}\hat{b}^{\dagger}_{L,+}\hat{b}^{\dagger}_{L,-}|0\rangle\,. \tag{5.26}$$

The molecular orbital with only one electron could also have the same electron but with the opposite spin. These two extra configurations would not add anything new to the system because the other molecular orbital has already two electrons with opposite spins, i.e., interchanging the directions of the spins gives the same state. The eigenenergies corresponding to the eigenstates in Eq. (5.26) are

$$\langle 1|\hat{H}_{\text{mol}}|1\rangle = 3\xi_H + \Delta_0 + U_0 + 2U_{HL}\,, \quad \langle 2|\hat{H}_{\text{mol}}|2\rangle = 3\xi_H + 2\Delta_0 + U_0 + 2U_{HL}\,. \tag{5.27}$$

The molecule can also have four electrons but in this case it is fully occupied, and therefore only one electron configuration is possible:

$$|1\rangle = \hat{b}^{\dagger}_{H,+}\hat{b}^{\dagger}_{H,-}\hat{b}^{\dagger}_{L,+}\hat{b}^{\dagger}_{L,-}|0\rangle\,. \tag{5.28}$$

The energy of this state is

$$\langle 1|\hat{H}_{\text{mol}}|1\rangle = 4\xi_H + 2\Delta_0 + 2U_0 + 4U_{HL}\,. \tag{5.29}$$

We may now pay a little more attention to the parameters introduced in the molecular energy spectrum. We consider $\xi_H$ to be the lowest energy level and therefore use $\Delta_0 > 0$. Also the parameters for the Coulomb repulsion ($U_0$ and $U_{HL}$) are taken positive. Then choose the two-particle state $|1\rangle$ in Eq. (5.24) to be the ground state. The ground-state energy is to be the smallest, hence, comparing the ground state to the one-particle state $|1\rangle$ in Eq. (5.22) gives

$$2\xi_H + U_0 < \xi_H \qquad \Rightarrow \qquad \xi_H < -U_0\,. \tag{5.30}$$

We can also deduce that two particles in the HOMO level must be lower in energy than one particle in the HOMO level and one particle in the LUMO level [$|2\rangle$ and $|3\rangle$ in Eq. (5.24)], i.e.,

$$2\xi_H + U_0 < 2\xi_H + \Delta_0 + U_{HL} \qquad \Rightarrow \qquad \Delta_0 + U_{HL} > U_0\,. \tag{5.31}$$

Clearly, the ground state must also be lower in energy than a three-particle state $|1\rangle$ in Eq. (5.26), i.e.,

$$2\xi_H + U_0 < 3\xi_H + \Delta_0 + U_0 + 2U_{HL} \qquad \Rightarrow \qquad \xi_H > -\Delta_0 - 2U_{HL}\,. \tag{5.32}$$

We have now got [from Eqs. (5.30) and (5.32)] a range of values for the energy in HOMO level

$$-\Delta_0 - 2U_{HL} < \xi_H < -U_0\,, \tag{5.33}$$

where also the condition from Eq. (5.31) is fulfilled since $-\Delta_0 - 2U_{HL} = -(\Delta_0 + U_{HL}) - U_{HL} < -U_0 - U_{HL} < -U_0$. A convenient choice for the Eq. (5.32) to be satisfied is when we have

$$\xi_H = -\frac{\Delta_0}{2} - \frac{U_0}{2} - U_{HL}\,. \tag{5.34}$$

### 5.2.3 Interaction between the molecule and the chain

The interaction term of the total Hamiltonian is in Eq. (5.4). We consider first the case with $t_{hyb} = 0$, i.e., the molecule and the chain interact only via the term $U_{ext}$. This approximation can be solved analytically. The number operator in the terminal site of the chain $\hat{n}_{\mathrm{ch}}$ needs to be converted to the basis we defined in Eqs. (5.5) and (5.6). We have then

$$\begin{aligned} \hat{n}_{\mathrm{ch}} &= \sum_{\sigma} \hat{c}^{\dagger}_{1,\sigma}\hat{c}_{1,\sigma} \\ &= \frac{2}{N+1}\sum_{\sigma}\sum_{j,k} \sin\left(\frac{\pi k}{N+1}\right)\sin\left(\frac{\pi j}{N+1}\right)\hat{d}^{\dagger}_{k,\sigma}\hat{d}_{j,\sigma} \,. \end{aligned} \tag{5.35}$$

We then get back to our truncated-chain example, and take two energy levels ($j,k = 1,2$) and two sites ($N = 2$). Then we have for the number operator in the terminal site of the chain

$$\begin{aligned} \hat{n}_{\mathrm{ch}} &= \frac{2}{3}\sum_{\sigma}\Big[\overbrace{\sin\left(\frac{\pi}{3}\right)}^{=\sqrt{3}/2}\overbrace{\sin\left(\frac{\pi}{3}\right)}^{\sqrt{3}/2}\hat{d}^{\dagger}_{1,\sigma}\hat{d}_{1,\sigma} + \overbrace{\sin\left(\frac{\pi}{3}\right)}^{=\sqrt{3}/2}\overbrace{\sin\left(\frac{2\pi}{3}\right)}^{=\sqrt{3}/2}\hat{d}^{\dagger}_{1,\sigma}\hat{d}_{2,\sigma} \\ &\quad + \underbrace{\sin\left(\frac{2\pi}{3}\right)}_{=\sqrt{3}/2}\underbrace{\sin\left(\frac{\pi}{3}\right)}_{=\sqrt{3}/2}\hat{d}^{\dagger}_{2,\sigma}\hat{d}_{1,\sigma} + \underbrace{\sin\left(\frac{2\pi}{3}\right)}_{=\sqrt{3}/2}\underbrace{\sin\left(\frac{2\pi}{3}\right)}_{=\sqrt{3}/2}\hat{d}^{\dagger}_{2,\sigma}\hat{d}_{2,\sigma}\Big] \\ &= \frac{1}{2}\left(\hat{n}_1 + \hat{n}_2 + \hat{d}^{\dagger}_{1,+}\hat{d}_{2,+} + \hat{d}^{\dagger}_{2,+}\hat{d}_{1,+} + \hat{d}^{\dagger}_{1,-}\hat{d}_{2,-} + \hat{d}^{\dagger}_{2,-}\hat{d}_{1,-}\right) \,. \end{aligned} \tag{5.36}$$

With Eq. (5.36) we can rewrite Eq. (5.4) (when $t_{hyb} = 0$) as

$$\hat{V} = U_{\mathrm{ext}}\left(\hat{n}_{\mathrm{mol}} - 2\right)\left[\frac{1}{2}\left(\hat{n}_1 + \hat{n}_2 + \hat{d}^{\dagger}_{1,+}\hat{d}_{2,+} + \hat{d}^{\dagger}_{2,+}\hat{d}_{1,+} + \hat{d}^{\dagger}_{1,-}\hat{d}_{2,-} + \hat{d}^{\dagger}_{2,-}\hat{d}_{1,-}\right) - 1\right] \,. \tag{5.37}$$

The operator $\hat{n}_{\mathrm{mol}}$ in Eq. (5.37) is already in correct basis, i.e, it gives only the number of electrons on the molecule. From this we can deduce that when there is two electrons on the molecule, the interaction vanishes.

We can now study different systems with our two-site molecule and two-site chain. The simplest case is to put one electron to the molecule and one electron to the chain. For this set-up we can distinguish four different electron configurations

$$|1\rangle = \hat{b}^{\dagger}_{H,+}\hat{d}^{\dagger}_{1,+}|0\rangle \,, \quad |2\rangle = \hat{b}^{\dagger}_{H,+}\hat{d}^{\dagger}_{2,+}|0\rangle \,, \quad |3\rangle = \hat{b}^{\dagger}_{L,+}\hat{d}^{\dagger}_{1,+}|0\rangle \,, \quad |4\rangle = \hat{b}^{\dagger}_{L,+}\hat{d}^{\dagger}_{2,+}|0\rangle \,. \tag{5.38}$$

The different combinations for the spin index do not give any extra information about the system, because the electron on the molecule cannot depend on the spin of the electron on the chain, and vice versa. Operating to the eigenkets in Eq. (5.38) with the total Hamiltonian operator [in Eq. (5.1)] we get the Hamiltonian matrix whose eigenvalues are the eigenenergies of the system. Because the $\hat{H}_{\mathrm{ch}}$ and $\hat{H}_{\mathrm{mol}}$ parts of the Hamiltonian are diagonal, the contribution from these is readily calculated [in fact, for the molecule we already calculated the eigenenergies in Eq. (5.23)]

$$\hat{H}_{\mathrm{ch}}|1\rangle = t|1\rangle \,, \quad \hat{H}_{\mathrm{ch}}|2\rangle = -t|2\rangle \,, \quad \hat{H}_{\mathrm{ch}}|3\rangle = t|3\rangle \,, \quad \hat{H}_{\mathrm{ch}}|4\rangle = -t|4\rangle \,, \tag{5.39}$$

$$\hat{H}_{\mathrm{mol}}|1\rangle = \xi_H|1\rangle \,, \; \hat{H}_{\mathrm{mol}}|2\rangle = \xi_H|2\rangle \,, \; \hat{H}_{\mathrm{mol}}|3\rangle = \left(\xi_H + \Delta_0\right)|3\rangle \,, \; \hat{H}_{\mathrm{mol}}|4\rangle = \left(\xi_H + \Delta_0\right)|4\rangle \,. \tag{5.40}$$

For the interaction part, we have to operate with Eq. (5.37) to the states in Eq. (5.38). From this calculation we get (note that $\langle \hat{n}_{\text{mol}} \rangle = 1$)

$$\begin{aligned}
\hat{V}|1\rangle &= \frac{1}{2}U_{\text{ext}}|1\rangle + \frac{1}{2}U_{\text{ext}}|2\rangle \\
\hat{V}|2\rangle &= \frac{1}{2}U_{\text{ext}}|2\rangle + \frac{1}{2}U_{\text{ext}}|1\rangle \\
\hat{V}|3\rangle &= \frac{1}{2}U_{\text{ext}}|3\rangle + \frac{1}{2}U_{\text{ext}}|4\rangle \\
\hat{V}|4\rangle &= \frac{1}{2}U_{\text{ext}}|4\rangle + \frac{1}{2}U_{\text{ext}}|3\rangle \, .
\end{aligned}$$

We are now ready to write down the total Hamiltonian matrix

$$\left(\hat{H}_{\text{tot}}\right)_{ij} = \begin{pmatrix}
\langle 1|\hat{H}_{\text{tot}}|1\rangle & \langle 1|\hat{H}_{\text{tot}}|2\rangle & \langle 1|\hat{H}_{\text{tot}}|3\rangle & \langle 1|\hat{H}_{\text{tot}}|4\rangle \\
\langle 2|\hat{H}_{\text{tot}}|1\rangle & \langle 2|\hat{H}_{\text{tot}}|2\rangle & \langle 2|\hat{H}_{\text{tot}}|3\rangle & \langle 2|\hat{H}_{\text{tot}}|4\rangle \\
\langle 3|\hat{H}_{\text{tot}}|1\rangle & \langle 3|\hat{H}_{\text{tot}}|2\rangle & \langle 3|\hat{H}_{\text{tot}}|3\rangle & \langle 3|\hat{H}_{\text{tot}}|4\rangle \\
\langle 4|\hat{H}_{\text{tot}}|1\rangle & \langle 4|\hat{H}_{\text{tot}}|2\rangle & \langle 4|\hat{H}_{\text{tot}}|3\rangle & \langle 4|\hat{H}_{\text{tot}}|4\rangle
\end{pmatrix}$$

$$= \begin{pmatrix}
t + \xi_H + \frac{1}{2}U_{\text{ext}} & \frac{1}{2}U_{\text{ext}} & 0 & 0 \\
\frac{1}{2}U_{\text{ext}} & -t + \xi_H + \frac{1}{2}U_{\text{ext}} & 0 & 0 \\
0 & 0 & t + \xi_H + \Delta_0 + \frac{1}{2}U_{\text{ext}} & \frac{1}{2}U_{\text{ext}} \\
0 & 0 & \frac{1}{2}U_{\text{ext}} & -t + \xi_H + \Delta_0 + \frac{1}{2}U_{\text{ext}}
\end{pmatrix} . \tag{5.41}$$

The matrix in Eq. (5.41) is block diagonal, and the diagonalization of the matrix can be done separately for the two-by-two parts. The eigenenergies are

$$E_{1,2} = \frac{1}{2}\left(2\xi_H + U_{\text{ext}} \pm \sqrt{4t^2 + U_{\text{ext}}^{\;2}}\right) \tag{5.42}$$

$$E_{3,4} = \frac{1}{2}\left(2\xi_H + \Delta_0 + U_{\text{ext}} \pm \sqrt{4t^2 + U_{\text{ext}}^{\;2}}\right) . \tag{5.43}$$

By this manner, we can construct the Hamiltonian matrices for all systems we want to study. Finding the eigenenergies of the studied system is then a matter of diagonalizing the Hamiltonian matrix. As an example, we calculate the lowest energies (ground-state energies) for a system of two electrons on the chain with varying number of electrons on the molecule. We use parameter values $U_0 = U_{HL} = \Delta_0 = -t = 1$ with $\xi_H = -2$ and plot the ground-state energies versus the number of electrons on the molecule $N_{\text{mol}}$ with different values of $U_{\text{ext}}$ in Fig. 5.3a. We also calculate the electron densities in the terminal site of the chain from the corresponding electron wave function in Fig. 5.3b.[2]

Let us then look at an application of the studied model. Consider the system of two-site molecule and two-site chain to be two electrons on the molecule and two electrons on the chain. The ground state of this system is, naturally, the electrons occupying the states that are the lowest in energy:

---

[2] This calculation is explained more in detail in Sec. 5.5 on page 86.

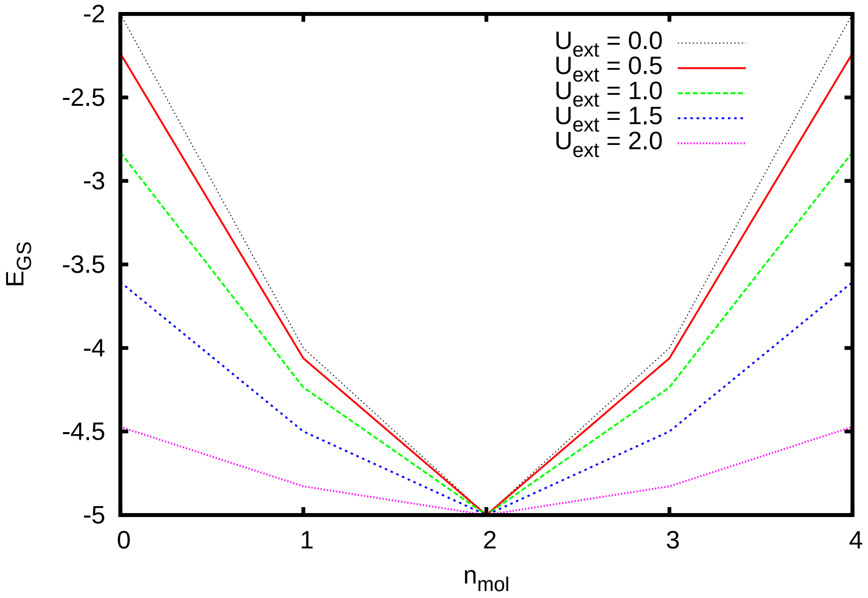

(a) Ground-state energies versus the number of electrons in the molecule.

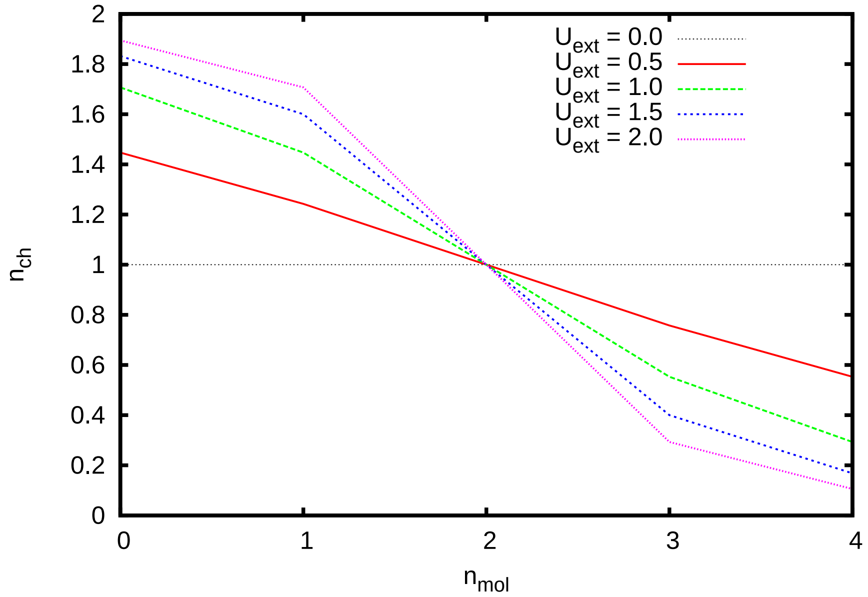

(b) Electron densities in the terminal site of the chain versus the number of electrons in the molecule.

Figure 5.3: (a) Ground-state energies in a system of two electrons on the chain, (b) electron densities in the terminal site of the chain.

$$|\Psi_0\rangle = \hat{b}^\dagger_{H,+}\hat{b}^\dagger_{H,-}\hat{d}^\dagger_{1,+}\hat{d}^\dagger_{1,-}|0\rangle$$

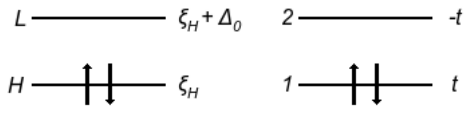

Since we have two electrons on the molecule, the interaction between the molecule and the chain vanishes as $\hat{n}_{\text{mol}} - 2 = 0$ in Eq. (5.4). We can then simply state that the ground state energy is given by [see Eqs. (5.21) and (5.25)]

$$\hat{H}_{\text{tot}}|\Psi_0\rangle = E_0|\Psi_0\rangle \qquad \text{with} \qquad E_0 = 2\xi_H + U_0 + 2t\,. \tag{5.44}$$

Then we add one electron to the molecule which will then occupy the LUMO level as the HOMO level is already fully occupied. We hereby have the molecular state

$$|\Psi_{\text{mol}}\rangle = \hat{b}^\dagger_{H,+}\hat{b}^\dagger_{H,-}\hat{b}^\dagger_{L,+}|0\rangle\,. \tag{5.45}$$

Now $\langle\hat{n}_{\text{mol}}\rangle = 3$ and the interaction between the molecule and the chain is not zero anymore. In fact, the interaction becomes repulsive as the molecule becomes negatively charged, and therefore the electrons on the terminal site of the chain are being pushed away from the molecule. The two electrons on the chain can arrange themselves in four different combinations as in Eq. (5.20). To evaluate the energies of the whole system, we need to add the contribution from the interaction, as we did when we calculated the eigenenergies in Eq. (5.42). We can now similarly construct all the different electron configurations and operate to these states with $\hat{H}_{\text{tot}}$ in order to obtain the total Hamiltonian matrix. The energies of the system are again found by evaluating the eigenvalues of the Hamiltonian matrix. This is a straightforward calculation and we state here the results for the eigenvalues. As there is four different states that the electrons on the chain can form, we have four eigenvalues, and two of them are the same because kets $|2\rangle$ and $|3\rangle$ in Eq. (5.20) are same in energy. We then have

$$E_1 = 3\xi_H - \Delta_0 + U_0 + 2U_{HL} - \sqrt{4t^2 + {U_{\text{ext}}}^2} \tag{5.46}$$
$$E_2 = 3\xi_H - \Delta_0 + U_0 + 2U_{HL} \tag{5.47}$$
$$E_3 = 3\xi_H - \Delta_0 + U_0 + 2U_{HL} + \sqrt{4t^2 + {U_{\text{ext}}}^2}\,, \tag{5.48}$$

where $E_1$ corresponds to a state with both electrons on the chain being on the lower energy level, $E_2$ to a state with the two electrons on the chain being on different energy levels, and $E_3$ to a state with both electrons on the chain being on the higher energy level. We can now calculate the energy difference between the ground state (two electrons on the molecule and two electrons on the chain) and the added-electron states. These energy differences give us the addition energies of the ($\langle\hat{n}_{\text{mol}}\rangle = 3$) -system. Taking parameters $-t = \Delta_0 = U_0 = U_{HL} = 1$ and $\xi_H = -2$ [see Eq. (5.34)] we have from Eqs. (5.44), (5.46), (5.47) and (5.48)

$$\Delta_1 = E_1 - E_0 = 3 - \sqrt{4 + {U_{\text{ext}}}^2} \tag{5.49}$$
$$\Delta_2 = E_2 - E_0 = 3 \tag{5.50}$$
$$\Delta_3 = E_3 - E_0 = 3 + \sqrt{4 + {U_{\text{ext}}}^2}\,. \tag{5.51}$$

We will get back to these results later in Chap. 6 with the corresponding results from the perturbation-theory calculations.

## 5.3 Solution via perturbative expansion

In Sec. 5.2 we were studying our model exactly with the formalism of second quantization. We can also apply the formalism of many-particle perturbation theory to this particular model. In this manner, we first need to construct the non-interacting Green's function, $G^0$, for our system – the molecule and chain. After this, we can compute the self-energy $\Sigma$ from the Feynman diagrams, and finally apply the Dyson equation to obtain the total Green's function.

Our goal is to evaluate the addition energies of the system as we did in the previous section in Eqs. (5.49), (5.50) and (5.51). Although the perturbation-theoretical approach to this small system is quite an overkill, it is an educational study of the functionality of the perturbation theory. When we treat our $N$-particle system perturbatively, we get information about the $N-1$ and $N+1$ particle systems without ever calculating them explicitly.

### 5.3.1 Non-interacting Green's function for the molecule

We start with the definition

$$G^0_{(1)}(\mathbf{x},z;\mathbf{x}',z') = \mathrm{i}\langle\Psi_0|\mathcal{T}_C[\hat{\psi}_H(\mathbf{x},z)\hat{\psi}^\dagger_H(\mathbf{x}',z')]|\Psi_0\rangle\,, \tag{5.52}$$

where $\mathcal{T}_C$ is the time-ordering operator for which

$$\mathcal{T}_C[A(z)B(z')] = \theta(z-z')A(z)B(z') - \theta(z'-z)B(z')A(z)\,, \tag{5.53}$$

with

$$\theta(z) = \begin{cases} 1 & \text{when } z \geq 0 \\ 0 & \text{when } z < 0 \end{cases} \tag{5.54}$$

being the Heaviside step function. The subscripts $H$ stand for Heisenberg operators, and the spin index $\sigma$ is included in the $\mathbf{x}$ coordinate by $\mathbf{x} = (\mathbf{r},\sigma)$. As we are dealing only with one-particle Green's functions here, no mix-ups should occur if we omit the subscript notation in Eq. (5.52) and write simply $G^0$. We can express the field operators in a the molecular orbital basis by

$$\hat{\psi}^\dagger_H(\mathbf{x},z) = \sum_{k,\sigma} \varphi^{(*)}_{k,\sigma}(\mathbf{r})\hat{b}^{(\dagger)}_{k,\sigma,H}(z)\,, \tag{5.55}$$

where the parentheses around † and ∗ mean that we have definitions for both creation and annihilation operators. We also emphasize that these creation and annihilation operators correspond to the molecule as in Hamiltonian (5.3). We can transform from Heisenberg picture into Schrödinger picture by writing the Heisenberg operators as

$$\hat{\psi}^{(\dagger)}_H(\mathbf{x},z) = \mathrm{e}^{\mathrm{i}\hat{H}_0 z}\hat{\psi}^{(\dagger)}(\mathbf{x},z)\mathrm{e}^{-\mathrm{i}\hat{H}_0 z}\,, \tag{5.56}$$

where $\hat{H}_0$ is the time-independent Hamiltonian. With Eq. (5.56) we get

$$\hat{b}^{(\dagger)}_{k,H}(z) = \mathrm{e}^{\mathrm{i}\hat{H}_0 z}\hat{b}^{(\dagger)}_k(z)\mathrm{e}^{-\mathrm{i}\hat{H}_0 z}\,. \tag{5.57}$$

Now insert these expressions into Eq. (5.52)

$$\begin{aligned} G^0(\mathbf{x},z;\mathbf{x}',z') &= \mathrm{i}\sum_{\substack{k,k'\\ \sigma,\sigma'}} \Big[\theta(z-z')\varphi_{k,\sigma}(\mathbf{r})\varphi^*_{k',\sigma'}(\mathbf{r}')\langle\Psi_0|\mathrm{e}^{\mathrm{i}\hat{H}_0 z}\hat{b}_{k,\sigma}(z)\mathrm{e}^{-\mathrm{i}\hat{H}_0 z}\mathrm{e}^{\mathrm{i}\hat{H}_0 z'}\hat{b}^\dagger_{k',\sigma'}(z')\mathrm{e}^{-\mathrm{i}\hat{H}_0 z'}|\Psi_0\rangle \\ &\quad - \theta(z'-z)\varphi^*_{k',\sigma'}(\mathbf{r}')\varphi_{k,\sigma}(\mathbf{r})\langle\Psi_0|\mathrm{e}^{-\mathrm{i}\hat{H}_0 z'}\hat{b}^\dagger_{k',\sigma'}(z')\mathrm{e}^{\mathrm{i}\hat{H}_0 z'}\mathrm{e}^{-\mathrm{i}\hat{H}_0 z}\hat{b}_{k,\sigma}(z)\mathrm{e}^{\mathrm{i}\hat{H}_0 z}|\Psi_0\rangle\Big]\,. \end{aligned} \tag{5.58}$$

We may also insert a complete set of $N+1$ and $N-1$ particle states, in the form of $\sum_n |\Psi_n\rangle\langle\Psi_n| = \mathbb{1}$, into this expression

$$\begin{aligned}
&G^0(\mathbf{x},z;\mathbf{x}',z') \\
&= \mathrm{i}\sum_{\substack{k,k'\\ \sigma,\sigma'\\ n,m}} \Big[\theta(z-z')\varphi_{k,\sigma}(\mathbf{r})\varphi^*_{k',\sigma'}(\mathbf{r}')\langle\Psi_0|\mathrm{e}^{\mathrm{i}\hat{H}_0 z}\hat{b}_{k,\sigma}(z)\mathrm{e}^{-\mathrm{i}\hat{H}_0 z}|\Psi_n^{N+1}\rangle\langle\Psi_n^{N+1}|\mathrm{e}^{-\mathrm{i}\hat{H}_0 z'}\hat{b}^\dagger_{k',\sigma'}(z')\mathrm{e}^{-\mathrm{i}\hat{H}_0 z'}|\Psi_0\rangle \\
&\quad - \theta(z'-z)\varphi^*_{k',\sigma'}(\mathbf{r}')\varphi_{k,\sigma}(\mathbf{r})\langle\Psi_0|\mathrm{e}^{\mathrm{i}\hat{H}_0 z'}\hat{b}^\dagger_{k',\sigma'}(z')\mathrm{e}^{-\mathrm{i}\hat{H}_0 z'}|\Psi_m^{N-1}\rangle\langle\Psi_m^{N-1}|\mathrm{e}^{-\mathrm{i}\hat{H}_0 z}\hat{b}_{k,\sigma}(z)\mathrm{e}^{-\mathrm{i}\hat{H}_0 z'}|\Psi_0\rangle\Big] \\
&= \mathrm{i}\sum_{\substack{k,k'\\ \sigma,\sigma'\\ n,m}} \Big[\theta(z-z')\varphi_{k,\sigma}(\mathbf{r})\varphi^*_{k',\sigma'}(\mathbf{r}')\mathrm{e}^{\mathrm{i}\left(E_0-E_n^{N+1}\right)(z-z')}\langle\Psi_0|\hat{b}_{k,\sigma}(z)|\Psi_n^{N+1}\rangle\langle\Psi_n^{N+1}|\hat{b}^\dagger_{k',\sigma'}(z')|\Psi_0\rangle \\
&\quad - \theta(z'-z)\varphi^*_{k',\sigma'}(\mathbf{r}')\varphi_{k,\sigma}(\mathbf{r})\mathrm{e}^{\mathrm{i}\left(E_0-E_m^{N-1}\right)(z'-z)}\langle\Psi_0|\hat{b}^\dagger_{k',\sigma'}(z')|\Psi_m^{N-1}\rangle\langle\Psi_m^{N-1}|\hat{b}_{k,\sigma}(z)|\Psi_0\rangle\Big]\ . \qquad (5.59)
\end{aligned}$$

We notice how the expression in Eq. (5.59) depends on the relative time coordinate $\tau := z - z'$. For the ground state $\Psi_0$ we are considering a simple Fermi sphere, i.e., a three-dimensional region in momentum space with $N$ particles inside, all having their momentum less than the value corresponding to the surface of the sphere. Then we deal with the matrix elements inside the sum in Eq. (5.59). The states with $N+1$ and $N-1$ particles are operated with the annihilation and creation operators $\hat{b}_{k,\sigma}$ and $\hat{b}^\dagger_{k',\sigma'}$, respectively. These operations give a non-zero contribution only if we have $n = k, k'$ and $m = k, k'$, and this observation kills the summations over $n$ and $m$. The contribution from these operations may, or may not, overlap with the ground state $\Psi_0$, and for this purpose we introduce step functions inside the Fermi sphere. For the $N+1$ and $N-1$ particle energies we have $E_k^{N\pm1} = E_0 \pm \epsilon_k$. We can then simplify the expression in Eq. (5.59), with the ideas presented above, as

$$\begin{aligned}
G^0(\mathbf{x},\mathbf{x}';\tau) &= \mathrm{i}\sum_{\substack{k,k'\\ \sigma,\sigma'}} \Big[\theta(\tau)\varphi_{k,\sigma}(\mathbf{r})\varphi^*_{k',\sigma'}(\mathbf{r}')\mathrm{e}^{\mathrm{i}(\cancel{E_0-E_0}-\epsilon_k)\tau}\theta\left(\frac{N}{2}-k\right)\delta_{k,k'}\delta_{\sigma,\sigma'} \\
&\quad - \theta(-\tau)\varphi^*_{k',\sigma'}(\mathbf{r}')\varphi_{k,\sigma}(\mathbf{r})\mathrm{e}^{\mathrm{i}(\cancel{E_0-E_0}+\epsilon_k)(-\tau)}\theta\left(k'-\frac{N}{2}\right)\delta_{k,k'}\delta_{\sigma,\sigma'}\Big] \\
&= \mathrm{i}\sum_{\substack{k\le N/2\\ \sigma}} \theta(\tau)\varphi_{k,\sigma}(\mathbf{r})\varphi^*_{k,\sigma}(\mathbf{r}')\mathrm{e}^{-\mathrm{i}\epsilon_k\tau} - \mathrm{i}\sum_{\substack{k>N/2\\ \sigma}} \theta(-\tau)\varphi^*_{k,\sigma}(\mathbf{r}')\varphi_{k,\sigma}(\mathbf{r})\mathrm{e}^{-\mathrm{i}\epsilon_k\tau}\ . \qquad (5.60)
\end{aligned}$$

Then we insert a useful form of the step function

$$\theta(x) = \lim_{\eta\to0^+}\frac{-1}{2\pi\mathrm{i}}\int_{-\infty}^{\infty}\frac{\mathrm{e}^{\mathrm{i}\lambda x}}{\lambda+\mathrm{i}\eta}\mathrm{d}\lambda \qquad (5.61)$$

into Eq. (5.60) to obtain

$$\begin{aligned}
G^0(\mathbf{x},\mathbf{x}';\tau) &= \mathrm{i}\sum_{\substack{k\le N/2\\ \sigma}} \varphi_{k,\sigma}(\mathbf{r})\varphi^*_{k,\sigma}(\mathbf{r}')\left(-\frac{1}{2\pi\mathrm{i}}\right)\int_{-\infty}^{\infty}\mathrm{d}\lambda\frac{\mathrm{e}^{\mathrm{i}\lambda\tau}}{\lambda+\mathrm{i}\eta}\mathrm{e}^{-\mathrm{i}\epsilon_k\tau} \\
&- \mathrm{i}\sum_{\substack{k>N/2\\ \sigma}} \varphi^*_{k,\sigma}(\mathbf{r}')\varphi_{k,\sigma}(\mathbf{r})\left(-\frac{1}{2\pi\mathrm{i}}\right)\int_{-\infty}^{\infty}\mathrm{d}\lambda\frac{\mathrm{e}^{-\mathrm{i}\lambda\tau}}{\lambda+\mathrm{i}\eta}\mathrm{e}^{-\mathrm{i}\epsilon_k\tau}\ , \quad \left(\eta\to0^+\right)\ . \qquad (5.62)
\end{aligned}$$

Then we take Fourier transforms with respect to the relative time coordinate $\tau$, and evaluate the integrals

$$\begin{aligned}
G^0(\mathbf{x},\mathbf{x}';\omega) &= -\frac{1}{2\pi}\sum_{\substack{k\leq N/2\\ \sigma}} \varphi_{k,\sigma}(\mathbf{r})\varphi^*_{k,\sigma}(\mathbf{r}') \int_{-\infty}^{\infty}\frac{\mathrm{d}\lambda}{\lambda+\mathrm{i}\eta}\int_{-\infty}^{\infty}\mathrm{d}\tau \mathrm{e}^{\mathrm{i}\omega\tau}\mathrm{e}^{\mathrm{i}\lambda\tau}\mathrm{e}^{-\mathrm{i}\epsilon_k\tau} \\
&+ \frac{1}{2\pi}\sum_{\substack{k>N/2\\ \sigma}} \varphi^*_{k,\sigma}(\mathbf{r}')\varphi_{k,\sigma}(\mathbf{r}) \int_{-\infty}^{\infty}\frac{\mathrm{d}\lambda}{\lambda+\mathrm{i}\eta}\int_{-\infty}^{\infty}\mathrm{d}\tau \mathrm{e}^{\mathrm{i}\omega\tau}\mathrm{e}^{-\mathrm{i}\lambda\tau}\mathrm{e}^{-\mathrm{i}\epsilon_k\tau}\,, \quad \left(\eta\to 0^+\right) \\
&= -\frac{1}{2\pi}\sum_{\substack{k\leq N/2\\ \sigma}} \varphi_{k,\sigma}(\mathbf{r})\varphi^*_{k,\sigma}(\mathbf{r}') \int_{-\infty}^{\infty}\frac{\mathrm{d}\lambda}{\lambda+\mathrm{i}\eta}\overbrace{\int_{-\infty}^{\infty}\mathrm{d}\tau \mathrm{e}^{\mathrm{i}(\omega+\lambda-\epsilon_k)\tau}}^{=2\pi\delta(\omega+\lambda-\epsilon_k)} \\
&+ \frac{1}{2\pi}\sum_{\substack{k>N/2\\ \sigma}} \varphi^*_{k,\sigma}(\mathbf{r}')\varphi_{k,\sigma}(\mathbf{r}) \int_{-\infty}^{\infty}\frac{\mathrm{d}\lambda}{\lambda+\mathrm{i}\eta}\underbrace{\int_{-\infty}^{\infty}\mathrm{d}\tau \mathrm{e}^{\mathrm{i}(\omega-\lambda-\epsilon_k)\tau}}_{=2\pi\delta(\omega-\lambda-\epsilon_k)}\,, \quad \left(\eta\to 0^+\right) \\
&= -\sum_{\substack{k\leq N/2\\ \sigma}} \varphi_{k,\sigma}(\mathbf{r})\varphi^*_{k,\sigma}(\mathbf{r}') \int_{-\infty}^{\infty}\mathrm{d}\lambda\frac{\delta(\omega+\lambda-\epsilon_k)}{\lambda+\mathrm{i}\eta} \\
&+ \sum_{\substack{k>N/2\\ \sigma}} \varphi^*_{k,\sigma}(\mathbf{r}')\varphi_{k,\sigma}(\mathbf{r}) \int_{-\infty}^{\infty}\mathrm{d}\lambda\frac{\delta(\omega-\lambda-\epsilon_k)}{\lambda+\mathrm{i}\eta}\,, \quad \left(\eta\to 0^+\right) \\
&= \sum_{\substack{k\leq N/2\\ \sigma}} \varphi_{k,\sigma}(\mathbf{r})\varphi^*_{k,\sigma}(\mathbf{r}')\frac{1}{\omega-\epsilon_k-\mathrm{i}\eta} + \sum_{\substack{k>N/2\\ \sigma}} \varphi^*_{k,\sigma}(\mathbf{r}')\varphi_{k,\sigma}(\mathbf{r})\frac{1}{\omega-\epsilon_k+\mathrm{i}\eta}\,, \quad \left(\eta\to 0^+\right) \\
&= \sum_{k,\sigma} \varphi_{k,\sigma}(\mathbf{r})\varphi^*_{k,\sigma}(\mathbf{r}')\frac{1}{\omega-\epsilon_k+\mathrm{i}\eta\,\mathrm{sgn}(\epsilon_k)}\,, \quad \left(\eta\to 0^+\right)\,. \qquad (5.63)
\end{aligned}$$

On the last line we defined

$$\mathrm{sgn}(\epsilon_k) = \begin{cases} +1 \text{ when } k > N/2 & \text{i.e. outside the Fermi sphere, unoccupied} \\ -1 \text{ when } k \leq N/2 & \text{i.e. inside the Fermi sphere, occupied.} \end{cases} \qquad (5.64)$$

We can finally sum over the molecular orbitals to obtain the non-interacting Green's function for the molecule in frequency space

$$G^0_{\substack{k,k'\\ \sigma,\sigma'}}(\omega) = \frac{\delta_{k,k'}\delta_{\sigma,\sigma'}}{\omega-\epsilon_k+\mathrm{i}\eta\,\mathrm{sgn}(\epsilon_k)}\,, \quad \left(\eta\to 0^+\right)\,. \qquad (5.65)$$

We keep the term $\eta$ still inside the expression for the non-interacting Green's function because we eventually want to do Feynman-diagram calculations with the non-interacting Green's function, and we take the limit $\eta \to 0^+$ after these calculations.

### 5.3.2 Non-interacting Green's function for the TB chain

For the TB chain, the derivation of non-interacting Green's function is slightly different than for the molecule. This is due to the fact that, as in Hamiltonian (5.2), we have the creation and annihilation operators for the chain in site basis and we must transform into energy eigenbasis as done in Sec. 5.2. In the exact calculation we used a linear transformation of the form (5.5), but now we will only refer to a *unitary* transformation that diagonalizes the tight-binding Hamiltonian. We will find the form of this transformation after we have derived the non-interacting Green's function. We hereby have

$$\hat{d}^{(\dagger)}_{k,\sigma} = \sum_{l,\sigma'} U^{(\dagger)}_{\substack{k,l\\ \sigma,\sigma'}} \hat{c}^{(\dagger)}_{l,\sigma'} \,, \tag{5.66}$$

where $U^{\dagger}_{\substack{k,l\\ \sigma,\sigma'}} = U^{*}_{\substack{l,k\\ \sigma',\sigma}}$ is the usual hermitean conjugate of a matrix. Also in this basis, the ground state is simply a Fermi sphere and we can do the derivation identical to the case of molecule as far as Eq. (5.59), but we must keep the unitary matrices connected to the creation and annihilation operators. We, thus, expand the field operators in Eq. (5.52) within a basis of functions $\varphi_{k,\sigma}(\mathbf{r})$ and expand the creation and annihilation operators again as in Eq. (5.66). This procedure involves a little more book keeping with the summing indices, and this way we get

$$\begin{aligned}
&G^0(\mathbf{x},z;\mathbf{x}',z') \\
&= \mathrm{i} \sum_{\substack{k,k'\\ \sigma_1,\sigma_1'\\ n}} \sum_{\substack{l,l'\\ \sigma_2,\sigma_2'\\ m}} \Big[ \theta(z-z')\varphi_{k,\sigma}(\mathbf{r})\varphi^{*}_{k',\sigma'}(\mathbf{r}')\mathrm{e}^{\mathrm{i}\left(E_0-E_n^{N+1}\right)(z-z')} \times \\
&\qquad \times \langle\Psi_0|U_{\substack{k,l\\ \sigma_1,\sigma_2}} \hat{c}_{l,\sigma_2}(z)|\Psi_n^{N+1}\rangle\langle\Psi_n^{N+1}|U^{*}_{\substack{l',k'\\ \sigma_2',\sigma_1'}} \hat{c}^{\dagger}_{l',\sigma_2'}(z')|\Psi_0\rangle \\
&- \theta(z'-z)\varphi^{*}_{k',\sigma'}(\mathbf{r}')\varphi_{k,\sigma}(\mathbf{r})\mathrm{e}^{\mathrm{i}\left(E_0-E_m^{N-1}\right)(z'-z)} \times \\
&\qquad \times \langle\Psi_0|U^{*}_{\substack{l',k'\\ \sigma_2',\sigma_1'}} \hat{c}^{\dagger}_{l',\sigma_2'}(z')|\Psi_m^{N-1}\rangle\langle\Psi_m^{N-1}|U_{\substack{k,l\\ \sigma_1,\sigma_2}} \hat{c}_{l,\sigma_2}(z)|\Psi_0\rangle \Big] .
\end{aligned} \tag{5.67}$$

Also in this case, we write the step functions by using Eq. (5.61) and Fourier transform with respect to the relative time coordinate $\tau := z - z'$. We also notice that the sums over $n$ and $m$ are done away with the fact that $n = l, l'$ and $m = l, l'$. First we get

$$\begin{aligned}
G^0(\mathbf{x},z;\mathbf{x}',z') &= \mathrm{i} \sum_{\substack{k,k'\\ \sigma_1,\sigma_1'\\ n}} \sum_{\substack{l,l'\leq N/2\\ \sigma_2,\sigma_2'\\ m}} \theta(\tau)\varphi_{k,\sigma}(\mathbf{r})\varphi^{*}_{k',\sigma'}(\mathbf{r}')\mathrm{e}^{-\mathrm{i}\epsilon_l\tau} U_{\substack{k,l\\ \sigma_1,\sigma_2}} U^{*}_{\substack{l',k'\\ \sigma_2',\sigma_1'}} \delta_{l,l'}\delta_{\sigma_2,\sigma_2'} \\
&- \mathrm{i} \sum_{\substack{k,k'\\ \sigma_1,\sigma_1'\\ n}} \sum_{\substack{l,l'> N/2\\ \sigma_2,\sigma_2'\\ m}} \theta(-\tau)\varphi_{k,\sigma}(\mathbf{r})\varphi^{*}_{k',\sigma'}(\mathbf{r}')\mathrm{e}^{-\mathrm{i}\epsilon_l\tau} U^{*}_{\substack{l',k'\\ \sigma_2',\sigma_1'}} U_{\substack{k,l\\ \sigma_1,\sigma_2}} \delta_{l,l'}\delta_{\sigma_2,\sigma_2'} \,,
\end{aligned} \tag{5.68}$$

and then we Fourier transform and insert the definition for the step function to obtain [the evaluation of the integrals goes exactly the same way as in Eq. (5.63)]

$$\begin{aligned}
G^0(\mathbf{x},\mathbf{x}';\omega) &= \sum_{\substack{k,k'\\ l,\sigma_2}} \varphi_{k,\sigma_1}(\mathbf{r})\varphi_{k',\sigma_1'}(\mathbf{r}') U_{\substack{k,l\\ \sigma_1,\sigma_2}} U^{*}_{\substack{l,k'\\ \sigma_2,\sigma_1'}} \frac{1}{\omega-\epsilon_l+\mathrm{i}\eta\,\mathrm{sgn}(\epsilon_l)} \,, \quad \left(\eta\to 0^+\right) \\
\Rightarrow \qquad G^0_{\substack{k,k'\\ \sigma_1,\sigma_1'}}(\omega) &= \sum_{l,\sigma_2} \frac{U_{\substack{k,l\\ \sigma_1,\sigma_2}} U^{*}_{\substack{l,k'\\ \sigma_2,\sigma_1'}}}{\omega-\epsilon_l+\mathrm{i}\eta\,\mathrm{sgn}(\epsilon_l)} \,, \quad \left(\eta\to 0^+\right) .
\end{aligned} \tag{5.69}$$

In this case the sign of $\mathrm{i}\eta$ is $+$ for an excited state, and $-$ for the ground state.

### 5.3.3 Hamiltonian and interactions

As we are dealing with calculations that include expansions of the interaction, we would want to keep the interactions as simple as possible, and include the more complicated terms inside the Hamiltonian. The interaction part of the Hamiltonian in Eq. (5.4), $U_{\mathrm{ext}}\left(\hat{n}_{\mathrm{ch}}-1\right)\left(\hat{n}_{\mathrm{mol}}-2\right)$, contains both one-particle and two-particle terms. We would like this term to be in the form of $U_{\mathrm{ext}}\hat{n}_{\mathrm{ch}}\hat{n}_{\mathrm{mol}}$ so that we could handle the interactions with

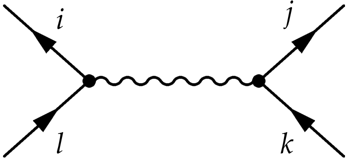

$$V_{ijkl} \;=\; V_{ij}\delta_{i,l}\delta_{j,k}\,. \tag{5.70}$$

Expanding the term in Eq. (5.4) we get

$$\hat{V}=U_{\mathrm{ext}}\left(\hat{n}_{\mathrm{ch}}\hat{n}_{\mathrm{mol}}-2\hat{n}_{\mathrm{ch}}-\hat{n}_{\mathrm{mol}}+2\right)\;, \tag{5.71}$$

where the number operator on the molecule is $\hat{n}_{\mathrm{mol}}=\hat{n}_H+\hat{n}_L$. These terms we can adapt to the molecular part of the Hamiltonian, i.e., we get for the Eq. (5.3)

$$\hat{\hat{H}}_{\mathrm{mol}}=\left(\xi_H-U_{\mathrm{ext}}\right)\hat{n}_H+\left(\xi_H+\Delta_0-U_{\mathrm{ext}}\right)\hat{n}_L+U_0\hat{n}_{H,+}\hat{n}_{H,-}+U_0\hat{n}_{L,+}\hat{n}_{L,-}+U_{HL}\hat{n}_H\hat{n}_L\,. \tag{5.72}$$

There is also a constant term in Eq. (5.71), $2U_{\mathrm{ext}}$, which we will neglect as adding a constant to the Hamiltonian does not change its properties. The third term to be considered is $-2U_{\mathrm{ext}}\hat{n}_{\mathrm{ch}}$, which unfortunately cannot be included in the other parts of the Hamiltonian. But, fortunately, we can take this term into account when calculating the self-energy. This idea is seen from the Dyson equation. We define the non-interacting Green's function $G^0$ through

$$\left(\mathrm{i}\partial_t-\hat{h}(1)\right)G^0(1,1')=\delta(1,1')\,, \tag{5.73}$$

and the full Green's function $G$ through

$$\left(\mathrm{i}\partial_t-\hat{h}(1)-\delta V\right)G(1,1')=\delta(1,1')+\int \mathrm{d}2\,\Sigma(1,2)G(2,1)\,, \tag{5.74}$$

where $\delta V$ is a small perturbation that is not included in the Hamiltonian $\hat{h}$. (In our case $\delta V$ is the part we could not include in the Hamiltonian, i.e., $-2U_{\mathrm{ext}}\hat{n}_{\mathrm{ch}}$.) We can manipulate Eq. (5.74) by moving the $\delta V$ term to the other side of the equation. In this way we get

$$\left(\mathrm{i}\partial_t-\hat{h}(1)\right)G(1,1')=\delta(1,1')+\int \mathrm{d}2\;\underbrace{\left[\Sigma(1,2)+\delta(1,2)\delta V\right]}_{=:\Sigma'}G(2,1)\,. \tag{5.75}$$

This trick is completely allowed since the solution of the Dyson equation remains as

$$G=G^0+G^0\Sigma' G\,, \tag{5.76}$$

as can be checked by operating from left with $\left(\mathrm{i}\partial_t-\hat{h}(1)\right)$. The term to be added to the self-energy is then simply a constant $-2U_{\mathrm{ext}}$ regarding the first site of the chain, i.e.,

$$\delta V_{ij}=\begin{pmatrix} 0 & 0 & 0 & 0\\ 0 & 0 & 0 & 0\\ 0 & 0 & -2U_{\mathrm{ext}} & 0\\ 0 & 0 & 0 & 0 \end{pmatrix}. \tag{5.77}$$

### 5.3.4 Two-site molecule and two-site TB chain

For this particular system of a two-site molecule next to a two-site TB chain we can determine the non-interacting Green's function $G^0$ by means of Eqs. (5.65) and (5.69). We take the indices for the $G^0$ matrix to be as $i, j \in \{H, L, 1, 2\}$, where $H$ and $L$ refer to the HOMO and LUMO levels of the molecule, respectively, and 1 and 2 refer to the first and second site of the chain. For the molecule part, the matrix is diagonal as Eq. (5.65) indicates, and we only need to insert proper energies in $\epsilon_k$. For the two-site chain, the Hamiltonian matrix is

$$\left(\hat{H}_{\text{ch}}\right)_{ij} = \begin{pmatrix} 0 & -t \\ -t & 0 \end{pmatrix}, \tag{5.78}$$

where $t$ is the hopping probability. A unitary matrix that diagonalizes this matrix is given by

$$U_{ij} = \frac{1}{\sqrt{2}} \begin{pmatrix} 1 & 1 \\ 1 & -1 \end{pmatrix}. \tag{5.79}$$

Hence, we have from Eq. (5.69) for the chain part

$$G^0_{ij}(\omega) = \frac{1}{\sqrt{2}} \begin{pmatrix} 1 & 1 \\ 1 & -1 \end{pmatrix} \begin{pmatrix} \frac{1}{\omega-\epsilon_1-\mathrm{i}\eta} & 0 \\ 0 & \frac{1}{\omega-\epsilon_2+\mathrm{i}\eta} \end{pmatrix} \frac{1}{\sqrt{2}} \begin{pmatrix} 1 & 1 \\ 1 & -1 \end{pmatrix}, \tag{5.80}$$

where $\epsilon_1 = t$ and $\epsilon_2 = -t$ (as we are using $t < 0$, see Fig. 5.2). The product of matrices yields

$$G^0_{ij}(\omega) = \begin{pmatrix} \frac{1}{2}\left(\frac{1}{\omega-t-\mathrm{i}\eta} + \frac{1}{\omega+t+\mathrm{i}\eta}\right) & \frac{1}{2}\left(\frac{1}{\omega-t-\mathrm{i}\eta} - \frac{1}{\omega+t+\mathrm{i}\eta}\right) \\ \frac{1}{2}\left(\frac{1}{\omega-t-\mathrm{i}\eta} - \frac{1}{\omega+t+\mathrm{i}\eta}\right) & \frac{1}{2}\left(\frac{1}{\omega-t-\mathrm{i}\eta} + \frac{1}{\omega+t+\mathrm{i}\eta}\right) \end{pmatrix}. \tag{5.81}$$

We can then finally conclude that the non-interacting Green's function for our $(2+2)$-site system is

$$G^0_{ij}(\omega) = \begin{pmatrix} \frac{1}{\omega-\xi_H+U_{\text{ext}}-\mathrm{i}\eta} & 0 & 0 & 0 \\ 0 & \frac{1}{\omega-\xi_H-\Delta_0+U_{\text{ext}}+\mathrm{i}\eta} & 0 & 0 \\ 0 & 0 & \frac{1}{2}\left(\frac{1}{\omega-t-\mathrm{i}\eta} + \frac{1}{\omega+t+\mathrm{i}\eta}\right) & \frac{1}{2}\left(\frac{1}{\omega-t-\mathrm{i}\eta} - \frac{1}{\omega+t+\mathrm{i}\eta}\right) \\ 0 & 0 & \frac{1}{2}\left(\frac{1}{\omega-t-\mathrm{i}\eta} - \frac{1}{\omega+t+\mathrm{i}\eta}\right) & \frac{1}{2}\left(\frac{1}{\omega-t-\mathrm{i}\eta} + \frac{1}{\omega+t+\mathrm{i}\eta}\right) \end{pmatrix}. \tag{5.82}$$

It is now worth mentioning how the extra $U_{\text{ext}}$ terms appear in the energies of the molecule as explained earlier in Eq. (5.72). For the interaction matrix we have

$$V_{ij} = \begin{pmatrix} U_0 & U_{HL} & U_{\text{ext}} & 0 \\ U_{HL} & U_0 & U_{\text{ext}} & 0 \\ U_{\text{ext}} & U_{\text{ext}} & 0 & 0 \\ 0 & 0 & 0 & 0 \end{pmatrix}. \tag{5.83}$$

### 5.3.5 Self-energy calculations

Now we are ready to do an actual Feynman-diagram calculation. We first consider the Hartree–Fock approximation for the self-energy, i.e., we calculate only the tadpole and exchange diagrams in first order. In the following we have a non-interacting Green's function $G^0(\omega)$ joining the diagram at point $j$ and leaving at point $i$. In every vertex, the frequency must be conserved, and every internal index must be summed over as well as every internal frequency must be integrated over.

$$\Sigma^{\mathrm{HF}}_{ij}(\omega) \;=$$

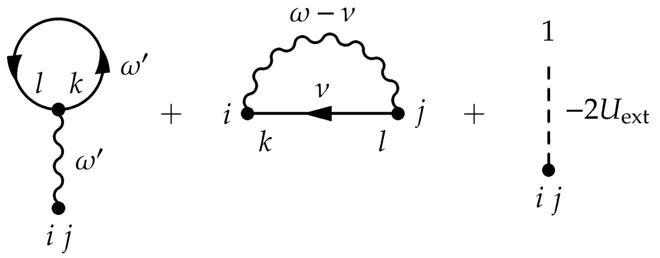

$$
\begin{aligned}
&= -\mathrm{i}\sum_{\substack{k,l\\ \sigma_k,\sigma_l}}\int_{\infty}^{\infty}\frac{\mathrm{d}\omega'}{2\pi}\mathrm{e}^{\mathrm{i}\omega'\eta}G^0_{kl}(\omega')\overbrace{\underset{\sigma_i\sigma_k\sigma_l\sigma_j}{V_{iklj}}}^{=V_{ik}\delta_{i,j}\delta_{k,l}\delta_{\sigma_i,\sigma_j}\delta_{\sigma_k,\sigma_l}} + \mathrm{i}\sum_{\substack{k,l\\ \sigma_k,\sigma_l}}\int_{-\infty}^{\infty}\frac{\mathrm{d}\nu}{2\pi}\mathrm{e}^{\mathrm{i}\nu\eta}G^0_{lk}(\nu)\overbrace{\underset{\sigma_i\sigma_l\sigma_j\sigma_k}{V_{iljk}}}^{=V_{il}\delta_{i,k}\delta_{l,j}\delta_{\sigma_i,\sigma_k}\delta_{\sigma_l,\sigma_j}} - 2U_{\mathrm{ext}}\delta_{i,1}\delta_{j,1}\\
&= -\mathrm{i}\sum_{k,\sigma_k}\int\frac{\mathrm{d}\omega'}{2\pi}\mathrm{e}^{\mathrm{i}\omega'\eta}G^0_{kk}(\omega')V_{ik}\delta_{i,j}\delta_{\sigma_i,\sigma_j} + \mathrm{i}\int\frac{\mathrm{d}\nu}{2\pi}\mathrm{e}^{\mathrm{i}\nu\eta}G^0_{ji}(\nu)V_{ij} - 2U_{\mathrm{ext}}\delta_{i,1}\delta_{j,1}\,. \qquad (5.84)
\end{aligned}
$$

From the expression in Eq. (5.84) we can calculate all the different components of the self-energy. All in all, we end up having to calculate 16 different elements, but fortunately, most of them are zero and that can be seen easily. It is also worthwile to notice that we now include the term discussed in Eq. (5.74) to the self-energy. In the first approximation only $\Sigma_{\mathrm{HH}}$ and $\Sigma_{\mathrm{LL}}$ are non-zero.

Let us calculate the '$HH$' component as an example. By inserting $i, j = H$ into expression in Eq. (5.84) and using Eqs. (5.82) and (5.83) we get

$$
\begin{aligned}
\Sigma^{\mathrm{HF}}_{HH}(\omega) &= -2\mathrm{i}\int\frac{\mathrm{d}\omega'}{2\pi}\mathrm{e}^{\mathrm{i}\omega'\eta}\Big[G^0_{HH}(\omega')V_{HH} + G^0_{LL}(\omega')V_{HL} + G^0_{11}(\omega')V_{H1} + G^0_{22}(\omega')V_{H2}\Big]\\
&\quad + \mathrm{i}\int\frac{\mathrm{d}\nu}{2\pi}\mathrm{e}^{\mathrm{i}\nu\eta}G^0_{HH}V_{HH}\\
&= -2\mathrm{i}\int\frac{\mathrm{d}\omega'}{2\pi}\mathrm{e}^{\mathrm{i}\omega'\eta}\Bigg[\frac{U_0}{\omega' - \xi_H + U_{\mathrm{ext}} - \mathrm{i}\eta} + \frac{U_{HL}}{\omega' - \xi_H - \Delta_0 + U_{\mathrm{ext}} + \mathrm{i}\eta}\\
&\qquad + \frac{U_{\mathrm{ext}}}{2}\Big(\frac{1}{\omega' - t - \mathrm{i}\eta} + \frac{1}{\omega' + t + \mathrm{i}\eta}\Big)\Bigg]\\
&\quad + \mathrm{i}\int\frac{\mathrm{d}\nu}{2\pi}\mathrm{e}^{\mathrm{i}\nu\eta}\frac{U_0}{\nu - \xi_H + U_{\mathrm{ext}} - \mathrm{i}\eta}\,. \qquad (5.85)
\end{aligned}
$$

Now we use Cauchy's integral formula (see Sec. 4.1) to calculate these integrals. We need the formula derived in Eq. (4.17) and also the idea from Eq. (4.22). We see that the terms with $\mathrm{i}\eta$ positive vanish, as these correspond to poles in the LHP, and the exponential convergence factor forces the integration via the UHP. Hence, we obtain

$$
\begin{aligned}
\Sigma^{\mathrm{HF}}_{HH}(\omega) &= -2\mathrm{i}\frac{1}{2\pi}2\pi\mathrm{i}\Big(U_0 + \frac{U_{\mathrm{ext}}}{2}\Big) + \mathrm{i}\frac{1}{2\pi}2\pi\mathrm{i}U_0\\
&= U_0 + U_{\mathrm{ext}}\,. \qquad (5.86)
\end{aligned}
$$

Similarly, we can calculate the '$LL$' component. All the other components give zero contribution, but it is essential to notice, that the tadpole diagram gives contribution $2U_{\mathrm{ext}}$ to the '11' component, which is then exactly cancelled by the added extra term in Eq. (5.77). This gives us the self-energy matrix for the first step of the calculation

$$\Sigma_{ij}^{\mathrm{HF}(1)}(\omega) = \begin{pmatrix} U_0 + U_{\mathrm{ext}} & 0 & 0 & 0 \\ 0 & 2U_{HL} + U_{\mathrm{ext}} & 0 & 0 \\ 0 & 0 & 0 & 0 \\ 0 & 0 & 0 & 0 \end{pmatrix} . \tag{5.87}$$

We can then insert the self-energy into Dyson equation to obtain the total Green's function for the first step

$$\begin{aligned} G_{ij}^{\mathrm{HF}(1)}(\omega) &= \left[\left(G_{ij}^0(\omega)\right)^{-1} - \Sigma_{ij}^{\mathrm{HF}(1)}(\omega)\right]^{-1} \\ &= \begin{pmatrix} \frac{1}{\omega-\xi_{\mathrm{H}}-U_0} & 0 & 0 & 0 \\ 0 & \frac{1}{\omega-\xi_{\mathrm{H}}-\Delta_0-2U_{HL}} & 0 & 0 \\ 0 & 0 & \frac{1}{2}\left(\frac{1}{\omega-t-\mathrm{i}\eta} + \frac{1}{\omega+t+\mathrm{i}\eta}\right) & \frac{1}{2}\left(\frac{1}{\omega-t-\mathrm{i}\eta} - \frac{1}{\omega+t+\mathrm{i}\eta}\right) \\ 0 & 0 & \frac{1}{2}\left(\frac{1}{\omega-t-\mathrm{i}\eta} - \frac{1}{\omega+t+\mathrm{i}\eta}\right) & \frac{1}{2}\left(\frac{1}{\omega-t-\mathrm{i}\eta} + \frac{1}{\omega+t+\mathrm{i}\eta}\right) \end{pmatrix} . \end{aligned} \tag{5.88}$$

The next step of the calculation is to take the derived Green's function $G^{\mathrm{HF}(1)}$ and to calculate the first order diagrams again, but this time with the new Green's function as a propagator. As an example, we calculate here the '$LL$' component of the second step:

$$\begin{aligned} \Sigma_{LL}^{\mathrm{HF}(2)}(\omega) &= -2\mathrm{i}\int \frac{\mathrm{d}\omega'}{2\pi}\mathrm{e}^{\mathrm{i}\omega'\eta}\left[\frac{U_{HL}}{\omega' - \xi_H - U_0 - \mathrm{i}\eta} + \frac{U_0}{\omega' - \xi_H - \Delta_0 - 2U_{HL} + \mathrm{i}\eta}\right. \\ &\qquad \left. + \frac{U_{\mathrm{ext}}}{2}\left(\frac{1}{\omega' - t - \mathrm{i}\eta} + \frac{1}{\omega' + t + \mathrm{i}\eta}\right)\right] \\ &\quad + \mathrm{i}\int \frac{\mathrm{d}\nu}{2\pi}\mathrm{e}^{\mathrm{i}\nu\eta}\frac{U_0}{\nu - \xi_H - \Delta_0 - 2U_{HL} + \mathrm{i}\eta} . \end{aligned} \tag{5.89}$$

Again we use Cauchy's integral formula, and see that the terms with $\mathrm{i}\eta$ positive vanish due to the orientation of the integration path. Simplifying the terms we obtain

$$\Sigma_{LL}^{\mathrm{HF}(2)}(\omega) = 2U_{HL} + U_{\mathrm{ext}} , \tag{5.90}$$

which is exactly the same result we got in the first step of the calculation. The same thing happens with all the other components as well. This implies that the perturbation sum converged after the first step of the calculation, and the Green's function we got in Eq. (5.88) is the full HF Green's function.

From the poles of the $G_{HH}(\omega)$ and $G_{LL}(\omega)$ components in Eq. (5.88) we find the removal and additional spectrum in the HOMO and LUMO levels, respectively. In Hartree–Fock approximation the LUMO spectral peaks then occur at

$$\omega = \xi_H + \Delta_0 + 2U_{HL} , \tag{5.91}$$

which gives $\omega = 1$ when we take $-t = \Delta_0 = U_0 = U_{HL} = 1$ and $\xi_H = -2$ [see Eq. (5.34)]. We notice that HF approximation does not see the interaction between the molecule and the chain as there is no dependency on the interaction strength $U_{\mathrm{ext}}$ in the addition energies. We also notice that when we compare this addition energy to the ones in Eqs. (5.49), (5.49) and (5.49), that HF approximation gives only one peak, whereas the exact result gives three peaks.

Next we would like to make our approximation better by calculating more terms in the perturbation series. After the HF calculations we can insert the obtained HF Green's function into second order diagrams. First, we introduce a second order diagram called the bubble diagram (here also a non-interacting Green's function $G^0(\omega)$ joins the diagram at $j$ and leaves the diagram at $i$)

$$\Sigma^{\mathrm{HFB}}_{ij}(\omega) \quad = $$

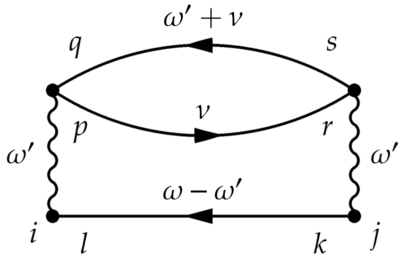

$$\begin{aligned}
&= -1\cdot \mathrm{i}^2 \sum_{\substack{k,l,p\\ q,r,s\\ \sigma_k,\sigma_l,\sigma_p\\ \sigma_q,\sigma_r,\sigma_s}} \int \frac{\mathrm{d}\omega'}{2\pi} \int \frac{\mathrm{d}\nu}{2\pi} \overbrace{V_{\substack{ipql\\ \sigma_i\sigma_p\sigma_q\sigma_l}}}^{=V_{ip}\delta_{i,l}\delta_{p,q}\delta_{\sigma_i,\sigma_l}\delta_{\sigma_p,\sigma_q}} \underbrace{V_{\substack{ksrj\\ \sigma_k\sigma_s\sigma_r\sigma_j}}}_{=V_{ks}\delta_{k,j}\delta_{s,r}\delta_{\sigma_k,\sigma_j}\delta_{\sigma_s,\sigma_r}} G^{\mathrm{HF}}_{kl}(\omega-\omega')G^{\mathrm{HF}}_{qs}(\nu)G^{\mathrm{HF}}_{rp}(\omega'+\nu) \\
&= \sum_{\substack{p,s\\ \sigma_p}} \int \frac{\mathrm{d}\omega'}{2\pi} \int \frac{\mathrm{d}\nu}{2\pi} V_{ip}V_{js}G^{\mathrm{HF}}_{ij}(\omega-\omega')G^{\mathrm{HF}}_{ps}(\nu)G^{\mathrm{HF}}_{sp}(\omega'+\nu)\,. \qquad (5.92)
\end{aligned}$$

From this expression we can again calculate all the different elements of the self-energy matrix. The calculations are straightforward although a bit tedious. Let us consider the '*HH*' component here. We insert $i, j = H$, $G^{\mathrm{HF}}$ from Eq. (5.88), and $V_{ij}$ from Eq. (5.83) into Eq. (5.92), and this gives

$$\begin{aligned}
\Sigma^{\mathrm{HFB}}_{HH}(\omega) &= 2\int \frac{\mathrm{d}\omega'}{2\pi} \int \frac{\mathrm{d}\nu}{2\pi} \Big[ \frac{{U_0}^2}{\omega-\omega'-\xi_H-U_0-\mathrm{i}\eta} \frac{1}{\nu-\xi_H-U_0-\mathrm{i}\eta} \frac{1}{\omega'+\nu-\xi_H-U_0-\mathrm{i}\eta} \\
&+ \frac{{U_{HL}}^2}{\omega-\omega'-\xi_H-U_0-\mathrm{i}\eta} \frac{1}{\nu-\xi_H-\Delta_0-2U_{HL}-\mathrm{i}\eta} \frac{1}{\omega'+\nu-\xi_H-\Delta_0-2U_{HL}-\mathrm{i}\eta} \\
&+ \frac{{U_{\mathrm{ext}}}^2}{\omega-\omega'-\xi_H-U_0-\mathrm{i}\eta} \frac{1}{2}\Big(\frac{1}{\nu-t-\mathrm{i}\eta} + \frac{1}{\nu+t+\mathrm{i}\eta}\Big) \frac{1}{2}\Big(\frac{1}{\omega'-t-\mathrm{i}\eta} + \frac{1}{\omega'+\nu+t+\mathrm{i}\eta}\Big)\Big]\,.
\end{aligned} \qquad (5.93)$$

From the expression in Eq. (5.93) we notice that in first two terms inside the square brackets, the integration over $\nu$ vanishes as the poles are both in the same side of the complex plane. The only contribution comes from the term with $U_{\mathrm{ext}}$. When we expand the expression inside the parentheses, we again get terms that vanish due to the position of the poles. The only terms that do not vanish are the cross terms, but also the other one from these vanish when we continue to the integration over $\omega'$. Therefore it is essential to do the calculations very carefully. Note that now we do not have the exponential convergence factor inside the integrals, as we did in the HF calculation. The integrals can therefore be done either in the UHP or in the LHP, and extra attention must be paid in order to get the overall sign correct. Proceeding with the calculation, we have

$$\begin{aligned}
\Sigma_{HH}^{\mathrm{HFB}}(\omega) &= \frac{{U_{\mathrm{ext}}}^2}{2}\int\frac{\mathrm{d}\omega'}{2\pi}\int\frac{\mathrm{d}\nu}{2\pi}\frac{1}{\omega-\omega'-\xi_H-U_0-\mathrm{i}\eta}\frac{1}{\nu+t+\mathrm{i}\eta}\frac{1}{\omega'+\nu-t-\mathrm{i}\eta}\\
&= \frac{{U_{\mathrm{ext}}}^2}{2}(-\mathrm{i})\int\frac{\mathrm{d}\omega'}{2\pi}\frac{1}{\omega-\omega'-\xi_H-U_0-\mathrm{i}\eta}\frac{1}{\omega'-2t-2\mathrm{i}\eta}\\
&= \frac{{U_{\mathrm{ext}}}^2}{2}(-\mathrm{i})\frac{\mathrm{i}}{\omega-\xi_H-U_0-2t-\mathrm{i}\eta}\\
&= \frac{\frac{1}{2}{U_{\mathrm{ext}}}^2}{\omega-\xi_H-U_0-2t}\,. \qquad (5.94)
\end{aligned}$$

Similarly we can evaluate the '$LL$' component, and all in all we have

$$\Sigma_{ij}^{\mathrm{HFB}(1)}(\omega) = \begin{pmatrix} \frac{\frac{1}{2}{U_{\mathrm{ext}}}^2}{\omega-\xi_H-U_0-2t} & 0 & 0 & 0\\ 0 & \frac{\frac{1}{2}{U_{\mathrm{ext}}}^2}{\omega-\xi_H-\Delta_0-2U_{HL}+2t} & 0 & 0\\ 0 & 0 & 0 & 0\\ 0 & 0 & 0 & 0 \end{pmatrix}. \qquad (5.95)$$

Then we insert the evaluated self-energy into Dyson equation to obtain the total Green's function for the first step in the bubble-diagram calculation. By doing this we get

$$G_{ij}^{\mathrm{HFB}(1)}(\omega) = \left[\left(G_{ij}^{0}(\omega)\right)^{-1} - \Sigma_{ij}^{\mathrm{HFB}(1)}(\omega)\right]^{-1} =$$

$$\begin{pmatrix} \frac{1}{\omega-\xi_H-U_0+\frac{\frac{1}{2}{U_{\mathrm{ext}}}^2}{\omega-\xi_H-U_0-2t}} & 0 & 0 & 0\\ 0 & \frac{1}{\omega-\xi_H-\Delta_0-2U_{HL}-\frac{\frac{1}{2}{U_{\mathrm{ext}}}^2}{\omega-\xi_H-\Delta_0-2U_{HL}+2t}} & 0 & 0\\ 0 & 0 & \frac{1}{2}\left(\frac{1}{\omega-t-\mathrm{i}\eta}+\frac{1}{\omega+t+\mathrm{i}\eta}\right) & \frac{1}{2}\left(\frac{1}{\omega-t-\mathrm{i}\eta}-\frac{1}{\omega+t+\mathrm{i}\eta}\right)\\ 0 & 0 & \frac{1}{2}\left(\frac{1}{\omega-t-\mathrm{i}\eta}-\frac{1}{\omega+t+\mathrm{i}\eta}\right) & \frac{1}{2}\left(\frac{1}{\omega-t-\mathrm{i}\eta}+\frac{1}{\omega+t+\mathrm{i}\eta}\right) \end{pmatrix}. \qquad (5.96)$$

This is now one step beyond Hartree–Fock approximation; we calculated a second order diagram by using the HF Green's function. The LUMO spectral peaks again occur at the poles of the $G_{LL}^{\mathrm{HFB}(1)}(\omega)$. Evaluating the quadratic equation we get two peaks at

$$\begin{aligned}
\omega_1 &= 2+\sqrt{1+\frac{1}{2}{U_{\mathrm{ext}}}^2} \qquad (5.97)\\
\omega_2 &= 2-\sqrt{1+\frac{1}{2}{U_{\mathrm{ext}}}^2}\,. \qquad (5.98)
\end{aligned}$$

From these we see that by including the bubble diagram in our calculation we now get a clear dependence on the interaction strength $U_{\mathrm{ext}}$. But still, when we compare these addition energies to the ones calculated exactly in Eqs. (5.49), (5.49) and (5.49), we see that one peak is missing.

Usually there is more second order diagrams to be considered. However, in the following we will show that the second order exchange diagram vanishes for the studied system. The exchange diagram in second order is of the form ($G^0(\omega)$ joins at $j$ and leaves at $i$)

$$\Sigma^{\mathrm{HFE}}_{ij}(\omega) \;=$$

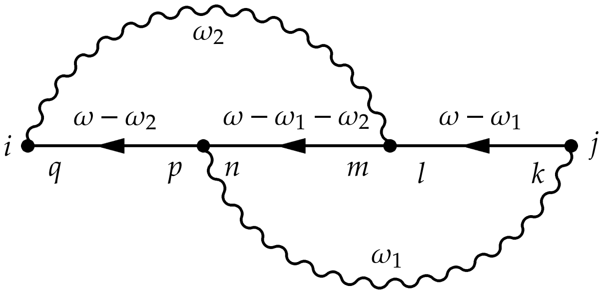

$$= \mathrm{i}^2 \sum_{\substack{k,l,m\\ n,p,q\\ \sigma_k,\sigma_l,\sigma_m\\ \sigma_n,\sigma_p,\sigma_q}} \int \frac{\mathrm{d}\omega_1}{2\pi} \int \frac{\mathrm{d}\omega_2}{2\pi} \overbrace{V_{\substack{ilnq\\ \sigma_i\sigma_l\sigma_n\sigma_q}}}^{=V_{il}\delta_{i,q}\delta_{l,m}\delta_{\sigma_i,\sigma_q}\delta_{\sigma_l,\sigma_m}} \underbrace{V_{\substack{kpnj\\ \sigma_k\sigma_p\sigma_n\sigma_j}}}_{=V_{kp}\delta_{k,j}\delta_{p,n}\delta_{\sigma_k,\sigma_j}\delta_{\sigma_p,\sigma_n}} G^{\mathrm{HF}}_{kl}(\omega-\omega_1) G^{\mathrm{HF}}_{mn}(\omega-\omega_1-\omega_2) G^{\mathrm{HF}}_{pq}(\omega-\omega_2)$$

$$= -\sum_{m,n} \int \frac{\mathrm{d}\omega_1}{2\pi} \int \frac{\mathrm{d}\omega_2}{2\pi} V_{im} V_{jn} G^{\mathrm{HF}}_{mj}(\omega-\omega_1) G^{\mathrm{HF}}_{nm}(\omega-\omega_1-\omega_2) G^{\mathrm{HF}}_{in}(\omega-\omega_2)\,. \tag{5.99}$$

If we then try to compute different components of the self-energy, we find that each one of them vanishes. When we integrate over the internal frequency $\omega_2$, we have the second and the third Green's function with poles at the same side of the complex plane. This is why the integrals over $\omega_2$ always vanish in this particular diagram, even if we used the non-interacting Green's function $G^0$ instead of the HF Green's function $G^{\mathrm{HF}}$.

We can then continue the calculation with the bubble diagram. Next we insert the obtained Green's function $G^{\mathrm{HFB}(1)}_{ij}$ back to the expression for the self-energy in Eq. (5.92), but first we need to factorize the components $G^{\mathrm{HFB}(1)}_{HH}(\omega)$ and $G^{\mathrm{HFB}(1)}_{LL}(\omega)$ so that we only get simple poles to be considered in the integration. Since we have two roots $\omega_1$ and $\omega_2$ for the denominators of the '*HH*' and '*LL*' components, we can modify the whole components in the following form

$$G^{\mathrm{HFB}(1)}_{HH,LL}(\omega) = \frac{a_1}{\omega-\omega_1} + \frac{a_2}{\omega-\omega_2}\,, \tag{5.100}$$

where $a_1$ and $a_2$ are the factors that we need to find. The procedure itself is a simple algebraic manipulation, and we find the factors for the '*HH*' component to be

$$a_1 = \frac{1}{2} - \frac{1}{\sqrt{4+2U_{\mathrm{ext}}{}^2}}\,, \qquad a_2 = \frac{1}{2} + \frac{1}{\sqrt{4+2U_{\mathrm{ext}}{}^2}}\,, \tag{5.101}$$

with roots of the denominator as

$$\omega_1 = -2 - \sqrt{1+\frac{1}{2}U_{\mathrm{ext}}{}^2}\,, \qquad \omega_2 = -2 + \sqrt{1+\frac{1}{2}U_{\mathrm{ext}}{}^2}\,. \tag{5.102}$$

Similarly for the '*LL*' component we find the factors to be

$$b_1 = \frac{1}{2} + \frac{1}{\sqrt{4+2U_{\mathrm{ext}}{}^2}}\,, \qquad b_2 = \frac{1}{2} - \frac{1}{\sqrt{4+2U_{\mathrm{ext}}{}^2}}\,, \tag{5.103}$$

with roots of the denominator as in Eqs. (5.97) and (5.98)

$$\omega_1 = 2 - \sqrt{1 + \frac{1}{2}{U_{\text{ext}}}^2}\,, \qquad \omega_2 = 2 + \sqrt{1 + \frac{1}{2}{U_{\text{ext}}}^2}\,. \tag{5.104}$$

A noteworthy point for the previous-step calculation is that the intensities of the spectral peaks in Eqs. (5.97) and (5.98) are given by the calculated factors in Eq. (5.103). For the factors we then naturally have $\sum_i a_i = 1 = \sum_i b_i$. Now we have, for the next-step calculation, the Green's function which has simple poles, and we can evaluate the integrals again by using Cauchy's integral formula. The calculation for the $\Sigma_{ij}^{\text{HFB}(2)}(\omega)$ is again straightforward but rather long, and we hereby state only the result. All the other components except *'HH'* and *'LL'* are again zero, and for the non-zero components we find (with $-t = \Delta_0 = U_0 = U_{HL} = 1$)

$$\Sigma_{HH}^{\text{HFB}(2)} = \frac{{U_{\text{ext}}}^2}{2}\left(\frac{\frac{1}{2} + \frac{1}{\sqrt{4+2{U_{\text{ext}}}^2}}}{\omega + \sqrt{1+\frac{1}{2}{U_{\text{ext}}}^2} + 4} + \frac{\frac{1}{2} + \frac{1}{\sqrt{4+2{U_{\text{ext}}}^2}}}{\omega + \sqrt{1+\frac{1}{2}{U_{\text{ext}}}^2} + 4}\right) \tag{5.105}$$

$$\Sigma_{LL}^{\text{HFB}(2)} = \frac{{U_{\text{ext}}}^2}{2}\left(\frac{\frac{1}{2} + \frac{1}{\sqrt{4+2{U_{\text{ext}}}^2}}}{\omega + \sqrt{1+\frac{1}{2}{U_{\text{ext}}}^2} + 4} + \frac{\frac{1}{2} + \frac{1}{\sqrt{4+2{U_{\text{ext}}}^2}}}{\omega + \sqrt{1+\frac{1}{2}{U_{\text{ext}}}^2} + 4}\right). \tag{5.106}$$

We then insert the evaluated self-energy into Dyson equation, and obtain the total Green's function. There is no point in writing down the obtained Green's function here, as it is quite a cryptic-looking matrix, but instead we are interested in the physical result for the studied model. We then again calculate the poles of the *'LL'* component to get the addition energy peaks for the LUMO level. These peaks arise at

$$\omega_1 = 3\,, \tag{5.107}$$

$$\omega_2 = 3 - \sqrt{4 + {U_{\text{ext}}}^2}\,, \tag{5.108}$$

$$\omega_3 = 3 + \sqrt{4 + {U_{\text{ext}}}^2}\,. \tag{5.109}$$

Naturally, the second-step calculation shows also a clear correspondence to the interaction strength $U_{\text{ext}}$. Comparing these addition energies to the exact ones in Eqs. (5.49), (5.49) and (5.49), we see that the difference is already zero, i.e., the perturbation series does not have any more diagrams with these particular initial conditions. This seems more like a coincidence, since when we apply the next step of the calculation we get closer to the so-called GW approximation which takes into account all the bubble diagrams in higher orders also.

Now we have three spectral peaks, and we are still able to factorize the components of the obtained Green's function. This way we can perform yet another step in the calculation, but as we are studying only the bubble diagram, the result found in Eqs. (5.107), (5.108) and (5.109) will get "worse". Although, we did not write down the total Green's function for the HFB(2) calculation, we state here the factors for the next step of the calculation

$$c_1 = \frac{{U_{\text{ext}}}^2}{8 + 2{U_{\text{ext}}}^2} \tag{5.110}$$

$$c_2 = \frac{1}{4} + \frac{1}{4 + {U_{\text{ext}}}^2} + \frac{1}{\sqrt{4 + {U_{\text{ext}}}^2}} \tag{5.111}$$

$$c_3 = \frac{1}{4} + \frac{1}{4 + {U_{\text{ext}}}^2} - \frac{1}{\sqrt{4 + {U_{\text{ext}}}^2}}\,, \tag{5.112}$$

and these factors give us also the intensities of the peaks found in Eqs. (5.107), (5.108) and (5.109), and we have $\sum_i c_i = 1$. When we have done the factorization we can again calculate the self-energy integrals by using Cauchy's integral formula, as we have only simple poles inside the integrand. We can then insert the evaluated self-energy into Dyson equation in order to obtain the total Green's function. This time, the poles of the '*HH*' and '*LL*' have four roots, and one of them must be unphysical, as there is only three addition spectral peaks in the exact result. This must be taken into account when solving the fourth-order roots. The addition energies for the next-step calculation were found to be

$$\omega_1 = \frac{1}{2}\left(8 - \sqrt{20 + 3U_{\text{ext}}{}^2 - \sqrt{256 + 96U_{\text{ext}}{}^2 + 5U_{\text{ext}}{}^4}}\right) \qquad (5.113)$$

$$\omega_2 = \frac{1}{2}\left(8 + \sqrt{20 + 3U_{\text{ext}}{}^2 - \sqrt{256 + 96U_{\text{ext}}{}^2 + 5U_{\text{ext}}{}^4}}\right) \qquad (5.114)$$

$$\omega_3 = \frac{1}{2}\left(8 - \sqrt{20 + 3U_{\text{ext}}{}^2 + \sqrt{256 + 96U_{\text{ext}}{}^2 + 5U_{\text{ext}}{}^4}}\right). \qquad (5.115)$$

The next steps of the calculation would eventually converge to the GW approximation, and the results in Eqs. (5.113), (5.114) and (5.115) only point the direction of the GW approximation.

We have mostly been interested in the Green's function $G$, and the physical quantities that can be deduced from it, but we have also put a lot of effort to obtaining the self-energy $\Sigma$. Because of its importancy, let us shortly see how the self-energy for, e.g., '*LL*' component looks like with respect to the frequency $\omega$. We have plotted Eqs. (5.90), (5.95), (5.106), and also for the third step of the calculation the self-energies as a function of the frequency $\omega$ in Fig. 5.4 with $-t = \Delta_0 = U_0 = U_{HL} = U_{\text{ext}} = 1$. The plots here are divided into three different regions of the frequency $\omega$ for clarity. It would be unnecessarily difficult to distinguish between the different curves if they were plotted in a same figure with, e.g., $\omega \in [0, 8]$. Now the figure is to be read as a comic book – from top to bottom. We will discuss the figure more in detail later in Chap. 6.

We have plotted also the calculated addition energies and the corresponding peak intensities from Eqs. (5.91), (5.97), (5.98), (5.107), (5.108), (5.109), (5.103), (5.110), (5.111) and (5.112) with the exact result in Fig. 5.5. We will review our calculation and compare the exact result to the results obtained by the perturbation theory later in Chap. 6.

## 5.4 Infinitely long chain

We are able to study also an infinitely long chain, i.e., an $N$-site TB chain with $N \to \infty$. This section is one part of the study presented in this thesis, which could not be done properly in our time frame. This, however, seems to be the case usually in research projects, but we will nevertheless present some of the key ideas regarding this problem.

The molecule part of the non-interacting Green's function remains the same as earlier, since we have not done any changes for the two-site molecule. The chain part, however, will change when we insert the solutions of the $N$-site TB chain from Eqs. (5.7) and (5.14) to the form of the

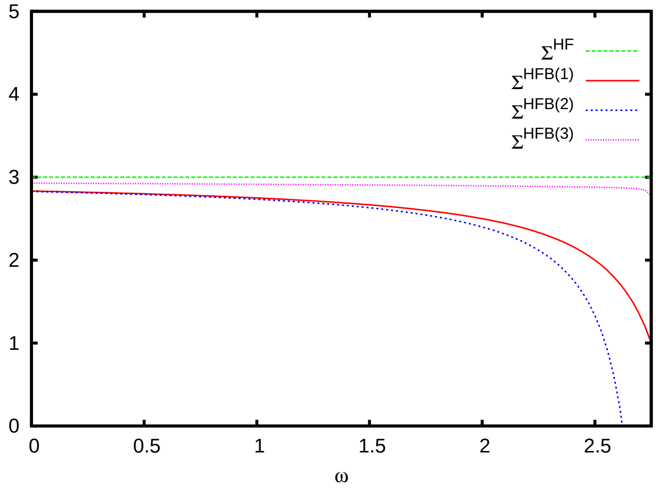

(a) $\omega \in [0.0, 2.75]$

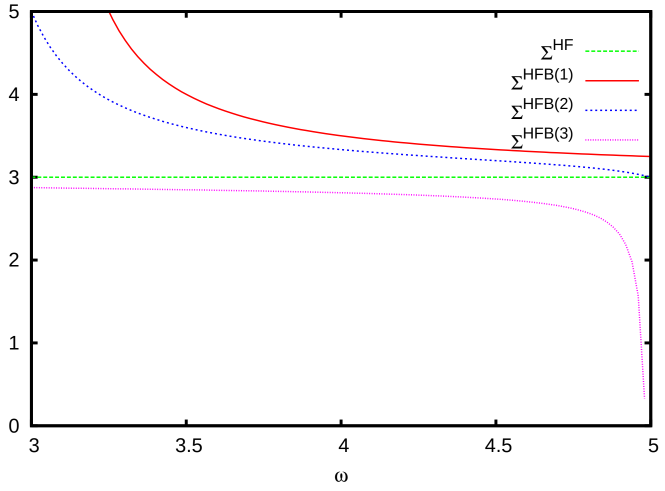

(b) $\omega \in [3.0, 5.0]$

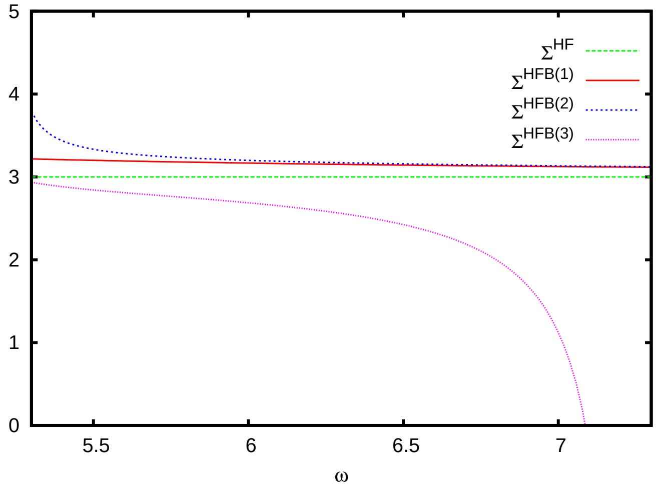

(c) $\omega \in [5.3, 7.3]$

Figure 5.4: LUMO components of the self-energy functions $\Sigma_{LL}(\omega)$ with respect to the frequency $\omega$ in different approximations.

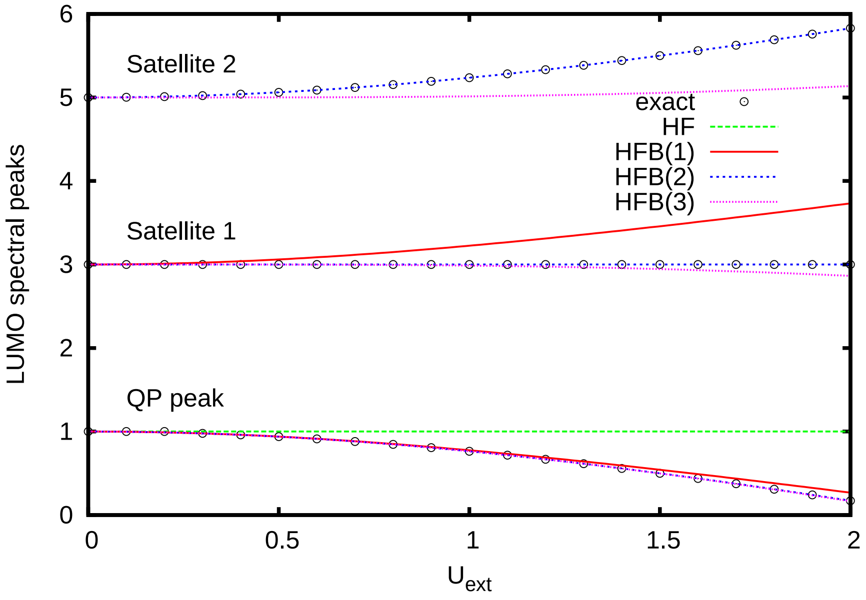

(a) Addition energies.

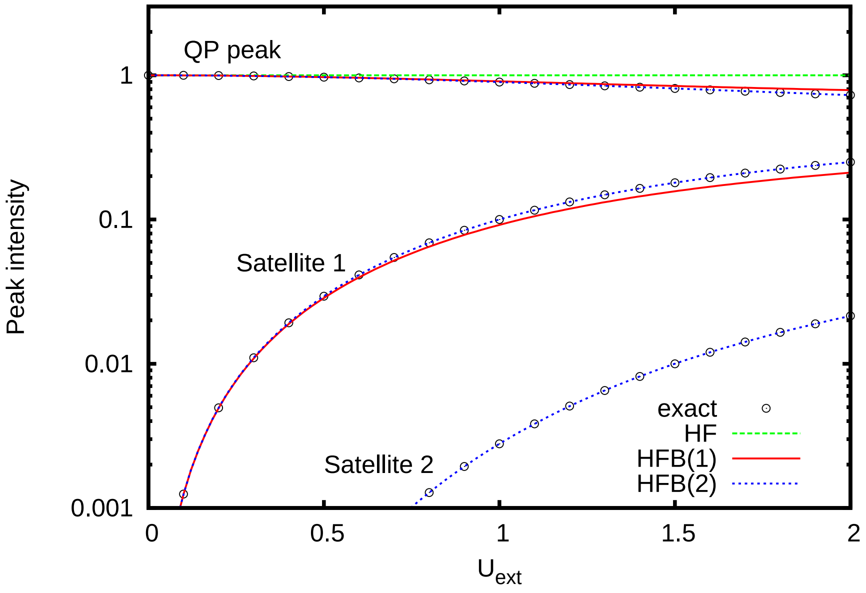

(b) Spectral peak intensities.

Figure 5.5: (a) Addition-energy spectrum of the LUMO level versus the interaction strength $U_{\text{ext}}$, (b) spectral peak intensities of the corresponding addition energy also versus the interaction strength $U_{\text{ext}}$.

non-interacting Green's function in Eq. (5.69). This way we obtain

$$G^0_{nm}(\omega) = \frac{2}{N+1}\sum_{k=1}^{N} \frac{\sin\left(\frac{\pi k n}{N+1}\right)\sin\left(\frac{\pi k m}{N+1}\right)}{\omega - 2t\cos\left(\frac{\pi k}{N+1}\right) + \mathrm{i}\,\mathrm{sgn}\left[2t\cos\left(\frac{\pi k}{N+1}\right)\right]\eta}\,, \tag{5.116}$$

for which we can perform a change of variables $x \equiv \frac{\pi k}{N+1}$ to obtain

$$G^0_{nm}(\omega) = \frac{2}{N+1}\sum_{k=1}^{N} \frac{\sin(nx)\sin(mx)}{\omega - 2t\cos x + \mathrm{i}\,\mathrm{sgn}(2t\cos x)\,\eta}\,. \tag{5.117}$$

This is now an expression for the TB part in the non-interacting Green's function $G^0$. We are then able to do the same self-energy calculations as in Sec. 5.3.5. For the tadpole diagram (Hartree approximation) we have

$$\Sigma^{\mathrm{H}}_{ij} = -\mathrm{i}\sum_{k,\sigma_k}\int \frac{\mathrm{d}\nu}{2\pi} \mathrm{e}^{\mathrm{i}\nu\eta} G^0_{kk}(\nu) V_{ik}\delta_{i,j}\delta_{\sigma_i,\sigma_j}\,. \tag{5.118}$$

For the '$HH$' component we therefore have, by inserting $k \in \{H, L\}$ for the molecule and $k \in \{1, 2, \ldots\}$ for the infinite chain,

$$\Sigma^{\mathrm{H}}_{HH} = 2U_0 - 2\mathrm{i}\frac{2}{N+1}\sum_{k=1}^{N}\int \frac{\mathrm{d}\nu}{2\pi}\mathrm{e}^{\mathrm{i}\nu\eta} \frac{\sin^2 x \cdot U_{\mathrm{ext}}}{\nu - 2t\cos x + \mathrm{i}\,\mathrm{sgn}(2t\cos x)\eta}\,, \tag{5.119}$$

where the first term on the right-hand side comes from the same calculation as earlier in Sec. 5.3.5, and for the second term we now need to do some careful thinking. The complex integral vanishes if the sign of the imaginary part of the denominator is positive. This is because the convergence factor $\mathrm{e}^{\mathrm{i}\nu\eta}$ forces the integration to be done in the UHP, hence, we need to have $2t\cos x < 0$ for the integral to give non-zero contribution. Because we are using $t < 0$ (see Fig. 5.2 on page 62), we have that

$$\begin{aligned} & \cos x > 0 \\ \Rightarrow\ & -\frac{\pi}{2} < x < \frac{\pi}{2} \\ \Rightarrow\ & -\frac{\cancel{\pi}}{2} < \frac{\cancel{\pi} k}{N+1} < \frac{\cancel{\pi}}{2} \\ \Rightarrow\ & -\frac{1}{2}(N+1) < k < \frac{1}{2}(N+1)\,. \end{aligned} \tag{5.120}$$

This constraint gives the limits for the sum in front of the integral, and we may evaluate the integral by using Cauchy's integral formula to give

$$\Sigma^{\mathrm{H}}_{HH} = 2U_0 + \frac{4U_{\mathrm{ext}}}{N+1}\sum_{k=1}^{\frac{1}{2}(N+1)} \sin^2 x\,. \tag{5.121}$$

Now we use the infinite chain argument and take $N \to \infty$. This converts the sum into an integral, and by change of variables[3] we get

$$\Sigma^{\mathrm{H}}_{HH} = 2U_0 + \frac{4U_{\mathrm{ext}}}{\cancel{N+1}}\frac{\cancel{N+1}}{\pi}\int_0^{\frac{\pi}{2}} \mathrm{d}x \sin^2 x\,, \tag{5.122}$$

---

[3] $x = \frac{\pi k}{N+1} \quad \Rightarrow \quad \mathrm{d}x = \frac{\pi}{N+1}\mathrm{d}k$

which can easily be integrated to give

$$\Sigma^{\mathrm{H}}_{HH} = 2U_0 + U_{\mathrm{ext}} \,. \tag{5.123}$$

Similarly we may compute the exchange diagram (Fock approximation)

$$\Sigma^{\mathrm{F}}_{ij} = \mathrm{i} \int \frac{\mathrm{d}\nu}{2\pi} \mathrm{e}^{\mathrm{i}\nu\eta} G^0_{ji}(\nu) V_{ij} \,, \tag{5.124}$$

and for the '$HH$' component we then have simply

$$\Sigma^{\mathrm{F}}_{HH} = \mathrm{i} \int \frac{\mathrm{d}\nu}{2\pi} \mathrm{e}^{\mathrm{i}\nu\eta} \frac{U_0}{\nu - \xi_H + U_{\mathrm{ext}} - \mathrm{i}\eta} = -U_0 \,. \tag{5.125}$$

By combining Eqs. (5.123) and (5.125) we then have the Hartree–Fock approximation for the infinite chain as

$$\Sigma^{\mathrm{HF}}_{HH} = U_0 + U_{\mathrm{ext}} \,, \tag{5.126}$$

and by comparing this to Eq. (5.86) for the truncated chain, we see that there is no difference at all. This means that the Hartree–Fock approximation for the interaction between the molecule and the terminal site of the chain is not affected by the total number of sites in the chain. For the '$LL$' component we find the same thing happening.

The bubble diagram for the infinite chain is then a real challenge. We will not go through the calculation here because of limited space but we state the outline for the '$HH$' component briefly. We must insert the non-interacting Green's function for the TB chain from Eq. (5.117) to the self-energy in Eq. (5.92). First we see that all other terms besides the ones with $U_{\mathrm{ext}}$ cancel due to the complex integrations as earlier in the truncated-chain calculation. Then we are left with one HF[4] Green's function for the '$HH$' component and two non-interacting Green's function for the '11' component inside the integrands. Also in this case we have to look at when the integrals give non-zero contribution with respect to the sign of the imaginary part of the denominators. This gives constraints for the summing indices in both of the '11' components. With these constraints we are able to evaluate the complex integrals and convert the sums from the $N$-site TB chains to integrals when taking the limit $N \to \infty$. These integrals then have the form of

$$\Sigma^{\mathrm{HFB}}_{HH}(\omega) = 8\left(\frac{U_{\mathrm{ext}}}{\pi}\right)^2 \int_{\frac{\pi}{2}}^{\pi} \mathrm{d}x \int_0^{\frac{\pi}{2}} \mathrm{d}y \frac{g(x,y)}{\omega - f(x,y) - \mathrm{i}\eta} \,, \tag{5.127}$$

where $g$ and $f$ are functions of $x$ and $y$ (in fact sines and cosines of $x$ and $y$) with the usual constants $\xi_H, \Delta_0, U_{HL}, t$. We see that the form of Eq. (5.127) is very close to the integral in Eq. (4.29) in Chap. 4. With some manipulations with the principal-value integrals, we finally arrive to an expression for the '$HH$' component of the self-energy's bubble-diagram approximation

$$\begin{aligned} \Sigma^{\mathrm{HFB}}_{HH}(\omega) &= 8\left(\frac{U_{\mathrm{ext}}}{2t\pi}\right)^2 \Bigg[ \mathcal{VP}\!\int_{2t}^{0} \mathrm{d}r \, \mathcal{VP}\!\int_0^{-2t} \mathrm{d}s \frac{\sqrt{1-\left(\frac{r}{2t}\right)^2}\sqrt{1-\left(\frac{s}{2t}\right)^2}}{\omega - \xi_H - U_0 + r - s} \\ &- \mathrm{i}\pi \int_{2t}^{0} \mathrm{d}r \, \theta(-2t - r - \omega + \xi_H + U_0)\theta(r + \omega - \xi_H - U_0) \\ &\times \sqrt{1-\left(\frac{r}{2t}\right)^2} \sqrt{1-\left(\frac{r + \omega - \xi_H - U_0}{2t}\right)^2} \Bigg] \,, \end{aligned} \tag{5.128}$$

---

[4] It is worthwile to note that we use the obtained HF Green's functions for the second-order expansion.

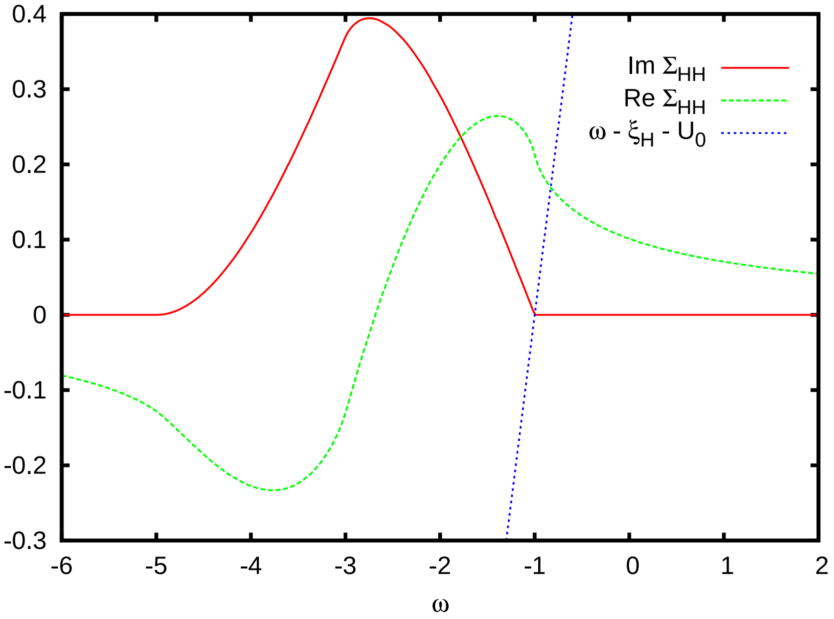

Figure 5.6: Real and imaginary parts of the '*HH*' component of the self-energy for the case of infinitely long TB chain.

where the step functions in the imaginary part give constraints for the integration variable $r$ with respect to the frequency $\omega$. It is a fair assumption that evaluating this integral by pen and paper is like squaring the circle, and for this purpose we have written a program which computes the integral numerically. This computation is explained more in detail in Sec. 5.5.2.

For an infinitely long TB chain we have obtained the self-energy for the interaction between the molecule and the terminal site of the chain, by using $U_0 = U_{HL} = \Delta_0 = U_{\text{ext}} = -t = 1$. The self-energy is a function of the frequency $\omega$ and has both real and imaginary parts. The imaginary and the real part of the self-energy's '*HH*' component are plotted in Fig. 5.6. In this figure we also have plotted a line $\omega - \xi_H - U_0$ for which the meaning will be discussed later in Chap. 6. Also the self-energy function $\Sigma^{\text{HFB}}_{HH}(\omega)$ itself will be analyzed more in detail in Chap. 6.

## 5.5 Computational methods

In this section we will clarify the computational methods used in the calculations of the studied systems.

### 5.5.1 Exact diagonalization

We present a brief introduction to Matti Manninen's FORTRAN code for exact diagonalization of Hubbardian type of models. This program was studied and modified for our purposes by Topi Korhonen [19].

The Hamiltonian in the beginning of this chapter [Eq. (5.1)] has dimension

$$\dim \hat{H}_{\text{tot}} = \binom{L}{n_+}\binom{L}{n_-}, \tag{5.129}$$

where $L = 2 + N$ is the number of sites in our system (2 for the molecule and $N$ for the chain), and $n_+$ ($n_-$) is the number of electrons with spin up (down). In the previous sections we were studying systems with truncated chain ($2 + 2$ sites) which can be diagonalized also by pen and paper in finite amount of time, but (at least for larger systems) we have made the diagonalizations with the help of computers.

The used program works in the occupation number representation, where the states are easily constructed: we take as many spin-up states as there are spin-up electrons, and for each spin-up state we take not more than the same amount of spin-down states. The input for the program for generating the basis is then the number of sites and the number of both spin-up and spin-down electrons.

After the basis is generated we need to construct the Hamiltonian $\hat{H}_{\text{tot}}$. The creation and annihilation operators are readily accessible as they simply change "zeros to ones", and vice versa, in the generated basis vectors. The Hamiltonian is constructed from these operations with some prefactors, not forgetting about the usual fermionic operator algebra. Then the generated basis vectors are operated with the Hamiltonian, and then the overlaps between the initial and final states are evaluated to give the elements for the Hamiltonian matrix.

The obtained Hamiltonian matrices can become quite large when the numbers of sites and electrons increase in Eq. (5.129). For the diagonalization of the matrix the program uses `LAPACK ZHEEVX`[5] routine, and the rest of the calculation is only a matter of computing power available.

From the obtained eigenvalues of the Hamiltonian matrix we have the eigenenergies of the corresponding system, and furthermore we are able to calculate the corresponding eigenvectors. From the eigenvectors we can also evaluate the electron densities in each site of the system.

### 5.5.2 Numerical integrations for the infinite chain

We will first consider the integral in the imaginary part of Eq. (5.128). This is a normal integral, although a challenging one, but we may compute the value of it numerically. A numerical grid for the frequency $\omega$ and for the integration variable $r$ are defined first, and then we compute the integral as a simple Riemann sum by inserting the correct values for the frequency to the loop. The step functions are considered as an `if` condition, which then in turn makes the integral non-zero in a particular region. For instance, in Fig. 5.6 we see that the imaginary part is non-zero only within the region $\omega \in [-5, -1]$. The numerical integrations were done by writing a simple `C++` program which was run by a regular desktop computer.

For the real part we need to figure out something more, as we have to take into account the principal-value integrals. First of all, it can be derived that the real part of the self-energy in Eq. (5.128) can be expressed qualitatively in a form

$$\operatorname{Re}\Sigma(\omega) = \mathcal{VP}\int_{-\infty}^{\infty} \mathrm{d}\omega' \ \operatorname{Im}\Sigma(\omega')h(\omega' - \omega) \,, \tag{5.130}$$

---

[5] LAPACK — Linear Algebra PACKage: `http://www.netlib.org/lapack/` , 27.1.2011

i.e., we use our result for the imaginary part to obtain the real part as a principal-value integral. This procedure is explained more in detail in [13], where it is found that the function $h$ in Eq. (5.130) is of the form $(\omega' - \omega)^{-1}$. We then notice that the integral for the real part of self-energy is of the similar form as in the Hilbert transform in Eq. (4.35). The numerical calculation for the principal-value integral is then performed by considering first the region where no singularities occur, and after this, adding the contribution around the singularity to the total value of the Riemann sum. The numerical considerations for the Hilbert transform are explained in detail in Ref. [31]. By using the idea of the Hilbert transform we wrote a `C++` program which computes the real part for the self-energy from the imaginary part. The program is a simple one, and it can be run by a regular desktop computer.

# Chapter 6

# Discussion

In this chapter we will present some results and discuss the meaning of these particular results.

## 6.1 Molecule and truncated chain

From the plots in Fig. 5.3 on page 67 we see that the behaviour of the system is very intuitive. The creation of an image charge lowers the ground-state energies of the $N+1$ and $N-1$ systems, and therefore lowers the addition and removal energies. Also, the absolute value of the image charge increases with the net charge on the molecule, and with the strength of the interaction $U_{\text{ext}}$.

The LUMO components of the self-energy function $\Sigma(\omega)$ are plotted against the frequency $\omega$ in Fig. 5.4 on page 82, where we use parameters $-t = \Delta_0 = U_0 = U_{HL} = U_{\text{ext}} = 1$. We see that for the HF approximation no singularities occur, and the self-energy $\Sigma$ seems to be simply a constant. From this finding we may deduce that, in the first order approximation, all the essential information about the system is determined by the non-interacting Green's function $G^0$, and only a ground-state contribution will be available from the full Green's function. However, when we take the second order approximation, already the first step shows a pole at $\omega \approx 3$. This result suggests that the first step of the second-order calculation will show an exited state with energy roughly $E = \omega \approx 3$. Another interesting feature of the studied system, which we see from Eq. (5.99), is that the exchange diagram in second order gives zero contribution. In fact, we noticed that all the other second-order diagrams except the bubble diagram vanish. It is therefore sufficient to calculate the second-order corrections from the bubble diagram only by inserting the obtained results iteratively until the perturbation series converges. The second and third steps of the calculation for the self-energy show two and three poles, respectively. This means that we do not only get more accurate results for the ground state but also information about the higher excited states as we are taking more diagrams into account.

In Fig. 5.5a on page 83 we have plotted the LUMO spectral peaks, i.e., the addition energies of the studied system. As suggested in the previous paragraph, the addition energy for the LUMO level in HF approximation is simply a constant with respect to the strength of the interaction $U_{\text{ext}}$, i.e., it does not follow the exact curve very well. Furthermore, we see only the ground-state contribution [quasiparticle (QP) peak], where the two electrons on the chain are both in the lower energy level. This electron configuration for the system is the most stable one, and is therefore called a 'quasiparticle' as a whole. The first step of the second-order calculation already takes the ground state quite close to the exact one, and we also see an excited state, where one electron on the chain has jumped to the higher energy level (Satellite 1). As we saw earlier, no other second-order diagrams need to be considered, and the higher excited states are obtained by inserting the obtained Green's functions back to the perturbation series iteratively. An extraordinary finding is that the second step of the calculation converges accurately to the exact result. This seems to be a coincidence more likely since the next step of the calculation already has more diagrams to be considered, and it starts to converge towards the so-called GW approximation. Similar pattern was obtained in Ref. [30] but without the 'accidental' success in the HFB(2)-step of our calculation. As the GW approximation deviates from the exact result, there still must be some higher order diagrams left in the perturbation series. By "creative thinking" we figured out that these remaining diagrams are so-called ladder diagrams, which are the same as the second-order bubble diagram, but with more interaction lines: (e.g. in fourth order)

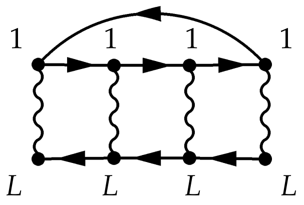

and the interaction lines can also be crossed in every possible way. This way we may, as in the figure above, connect the LUMO level of the molecule to the terminal site of the chain by an interaction line, and then propagate electrons on the LUMO level and on the terminal site, and again have an interaction. The ladder diagrams go up to infinite order since an infinite number of interaction lines (in infinite order by crossings) can be inserted. The contribution from these diagrams is quite minimal if we look at both Fig. 5.5a and Fig. 5.5b: The first excited state (Satellite 1) deviates very little from the exact result, and the main difference comes from the higher excited state (Satellite 2), where both electrons on the chain are on higher energy level. This difference is, however, a minimal one as well if we look at the intensities of the peaks from the lower figure. With $U_{\text{ext}} = 2$ the difference in energy between the exact result and the HFB(3) step is around one unit. In this case the peak intensity for the second satellite (to be even visible) is around 0.02 in relative scale. Hence, the results are mainly centered around the lower states (notice the logarithmic scale), and the GW approximation seems to fit well at least in the region $U_{\text{ext}} < 2$.

The main idea in the truncated-chain example was to test the accuracy of the perturbation theory, but in the process we also saw an interesting phenomenon (already from the exact result). The ground-state energies (QP peak) are lowered as the interaction strength is increased for the system with electron added to the LUMO level. This seems to be due to the effect that the added electron binds with its image charge on the chain. For the first excited state (Satellite 1), the electrons on the chain are in different energy levels (cancelling the effect from each other), and this is why the image-charge effect does not vary with respect to the interaction strength. The higher excited state (Satellite 2), however, has both electrons on the chain in higher energy level, and in this case the image-charge effect increases the energies of the system with added electron with respect to the interaction strength.

A remark concerning all the calculations done for the case of truncated chain. Having all the calculations done, we noticed that the Hamiltonian in Eq. (5.1) could have been divided by the hopping parameter $t$. In this case, we would measure energies in units of $t$. This seems to be more clever way to include an arbitrary hopping as all the other parameters in, e.g., Eqs. (5.42), (5.46), (5.47), (5.48), (5.91) would then be divided by $t$.

Now that we have compared the results, obtained from the diagrammatic calculations to the exact ones, and seen that they are congruent, we may consider also larger systems which would be very tedious to evaluate by using exact diagonalization. This task, however, seems to remain as a future plan. Also the mentioned image charge on the chain could be calculated, and especially it would be an interesting quantity on the terminal site. These calculations we will, however, exclude from this work, and get back to them in future.

## 6.2 Infinitely long chain

For an $N$-site TB chain, with $N \to \infty$, we had only little time to work with, regarding this thesis. We are still interested in the topic, and are considering it thoroughly for future purposes. Here we will review only the preliminary results and see where they can be applied to.

First of all, we noticed that the HF approximation for the self-energy is independent on the number of sites on the chain. We found the same results for the infinitely long chain as for the truncated chain. Therefore we studied the second order approximation by considering the bubble diagram.

In Fig. 5.6 we plotted the real and imaginary parts of the '$HH$' component of the self-energy $\Sigma(\omega)$ against the frequency $\omega$. In the figure we have also a line $\omega - \xi_H - U_0$, which corresponds to a part of the denominator of the Green's function [see Eq. (5.88)]. The other part of the denominator can be shown to be the real part of the self-energy $\Sigma$. Furthermore, we see the pole of the Green's function, i.e., the denominator going to zero, when the real part of the self-energy and the line $\omega - \xi_H - U_0$ intersect. This pole of the Green's function (as we are considering the '$HH$' component) corresponds to the removal energy of a particle from the HOMO level of the molecule. We are able to perform the numerical calculation in a loop where we vary the interaction strength $U_{\text{ext}}$ and then find the crossing point, and this way obtain a behaviour for the energy of the removed particle with respect to $U_{\text{ext}}$. This behaviour is shown in Fig. 6.1. We see that the behaviour is similar (although mirror-like) to the one in Fig. 5.5 for the truncated chain. When we increase the interaction strength $U_{\text{ext}}$, the ground-state energy is increased for the system with electron removed from the HOMO level. Although for the truncated chain we were studying the addition energy spectrum to the LUMO level, in here we have the removal energy spectrum from the HOMO level. In this work we did not study the LUMO level self-energies for the case of infinitely long chain.

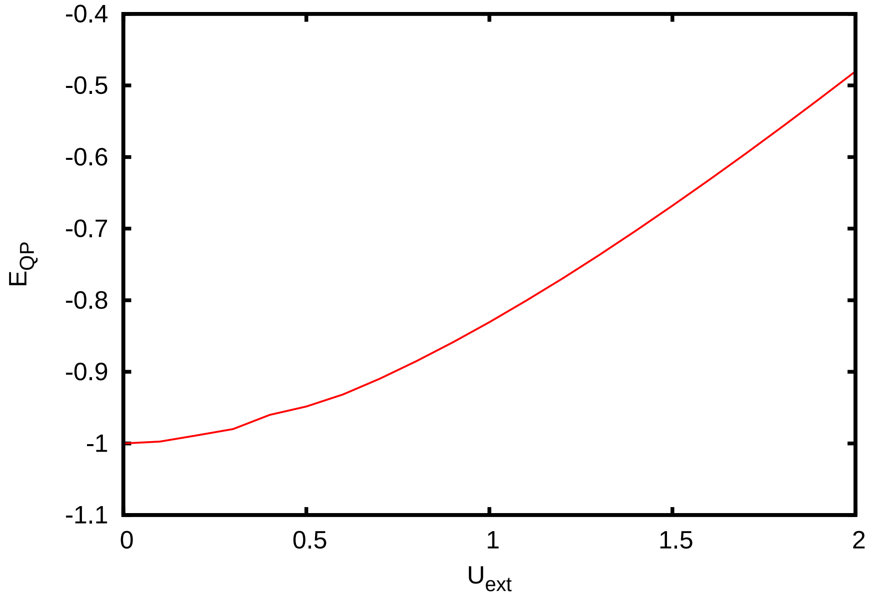

Figure 6.1: Quasiparticle energies corresponding to a removed particle from the molecule's HOMO level against the interaction strength $U_{\text{ext}}$ between the molecule and the terminal site of the infinitely long chain.

# Chapter 7

# Conclusion

This is a concluding chapter and we will give an overview of this thesis, and present some ideas and viewpoints for future considerations.

In this work we have presented the many-particle theory from quantum-field theoretical viewpoint. We started from essential field-theoretical ingredients including, e.g., second quantization, and advanced all the way to the many-particle perturbation theory. In the process we saw some interesting features of the theory. Mentioning few of them: such as, grand canonical ensemble; creating particles and holes (i.e. removing particles), propagators; how do particles move in spacetime, evolution on the Keldysh time contour, and eventually a lot of somewhat complicated mathematical equations which could be simplified by using pictorial representations called Feynman diagrams.

Although this thesis is about theoretical physics, we did not want to spend all the time available to going through the diversified background theory. Instead, after a lengthy introduction to this field of physics, we studied some applications which could, to some extent, be utilized in, e.g., nanotechnology and especially in quantum-size chips in electronics. We introduced a model with a two-site molecule and an $N$-site tight-binding chain, which could be thought of as an electrical device and a conduction wire, respectively. We wanted to study the interactions between the molecule's sites and the terminal site of the chain, in order to obtain information about, e.g., charge transport and currents.

The introduced model was then studied (with a truncated chain) by two different methods: first by exact diagonalization of the Hamiltonian, and then by considering the interactions between the molecule and the chain perturbatively. For small systems, the exact calculations were naturally easier to handle since it was straightforward to formulate the Hamiltonian matrix from all the possible electron configurations, and then to find the eigenvalues of that particular matrix. For larger systems, the possible electron configurations increased rapidly and so did the dimension of the Hamiltonian matrix to be diagonalized. At this stage the many-particle perturbation theory came in handy. Although there was lot to discuss, with non-interacting Green's functions, interactions, Feynman rules, self-energies, etc., the calculations could eventually be made analytically. These two methods for studying the model seemed to be fairly congruent, and for a closer review of the results we refer to the previous chapter.

Beyond the truncated-chain calculations we also put to the test a case for an infinitely long chain. For this purpose we first needed to take a closer look at the non-interacting Green's function of the system. It turned out that the calculations for the self-energy could be done for the infinite-chain case as well, but only numerically as the integrals became somewhat difficult to reach analytically. For this thesis we presented some preliminary results from the infinite-chain case, and these can be seen in the previous chapters. The actual reason of these calculations was to find a clever way how to tackle the problem rather than finding the right results at once. These topics are still under discussion and will definetely be a part of our future considerations.

There was also something obvious that was brushed aside, namely the true many-particle problem of the studied system. In this case, also the electron hoppings between the molecule and the chain, leading to charge transport, would have been allowed. For the parameter $t_{\text{hyb}} \neq 0$ the problem would have become more complicated because: 1) the dimension for the Hamiltonian matrix for exact diagonalization would have grown out of our computing power quite rapidly; and 2) the perturbative treatment would have had more components to be studied (embedding self-energy accounting for the hoppings between the molecule and the chain).

Since this paper is a thesis, we would like, as an epilogue, to review something we have learned. The learning process about the topics of many-particle quantum mechanics already started with courses before an explicit description of the given master's project. The project, however, was a great motivation to go through all the material from already finished courses, and develop some kind of an understading at grass-roots level. By writing down the background theory for the topics to be studied helped a lot in constructing the knowledge, piece by piece. The level reached, as stated, is still at the bottom of the pile – just a little above the ground level – and the studying seems to go on towards next projects.

# Bibliography

[1] A. A. Abrikosov, L. P. Gorkov, and I. E. Dzyaloshinski. *Quantum Field Theoretical Methods in Statistical Physics*. Pergamon Press, Oxford, UK, 2nd edition, 1965.

[2] G. B. Arfken and H. J. Weber. *Mathematical Methods for Physicists*. Elsevier Academic Press, San Diego, California, 6th edition, 2005.

[3] H. Bruus and K. Flensberg. *Many-Body Quantum Theory in Condensed Matter Physics: An Introduction*. Oxford University Press, Oxford, New York, 1st edition, 2004.

[4] C. Cercignani. *Ludwig Boltzmann: The Man Who Trusted Atoms*. Oxford University Press, Oxford, New York, 1st edition, 1998.

[5] P. Danielewicz. Quantum Theory of Nonequilibrium Processes. *Ann. Phys.*, **152**(239), 1984.

[6] P. Dirac. *Quantum mechanics*. PhD thesis, St. John's College, University of Cambridge, 1926.

[7] P. A. M. Dirac. The Quantum Theory of the Emission and Absorption of Radiation. *Proc. Roy. Soc.*, **A114**(243), 1927.

[8] A. L. Fetter and J. D. Walecka. *Quantum Theory of Many-Particle Systems*. McGraw-Hill, San Francisco, 1st edition, 1971.

[9] R. P. Feynman. *The Principle of Least Action in Quantum Mechanics*. PhD thesis, Princeton University, 1942.

[10] R. P. Feynman. Space-Time Approach to Quantum Electrodynamics. *Phys. Rev.*, **76**(769), 1949.

[11] R. P. Feynman. The Theory of Positrons. *Phys. Rev.*, **76**(749), 1949.

[12] V. Fock. Konfigurationsraum und zweite Quantelung. *Z. Phys.*, **75**(622), 1932.

[13] J. M. Garcia-Lastra, C. Rostgaard, A. Rubio, and K. S. Thygesen. Polarization-induced renormalization of molecular levels at metallic and semiconducting surfaces. *Phys. Rev.*, **B80**(245427), 2009.

[14] E. K. U. Gross, E. Runge, and O. Heinonen. *Many-Particle Theory*. Adam Hilger, Bristol, Philadelphia and New York, 2nd edition, 1991.

[15] W. Heisenberg. Über quantentheoretische Umdeutung kinematischer und mechanischer Beziehungen. *Z. Phys.*, **33**(879), 1925.

[16] J. Hubbard. Electron Correlations in Narrow Energy Bands. *Proc. Roy. Soc.*, **A276**(238), 1963.

[17] P. Jordan and O. Klein. Zum Mehrkörperproblem der Quantentheorie. *Z. Phys.*, **45**(751), 1927.

[18] L. V. Keldysh. Diagram technique for nonequilibrium processes. *Sov. Phys. JETP*, **47**(1515), 1964.

[19] T. Korhonen. Spectral Functions of Second Quantization Hamiltonians in Chains, Bachelor's thesis, University of Jyväskylä, Department of Physics, 2009.

[20] L. D. Landau and E. F. Lifshitz. *Quantum Mechanics: Non-Relativistic Theory*. Pergamon Press, Oxford, UK, 3rd edition, 1977.

[21] G. D. Mahan. *Many-Particle Physics*. Plenum Press, New York, 2nd edition, 1993.

[22] F. Mandl. *Statistical Physics*. Wiley, New York, 2nd edition, 1988.

[23] P. C. Martin and J. Schwinger. Theory of Many-Particle Systems. *Phys. Rev.*, **115**(1342), 1959.

[24] R. D. Mattuck. *A Guide to Feynman Diagrams in the Many-Body Problem*. Dover Publications, Mineola, New York, 2nd edition, 1992.

[25] W. Pauli. The Connection Between Spin and Statistics. *Phys. Rev.*, **58**(716), 1940.

[26] L. I. Schiff. *Quantum Mechanics*. McGraw-Hill, New York, 1st edition, 1949.

[27] E. Schrödinger. An Undulatory Theory of the Mechanics of Atoms and Molecules. *Phys. Rev.*, **28**(1049), 1926.

[28] F. Schwabl. *Advanced Quantum Mechanics*. Springer-Verlag, Heidelberg, Berlin, 4th edition, 2008.

[29] F. Smithies. *Cauchy and the Creation of Complex Function Theory*. Cambridge University Press, Cambridge, UK, 1st edition, 1997.

[30] K. S. Thygesen and A. Rubio. Renormalization of Molecular Quasiparticle Levels at Metal-Molecule Interfaces: Trends across Binding Regimes. *Phys. Rev. Lett.*, **102**(046802), 2009.

[31] X. Wang. Numerical Implementation of the Hilbert Transform. Master's thesis, University of Saskatchewan, Department of Electrical Engineering, 2006.

[32] E. Wigner and P. Jordan. Über das Paulische Äguivalenzverbot. *Z. Phys.*, **47**(631), 1928.

[33] A. M. Zagoskin. *Quantum Theory of Many-Body Systems*. Springer-Verlag, New York, 1st edition, 1998.